Microwave lattice mixers at 4.5 Ghz

J. R. Emmett

MICROWAVE LATTICE MIXERS AT 4.5 GHz

by

J. R. EMMETT B.Sc.

A thesis submitted to the Faculty of Science,

University of Durham, for the degree of

Doctor of Philosophy

Department of Applied Physics
and Electronics,
University of Durham, U.K.

September 1974

Microwave Lattice Mixers at 4.5 GHz

J.R. Emmett Ph.D. Thesis University of Durham 1974

ABSTRACT

The theory, development and construction is described, of a type of microwave mixer which has a very good noise performance due to a low conversion power loss. The conditions under which this performance is obtained are derived from a theory based on practical diode laws and operating conditions. The effect of input and output terminations on the conversion power loss are then analysed, and the open-circuit image rejection type is shown to be capable of the best performance.

Realisation of the open-circuit image termination is difficult at microwave frequencies because of losses involved in the passive input network. Part 1 of this thesis concerns the theory and development of a new type of T.E.M. mode cavity especially suited to these conditions. Performance of the cavity is analysed using lumped equivalent circuits, and the results confirmed on a 400 MHz experimental cavity. A double-balanced system is then described, with a new type of frequency independent phase inversion. This combination is shown to suit the requirements of the type of mixer considered, and a total of six experimental mixers at 4.5 GHz are constructed using this type of cavity. The results obtained are shown to be in accordance with the theories put forward, and noise measurements are used to support the values for conversion power loss put forward.

In the last chapter, the practical and commercial implications of a high performance mixer at microwave frequencies are considered, especially with regard to the intermediate frequency amplifier design.

ACKNOWLEDGEMENTS

The author is indebted to Dr. B.L.J. Kulesza for his supervision, patience and encouragement throughout this project.

The help of the other members of the Solid State Research Group is also gratefully acknowledged, especially that of Mr. J.P. Wright, Senior Lecturer at Newcastle-on-Tyne Polytechnic.

Thanks are also extended to Professor D.A. Wright, Head of the Department of Applied Physics and Electronics at the University of Durham, for placing the facilities of the department at the author's disposal, and to the U.K. Science Research Council for supporting the project.

CONTENTS

PART II 4.5 GHz LATTICE MIXERS

APPENDICIES AND REFERENCES

Part 1

Appendix 1 Impedance Analysis of a loss-less short-circuited Transmission Line

2 Simplifications in the calculations for loop coupling

3 Integration of the Magnetic Field in a Coaxial Cavity

4 The loaded Q value of an End-loaded Cavity

Part 2

Appendix 5 Output Components of Balanced and Double-Balanced Mixers

Parts 1 and 2

References

Paper presented at 1971 European Microwave Conference

LIST OF ILLUSTRATIONS

PREFACE

The two parts of this thesis represent the two connected projects undertaken at Durham in the period 1969-74.

The first project was started as a part-time M.Sc. with the general title of "Strip transmission lines." The basis of the mixer theory to be used later had just been laid down, and experimental verification was moving from mixers at a few hundred kilohertz, to a lumped component 1.5 Gigahertz version. The later mixer used some of the first glass encapsulated Schottky-barrier diodes available. Although the results obtained were good, it was obvious that any commercial mixer working at this frequency or higher could not employ the tiny, critically adjusted, filters and transformers. The answer seemed to lie, at the time, in the use of printed stripline components. However, after some practical experience of stripline at Microwave Instruments Ltd., and discussion with other workers in this field, problems of loss and compatibility became obvious.

The frequency for the next experimental mixer was established at 4.5 GHz because of interest in direct television reception from the geostationary satellites which use an atmospheric transmission "window" in this frequency region. The use of such a mixer in space vehicles was also considered, and so size as well as commercially repeatable results was important. Ancilliary projects for the 4.5 GHz mixer were concerned with diode evaluation and measurements (which led to the parasitic theory modifications used here), and also work on local oscillator sources. One early experimental device in the local oscillator project was a 1.5 to 4.5 GHz varactor multiplier. Size dictated the use of TEM mode components and for mechanical convenience a capacitively coupled input with a loop output was used on the resonators. Construction was a hybrid stripline-cavity arrangement, although lower

loss airspaced coaxial parts were used later. The unusual point about these resonators was the twin resonance, the expected one when the line was a quarter of a wavelength long, and the other when the line was slightly shorter. Now, the short-circuited transmission line exhibits an inductive reactance when slightly shorter than a quarter wavelength, and this could have resonated with the end coupling capacitance. If so, it was reasoned that this pseudo-series resonance would provide the image rejection filter required for the mixer. It ~~seen~~ became apparent that there was virtually no quantitative information on TEM mode cavity coupling in the literature, since the easy adjustments which may be made in the coaxial arrangement, allowed the use of empirical methods. The mixer project required more accuracy, since not only was there impedance matching to be done, but also, filtering of some accuracy.

Work on the theory of the end-loaded cavity took nearly a year, although a few mathematical problems lingered on until later. A test cavity at 400 MHz bore out the main points and confirmed the suitability of the arrangement for the mixer front end. In 1971 an S.R.C. award was obtained to work on the 4.5 GHz mixer, and the design of the balanced front end was started using end-loaded cavities. The problem was to obtain the phase inversion required for balanced operation. By reversing the current flow in the input coupling loop, a phase reversal was obtained in one cavity, and the double cavity system with a figure 8 input coupling was created. Suitable Schottky barrier diodes were by now becoming available for the 4.5 GHz mixer. Matching these into quads was surprisingly difficult due to the almost invisible size of the unencapsulated devices. Once the measurements had been made, the large parameter spreads of the early examples made matching difficult, as did the inevitable losses due to damage

to the very vunerable exposed junction areas. Initial results were given at the European Microwave Conference in Stockholm, and a copy of this paper is included in the Appendix.

Encouraged by the success of this model, later versions were produced with neater engineering and a printed substrate containing the diodes and associated components. This gave the required three dimensional symmetry, and will it is hoped, pave the way towards an integrated system incorporating a low noise balanced I.F. amplifier as well. Measurements on later mixers supported the input and output calculations from the theory, which itself was modified to include the effect of diode parasitics and imperfect image rejection. The best results were obtained using diodes only available very recently, and consisting of an integrated quad of silicon Schottky barrier diodes (mixer 6). This is most encouraging from the point of view of the integration in the future, of not only diodes, but also the capacitors and possibly the I.F. amplifier. The result of this could be to extend mixer performance into a region where at present only bulky and bandwidth restricting R.F. amplifiers can compete.

PART I - THE END-LOADED CAVITY

1. Introduction

In many microwave applications there are problems involved in impedance matching between solid state active devices and the passive circuits. In the past, thermionic counterparts of these active devices could usually be designed with impedance values to fit a particular circuit, but the impedance relationships of solid state devices are determined intrinsically, and any deviation would deteriorate the performance. Consequently many practical circuits are operated very inefficiently due to mismatches.

In mixer applications there is a need for an efficient frequency conversion, not only to obtain a match between the device and the rest of the circuit, but also to provide filtering. Due to the non ideal nature of components, a means of adjustment is also needed to optimise the performance. In this respect we are concerned in Part 2 with a double-balanced mixer utilising four semiconductor diodes connected in a lattice configuration.

In this type of mixer a balanced system was required which would provide a filter, together with impedance transformation. It was decided because of high Q possibilities at microwaves, to use a resonant coaxial cavity as the filter network.† Initially a coaxial cavity had to be constructed which would act as a series resonant circuit.†† The result was the end loaded resonant coaxial cavity.

† It is well known that a coaxial transmission line of just under a quarter wavelength long, shorted at one end and comparatively terminated at the other, will behave as a resonant element. In the usual application, because of the way in which the couplings are introduced, such a coaxial cavity can be represented as a parallel resonant circuit.

†† This was achieved by using the cavity resonance capacitance also as the coupling element to the load.

The theory of this cavity is presented in Chapter 3, and the experimental results in Chapter 4. Finally the identical end loaded cavities were combined to form a balanced system which is a part of the lattice mixer.

In practice the parameters of any cavity end associated coupling networks are often chosen arbitrarily, and the information available on the theory of the end loaded cavity is limited. In our application a more rigorous approach was necessary, and so equivalent circuits are proposed, based on the physical dimensions of the cavity and couplings. The circuits can then be analysed for optimum operational conditions in the normal way. The theoretical derivations obtained are compared in Chapter 4 with experimental results on low frequency cavities, before the 4.5 GHz cavities used for the mixer in Part 2 are described.

2. General Properties of Resonant Cavities

2.1 Historical Background

The history of the radio waves has been one of increasing frequency, advanced to a large extent by overcrowding of the lower end of the spectrum. It is not surprising, therefore, that the history of the cavity resonator at microwave frequencies is a fairly short one.

Long lines were, of course, used over a century ago in the field of electrical communications, but without any clear conception of their behaviour under A.C. conditions. Soon after the commercial development of telegraph systems in the early 1840's, it became obvious that the transmission in propagation was not fully explained by the D.C. theory of the time. In 1855 Lord Kelvin[1] introduced capacity and loss resistance into the theory. This was with reference

to a concentric undersea cable. Land lines of the time were, however, a single line against earth type, and inductive efforts predominated. Kirchoff[2] made an attempt at this analysis in 1857. The big jump in transmission line interest came in the 1880's with the introduction of the telephone. This required a much higher bandwidth than the telegraph and hence a better understanding of the transmission line. The immediate problems were solved by Heavyside[3] in 1886, although he only considered the forward wave. About this time, the theory of electromagnetic radiation was formulated culminating in Maxwell's equations. With this information available around the turn of the century, D.D. Thompson[4] and others produced the present day theory of transmission lines, including radiation effects and resonance possibilities.

About this period, the early electrical experimenters were concerned with waves of thousands of metres wavelength, but the foundations of short wavelength theory were being laid down in the acoustical field. The low propagation velocity of sound waves gave wavelengths of a few centimetres for frequencies in the audible range. The audible and often visible effects associated with these waves were quite an advantage from the point of view of generation and detection before electronic devices were available.

The earliest work on resonant cavities was done by the early organ builders. The physicists continued this work around the turn of the century[5] and a whole range of easily recognised acoustic analogues of microwave systems were produced[6]. Although interest in theoretical acoustic research soon lapsed, certain types of resonator are still of great interest today. In particular, an analogue of the end loaded cavity is used in loudspeaker cabinets. This is used to match the high acoustical impedance of the air by

means of a low Q resonance in the 30-100 Herz region. This was first theoretically described, I believe, by Jordan[7] and has the advantage, as does its microwave counterpart, of negligible higher spurious resonances due to the poor impedance match of these to the air. The advantage over the common Helmholtz (Bass Reflex) system is that of an easily adjusted impedance match, exactly as with the microwave counterpart.

When the radio experimenters were raising frequencies in the 1920's they used a resonant transmission line system in the form of "Lecher" lines for direct wavelength measurement. As a resonator, however, this type of line would have been very lossy due to radiation and non-optimum characteristic impedance. In 1936 two papers were published[8,9] which first described practical waveguides, and just two years later W.W. Hansen[10] published the basic paper on microwave cavity resonators. In recent years the design of cavity resonators has progressed into the optical region of the spectrum where the wavelength involved is far too small for a practical cavity to be made employing conventional theory. Any practical system must use a very high order mode of resonance and there is considerable difficulty in separating a usable mode from others close together in frequency. In 1958 Schaulow and Townes[11] pointed out that removing the sides of a resonator would eliminate many modes by radiating them. Whether there would be any usable modes left was in some doubt until Fox and Li[12] published a computer simulation of this type of cavity in 1961. This type of cavity made Laser and Maser systems possible, and at present the frequencies of these are pushing into the near ultra-violet region.

2.2 Fundamental Principles

The two fundamental features of a microwave resonant cavity are:-

(i) The physical size depends on the wavelength involved, and

(ii) the electromagnetic fields are totally confined within conducting walls, except where it is desired to radiate the energy.

In fact the second feature is an essential property of a cavity, since any circuit element of a size comparable with the wavelength involved will lose energy by radiation. The understanding of the operation of such a cavity is complicated by the fact that the lumped elements of the equivalent low frequency resonant circuit (inductance and capacitance), lose their validity. It is even possibly incorrect to use the word circuit with reference to a cavity.

There are two ways out of this complicated situation. We can abandon attempts to describe circuits in terms of a voltage, a current and an impedance, and restrict ourselves to the quantities occurring in the equations of the electromagnetic field, i.e. Maxwell's equations. Although it would be easy to state the problem this way, the solution would be difficult. An alternative is to consider only the external characteristics of the cavity; its behaviour as a circuit element. We must in this case include the elements that couple the cavity to the rest of the circuit, and then treat it as a one or two terminal pair network. Any cavity resonator is inherently a very complex network, it has an infinite number of natural frequencies of oscillation, and what is more, it may be excited in more than one mode. If we can arrange to have only one resonance in the frequency band of interest, however, the analysis of the cavity resonator is considerably simplified, and this method has formed the basis of most considerations in the past.

2.3 Theoretical Relations of a Coaxial Resonant Cavity

In the frequency bands up to 10 GHz, where waveguide systems were used, there are increasing demands for larger bandwidths and greater miniaturisation, and so the use of TEM mode transmission lines is becoming essential, despite the higher losses incurred compared to waveguide. Of the available TEM mode resonators compatible with this type of transmission line, the coaxial form offers the advantages of total screening and the lowest loss.

This type of resonator consists of a length of coaxial line reflectively terminated at both ends. The length is therefore governed by the electrical length at resonance, and is normally a multiple of a quarter wavelength. The designer has the choice of shape, cross sectional size and characteristic impedance. The shape can be chosen for practical convenience, but the size should be such that no modes other than TEM can be supported. This usually involves cross section dimensions much less than a half wavelength. The characteristic impedance can be chosen to be an optimum with respect to several different parameters. The most important of these in most cases is minimum loss at resonance (highest Q values). It is important to realise that this condition is not realised by optimising for the minimum A.C. resistance of the line which occurs when the inner and outer conductors are of the same diameter (i.e. characteristic impedance Zo=0). The attention constant of the line alone determines the loss of the resonator[14].

If we consider a coaxial line of inner conductor diameter = d, and outer conductor inner diameter = D:-

A.C. resistance R is proportional to

$$\left(\frac{1}{d} + \frac{1}{D}\right) \quad .. \quad .. \quad .. \quad .. \quad .. \quad .. \quad (1)$$

and the attenuation constant

$$\alpha = \frac{R}{2Z_o} \quad .. \quad .. \quad .. \quad .. \quad .. \quad .. \quad (2)$$

We know that for circular conductors:-

$$Z_o = 138 \log_{10} \left(\frac{D}{d}\right)$$

therefore:-

$$\alpha = \frac{K\left(\frac{1}{d} + \frac{1}{D}\right)}{\log_{10} \left(\frac{D}{d}\right)} \quad .. \quad .. \quad .. \quad .. \quad .. \quad (3)$$

where K is a constant of proportionality.

Minimising equation (3) with respect to D/d, we find an optimum value of Zo of approximately 77 ohms. As the conductor diameter ratio drops below this minimum ($\frac{D}{d} = 3.592$), the line resistance R continues to decrease, but the current required to transmit the same power increases at such a rate that the power loss is greater. For a low loss resonator, therefore, it is advisable to design for a characteristic impedance somewhere between 40 and 100 ohms.

2.4 Impedance Analysis

For mathematical simplicity in developing this analysis, the method of equivalent lumped elements is used. In the proposed equivalent circuit, each cavity and coupling is replaced with lumped element impedances which are of known magnitude and frequency dependence. To do this on a rigorous basis it is necessary to know the field distribution of a coupled cavity at all frequencies. However for coupled cavities with high Q values, the coupling does not significantly change the normal field distribution which may be found for simple shapes by solving the boundary conditions in Maxwell's equations.

The problem of finding the impedance function of a cavity and associated coupling system is similar to that of an n-mesh two terminal circuit (assumed lossless). This can be analysed using Foster's theorem, producing an input impedance that is purely imaginary, with poles and zeros alternating along the frequency axis. Two networks may be said to be equivalent if their poles and zeros correspond, and impedances are the same at any single non-resonant frequency. Two such equivalent circuits with poles at $w = 0$ and $w = \infty$ are shown in Fig.1. At the frequency close to one of the poles ($w = w_k$) we may approximate to the circuit by lumping together all non-resonant elements into one, as shown in Fig.2. This is allowable if the cavity resonance is the only one in the frequency band under consideration. In the case of a coaxial resonator used at the fundamental mode corresponding to the first pole of the equivalent circuit, the next resonance will be at twice or three times the fundamental and so may be ignored for the purposes of this analysis. As an example, a short circuited TEM mode transmission line resonator is analysed in Appendix 1. The error produced by lumping together elements is illustrated in Fig.3 where an admittance plot is given for one, five and infinity elements. Close to the first pole it can be seen that taking only one element introduces negligible error for the practical application of this type of analysis.

2.5 Filter Properties

If the element values of the equivalent lumped circuit of a cavity resonator are known, it becomes possible to design the required filter network (normally of the band-pass pattern)[15,16,17]. The usual starting point is a normalised low-pass prototype from

Fig. 1

Equivalent circuits for an n-mesh 2 pole with poles at $\omega = 0$ and ∞.

(a) Impedance form

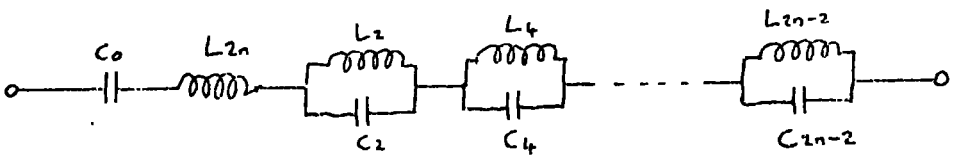

$$Z(\omega) = jA\omega \frac{(\omega^2-\omega_1^2/(\omega^2-\omega_3^2).....(\omega^2-\omega_{2H-1}^2)}{\omega^2(\omega^2-\omega_2^2)(\omega^2-\omega_4^2)...(\omega^2-\omega_{2H-2}^2)}$$

(b) Admittance form

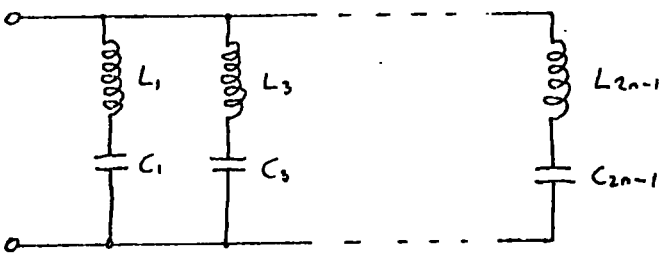

$$Y(\omega) = Z(\omega)^{-1}$$

Fig. 2

Fig. 1 simplified at one pole $\omega = \omega_k$

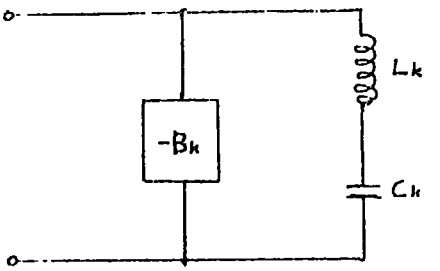

Fig. 3

Curves showing exact form of admittance function and two approximations.

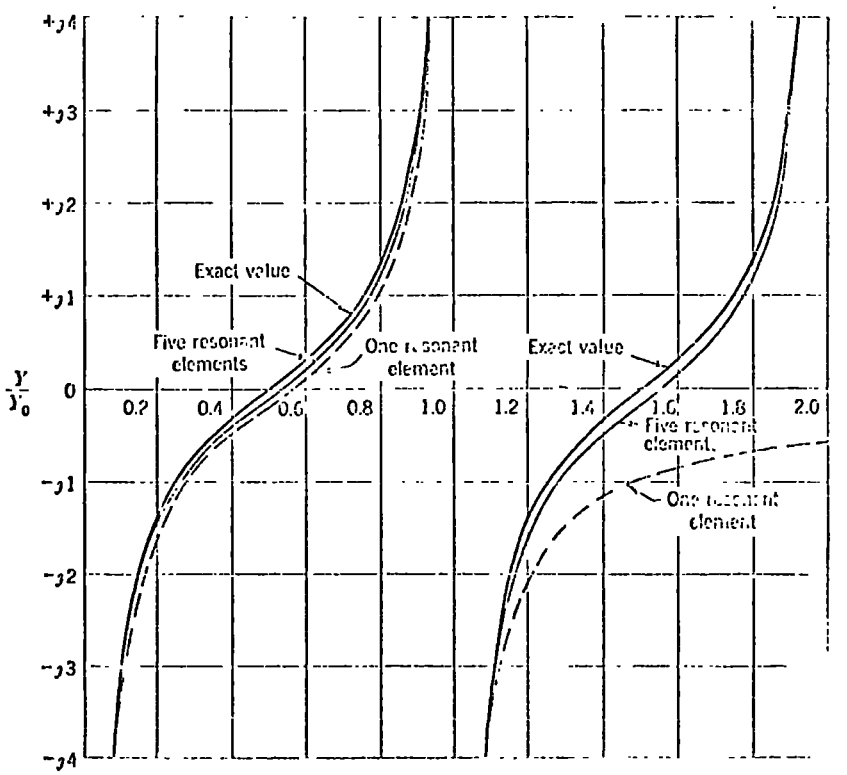

which a bandpass system may be evolved[18]. Except for special applications, transmission characteristics usually fall into one of two types, maximally flat or chebyshev response. For a given number of filter sections, the chebyshev system offers the highest out-of-band attenuation, but has the penalty of pass band ripple. Reducing this ripple reduces the out of band attenuation, and in the limit a maximally flat type of response results. This response is defined as having the largest number of response derivatives equal to zero at the centre frequency, and it corresponds to critical coupling between cavities. The equivalent circuit of a cavity depends to a large extent on the method of coupling and this may be divided into three types for the coaxial cavity. These are loop (magnetic field), coupling, probe (electric field) coupling or a combination of both which will be called direct coupling. As an example, the lumped component equivalent circuits for these coupling methods are given in Fig.4 for a filter consisting of three cavities. The networks have equal input and output impedances, but it is important to note that any single cavity is not normally a reciprocal network, as it forms a so called half section of the filter. The impedance values and coupling parameters of such a half-section must be derived directly from the physical characteristics of the cavity, before a filter can be constructed. This will be done later for the end loaded coaxial cavity, for which the half-section equivalent circuits are given in Fig.5.

2.6 Energy Storage

In general the electromagnetic energy in a cavity at resonance is stored in the electric and magnetic fields. The amount

Fig. 4

Equivalent circuits for 3 coupled cavities

(a) Mutual inductive (loop) coupling:-

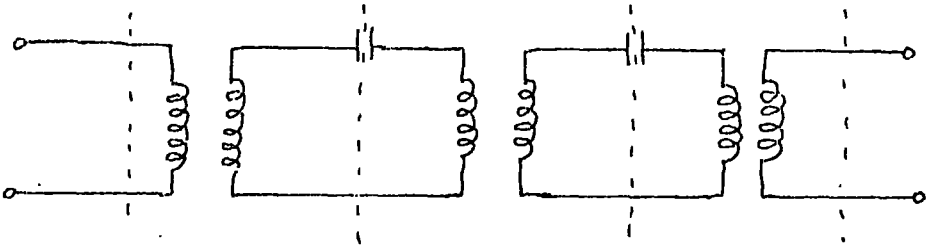

(b) Series capacitive (probe) coupling:-

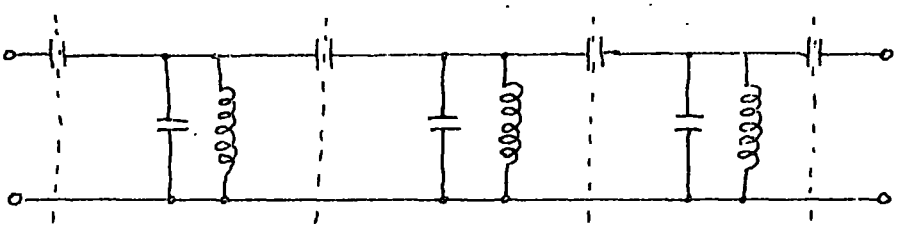

(c) Shunt inductive (direct) coupling:-

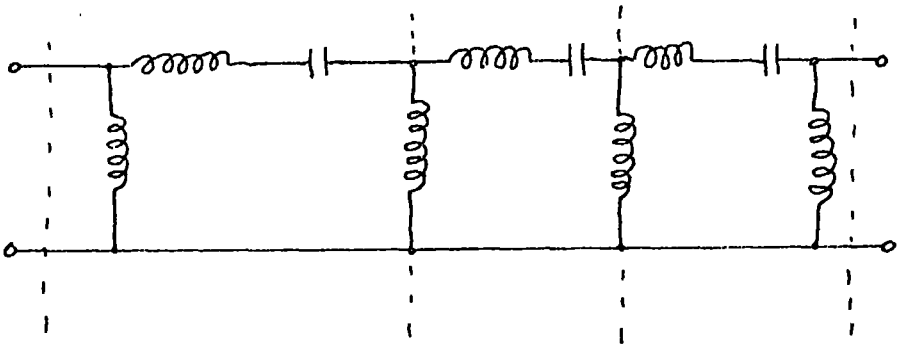

Fig. 5

Equivalent Circuits and Physical realisation for a half section of Figs. 4a, b, c

(a) Mutual inductive coupling:-

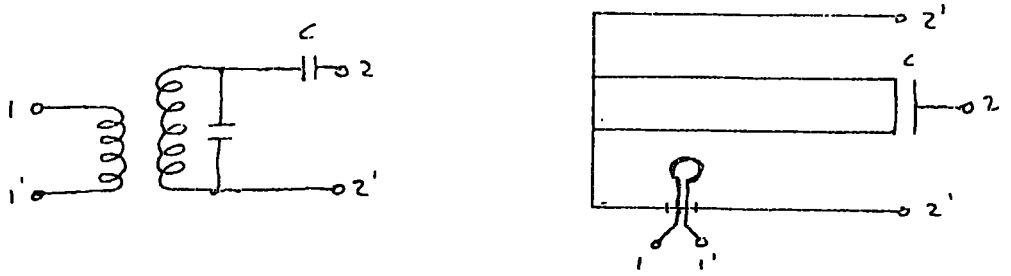

(b) Series capacitive (probe) coupling:-

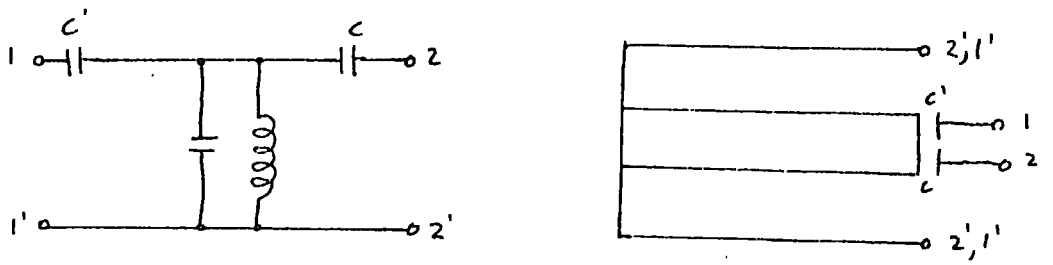

(c) Shunt inductive (direct) coupling:-

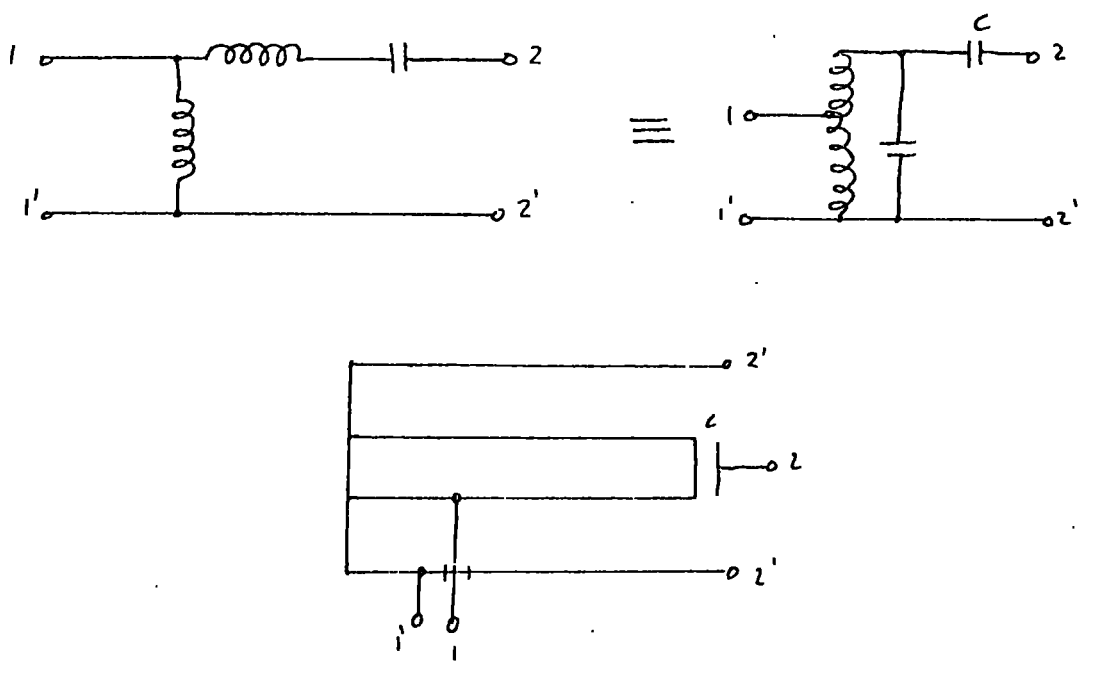

stored in each field will vary during the cycle, but their summation is always equal to the total energy content of the cavity[19]. If cavity loaded Q is reasonably high, the rate of stored to dissipated energy is high, and the average magnetic field density is equal to the average electric field density over a cycle. At two instants in the cycle the energy will be entirely in the field, and at two other instants the energy will be entirely in the electric field. With this knowledge we may calculate the total energy stored by finding the peak magnetic field energy. In a coaxial cavity, the magnetic field is created by the oscillatory currents flowing in the centre conductor, and if these currents can be calculated, the energy stored may also be found.

If we consider a resonant coaxial line of length x the energy stored in a segment is:-

$$\delta E = \frac{1}{2}(L\delta x)\hat{I}^2$$

where L = inductance per unit length

$\hat{I}$ = current flowing in segment.

Therefore, total energy stored in a length x is:-

$$E = \frac{1}{2} L \hat{I}_o^2 \int_o^2 \cos^2 \frac{2\pi x}{\pi_o} \, dx$$

$$= \frac{1}{4} L \hat{I}_o^2 \frac{\lambda_o}{2\pi} \left[\theta_o + \frac{1}{2} \sin 2\theta_o\right]$$

where λ_o = line wavelength

$\theta_o = \frac{2\pi x}{\lambda_o}$

$\hat{I}_o$ = current at node point on line.

But:- $L = \frac{Z_o}{\lambda_o f_o}$ where Z_o is characteristic line impedance, and f_o is frequency.

Therefore, $E = \frac{1}{4} \frac{Z_o}{2\pi f_o} \hat{I}_1^2 \left[\theta_o + \frac{1}{2} \sin 2\theta_o\right]$

Normally under resonant conditions θ_o is near $\frac{n\pi}{2}$ where n is an integer.

Therefore we can say

$$E \simeq \frac{nZ_o i_o^2}{8f_o} \quad .. \quad .. \quad .. \quad .. \quad .. \quad .. \quad .. \quad (4)$$

where i_o is the rms value of $\hat{I}_o$

2.7 Q Factor

The n factor of a resonator may be defined as

$$w_o \times \frac{\text{energy stored}}{\text{energy dissipated}}$$

The energy may be dissipated either in the losses inside the cavity or in the external circuit impedances to which the cavity is coupled. If there is no energy dissipated outside the cavity, the Q factor is known as the unloaded Q and is a measure of the energy dissipated in cavity losses. Obviously this factor cannot be measured directly since the introduction of energy into the cavity and the resultant measurements violate the condition of no external energy dissipation. In most circuits the cavity has a loaded Q value under working conditions which is usually several times lower than the unloaded value. This is to ensure that only a small fraction of the energy dissipated is lost in cavity losses, and the majority is available for use in the associated circuits. In the previous section we have calculated the energy stored in a short circuited transmission line of length $\frac{n\lambda}{4}$. To calculate the loaded Q factor we need to know the energy dissipated. We will assume that a negligible amount is lost in the cavity for practical convenience.

If the cavity is coupled to m external circuits of internal resistance R_1, R_2, R_3 .... R_m and in each circuit r.m.s. currents i_1, i_2, i_3, ... i_m are flowing, the total power dissipated will be:-

$$i_1^2 R_1 + i_2^2 R_2 + i_3^2 R_3 \ldots\ldots\ldots\ldots\ldots i_m^2 R_m$$

and the loaded Q value Q_L will be from equation (4):-

$$\frac{\omega_o \, n \, Z_o \, i_o^2}{8 f_o \, (i_1^2 R_1 + i_2^2 R_2 \ldots\ldots + i_m^2 R_m)} \quad .. \quad .. \quad .. \quad .. \quad .. \quad (5)$$

A special case of equation (5) is obtained if there is only one circuit coupled into the cavity or if there are two which are optimally matched to each other, and therefore dissipating the same amount of power. i.e.:-

$$Q_L = \frac{\pi \, n \, Z_o}{4 \, R_1} \left(\frac{i_o}{i_1}\right)^2 \quad .. \quad .. \quad .. \quad .. \quad .. \quad .. \quad (6)$$

(or half this value for two matched circuits).

Here we have ectracted the factor $\left(\frac{i_o}{i_1}\right)^2$ which may be regarded as the transformer ratio of the coupling to the cavity. This factor will later be used in coupling calculations for the end loaded cavity, and also as an aid in visualising equivalent circuits. In a lumped circuit i_o would be the current flowing through the inductance at resonate and i_1 the current flowing through the load. Thus $\left(\frac{i_o}{i_1}\right)^2$ is in effect the ratio of the energy stored to the energy dissipated in the load, and thus directly proportional to Q value.

3.0 Theory of the End Loaded Cavity

3.1 General

Of the many possible forms of coaxial transmission line resonator, the most common consists of a quarter wavelength (approximately) of line with one end short circuited and the other end open circuited. In the practical case, the open circuit end of the line has considerable short capacity due to fringing effects, and also radiation loss from this end must be taken into account. If the end of the cavity is screened to prevent this radiation loss, more shunt capacity is introduced, and the resonator now must be less than a quarter wavelength long (inductive) to resonate with the lumped end capacity.

By taking the end capacity not to earth but to an external connection, a different type of resonance response is produced. The associated equivalent circuit at and near reasonance is given in Fig.6. In the following chapter this resonance is taken to be the fundamental which occurs when the line is near to one quarter wavelength long. The next resonances are at three quarters wavelength and five quarters wavelength and so on. The effect of these higher resonances will be looked at in Section 3.4.

This then is the end loaded coaxial cavity, (Fig.6A) and there are two stages to the practical analysis of its behaviour as a circuit element. In the next section, the resonator is considered as a two terminal network, and in Section 3.3 an additional coupling is introduced to form a four terminal network.

3.2 Basic Relations

The lumped equivalent circuit of a cavity resonator is given in Fig.6B. This circuit meets all the requirements given

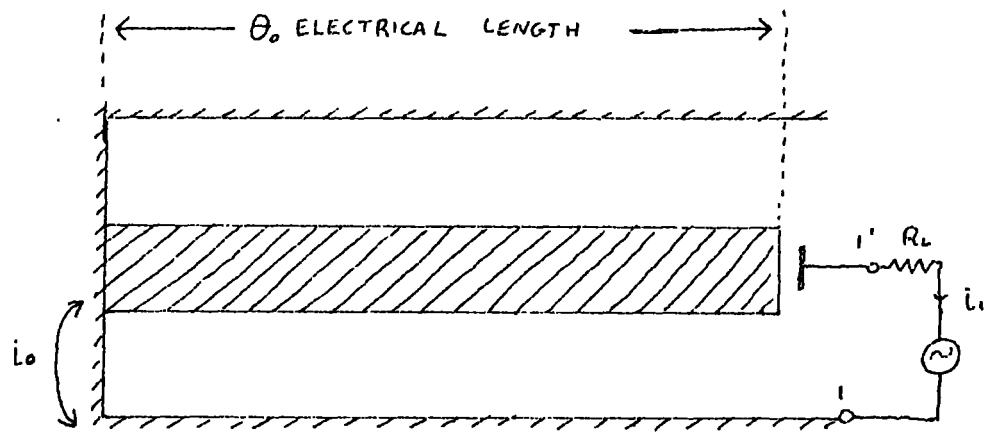

Fig. 6a Cavity fed by a voltage source

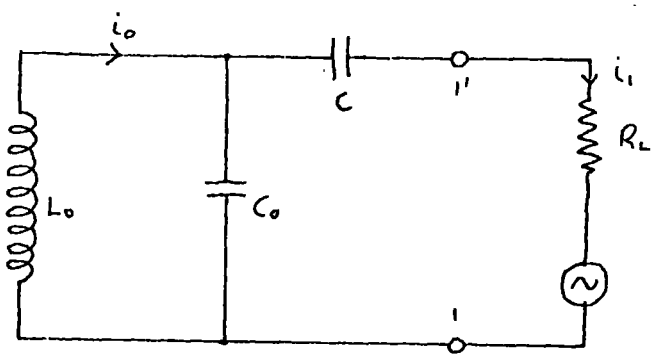

Fig. 6b Equivalent circuit of Fig.6a

in Section 2.4 for an equivalent circuit valid for frequencies in the vicinity of the fundamental resonance. From this circuit we can state the loaded Q at resonance:-

$$Q_L = \frac{\omega_o L_o}{R_L} \left(\frac{i_o}{i_1}\right)^2$$

From the stored energy in a cavity resonator, Equation (6), Section 2.7 gives the loaded Q in terms of cavity parameters. By equating these two values of Q_L and using the resonant frequency relationships, we can find a value for $\left(\frac{i_o}{i_1}\right)^2$ in terms of R_L and the cavity parameters. If we substitute this value back into Equation 6 and simplify the result by considering values of Q_L greater than one:-

$$Q_L = \frac{4Z_o \tan^2\theta_o}{\pi R_L} \quad \text{assuming } Q_L > 1 \quad .. \quad .. \quad .. \quad (7)$$

This calculation is covered in Appendix 4.

We now add a second coupling to the cavity. By finding the current flowing at resonance in the second load with respect to i_o, we may use the value of $\left(\frac{i_o}{i_1}\right)^2$ we have just found to determine the modified Q_L value of the resultant, and also the input to output matching conditions. This will now be done for three common forms of coupling.

3.3 Input Coupling

3.3.1 Loop Coupling

A coupling loop is inserted into the cavity at an electrical length ϕ degrees at resonance from the shorted end (Fig.7A). The lumped equivalent circuit (Fig.7B) is a transformer of turns ratio $\left(\frac{i_o}{i_2}\right)$ This circuit is redrawn as a T-equivalent and condensed by using Thevenins theorem (Fig.7D). The values of Re and Xe in this equivalent circuit may be found in terms of Rs, the mutual and the primary inductance values.

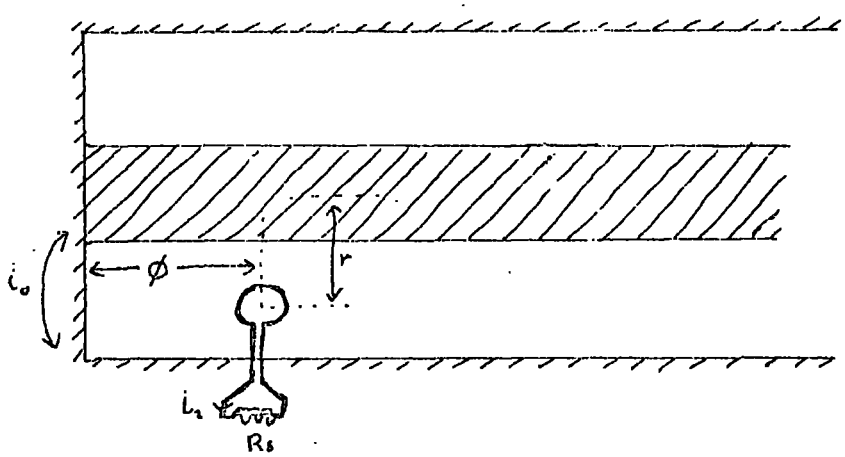

Fig. 7a Loop area A inserted in cavity

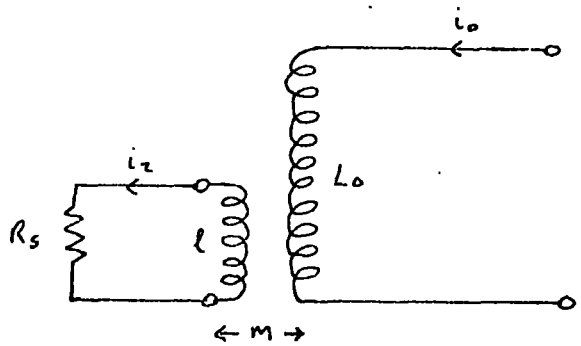

m = mutual inductance

ℓ = loop inductance

Fig. 7b Lumped equivalent circuit

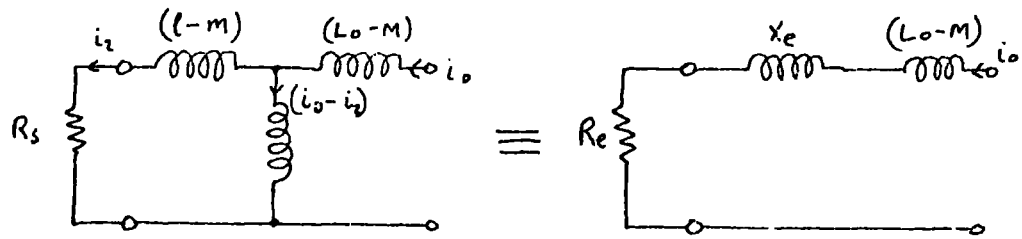

Fig.7c, 7d equivalent circuits of Fig. 7b.

Since the loop is entirely enclosed by the cavity it can be assumed that the coupling coefficient approaches unity. Also in the practical case, the ratio $\left(\frac{i_o}{i_2}\right)$ will be greater than unity. This allows certain simplifications in the equations for Re and Ze, which are given in Appendix 2. Since the loop will enclose a relatively small area of the total cavity, it can be assumed to lie in an area of constant magnetic flux density H. The mutual inductance M can then be found since:-

$$M = \frac{A \mu_o H}{i_2}$$

Therefore $$X_m = \frac{A \mu_o \omega_o \cos\phi}{2\pi t} \left(\frac{i_o}{i_2}\right)$$

in MKS units where μ_o is the permeability of free space ($= 4\pi \times 10^{-7}$).

The equivalence of Figs.7B and 7D means that the same power must be dissipated in Re and Rs.

Therefore $i_o^2 Re = i_2^2 R_S$ and Appendix 2 gives $Re = \frac{Xm^2}{R_S}$

So finally $\frac{i_o}{i_2}$ may be stated in terms of Rs, the resonant frequency and the loop physical dimensions.

$$\frac{i_o}{i_2} = \frac{R_S}{2A \omega_o \cos\phi \times 10^{-7}} \quad .. \quad .. \quad .. \quad .. \quad .. \quad (8)$$

For an optimum match between input and output of the four terminal resonator (Fig.8):-

$$i_1^2 R_L = i_2^2 R_S \text{ , i.e. } \frac{R_s}{R_L} = \left(\frac{i_1}{i_o}\right)^2 \left(\frac{i_o}{i_2}\right)^2$$

Substituting from Equation 8 for $\left(\frac{i_o}{i_2}\right)$ and the value of $\left(\frac{i_o}{i_1}\right)$ from Section 3.2

$$R_L/R_S = \left(\frac{A \cos\phi}{t}\right)^2 \left(\frac{4 \omega_o \times 10^{-7}}{\pi}\right)^2 \left(\frac{4Z_o \tan^2\theta_o - 4R_L \tan\theta_o + R_L\pi}{Z_o}\right)$$

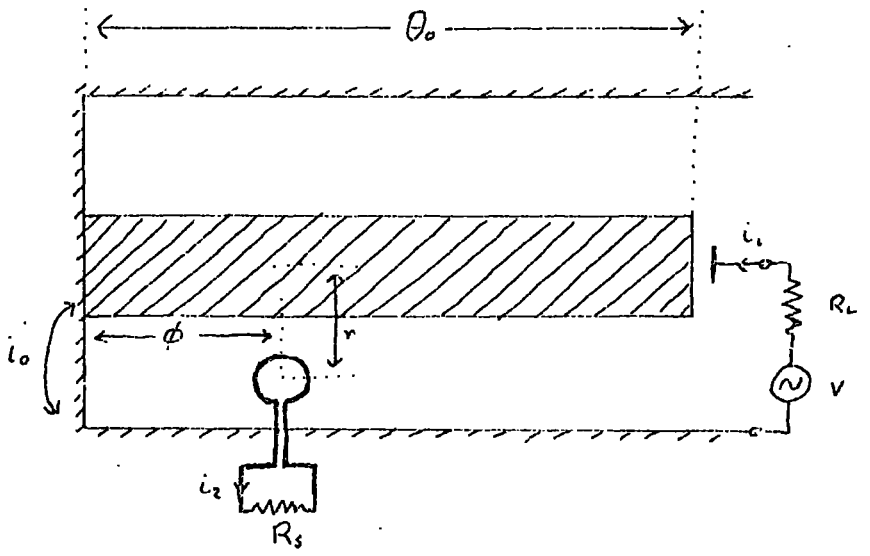

Fig. 8 A loaded series-resonant cavity

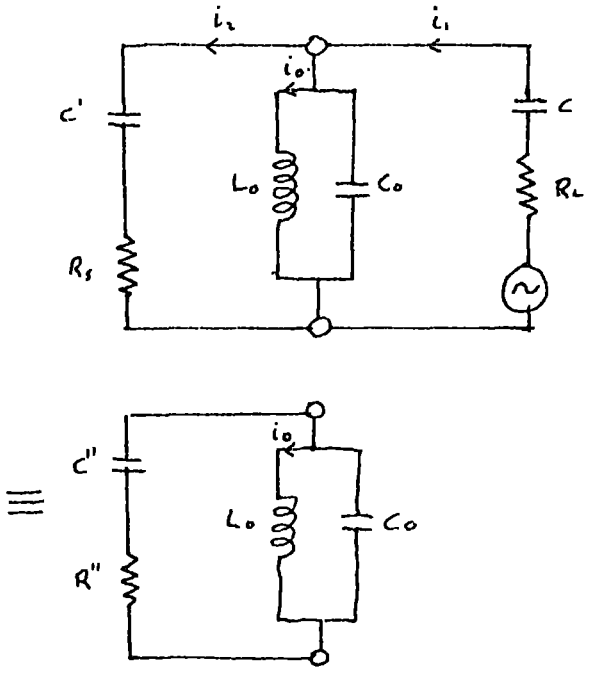

Fig.9 Probe coupling equivalent circuits

The "loop constant" $\frac{A\cos\phi}{r}$ may be put into a more practical equation by using the value of Q_L from Equation 7:-

$$\frac{A\cos\phi}{r} = \frac{1}{4\omega_o \times 10^{-7}} \sqrt{\frac{\pi R_s Z_o}{Q_L}} \quad .. \quad .. \quad .. \quad (9)$$

3.3.2 Probe Coupling

The end loading of this type of cavity is, in itself, a form of heavily overcoupled capacitive probe. The best way to treat an additional coupling is by combining it with the first branch in parallel. The combined branch components can then be used in the equations of Section 3. Fig.9 shows how this may be done but in the general case this combination of branches will produce an unmanageable expression for the resultant components. If we can make one of two simplifying assumptions, however, the currents flowing in each of the branches can be taken to be in phase. The assumptions are that : either $Q_L >> 1$, or that the load resistances are of a similar value. Taking this to be the case, the expressions for R" and C" are as follows:-

$$C'' = C + C'$$

$$R'' = R_L \left(\frac{C}{C+C'}\right)^2 + R_S \left(\frac{C'}{C+C'}\right)^2$$

For an optimum match between R_L and R_S:-

$$\frac{R_L}{R_S} = \left(\frac{C'}{C}\right)^2$$

Under which conditions:-

$$R'' = 2R_L \left(\frac{C}{C+C'}\right)^2 = 2R_S \left(\frac{C}{C+C'}\right)^2$$

And $$Q_L' = \frac{4Z_o \tan^2 \theta_o}{\pi_1 R''} - \frac{4\tan \theta_o}{\pi} + 1$$

Where $$\tan \theta_o = \frac{1}{\omega_o Z_o C''}$$ (Resonance Condition).

3.3.3 Direct Coupling

Direct coupling may be looked upon as a limiting case of loop coupling. In the usual form a radial tap is made on to the centre conductor of the cavity (Fig.10A). The auto-transformer type of equivalent circuit (Fig.10B), can be treated exactly as the transformer case was in Section 3.3.1. The area of the magnetic flux enclosed by the tap is that between the tap and the short circuited end of the cavity, bounded by the outer wall and the inner conductor. This area cannot be assumed to have constant flux density as was taken to be the case for the loop case. Integration is therefore required in the calculation for Xm. This calculation is done in Appendix 3 and Fig.10B shows the method used.

Once the value of Xm is obtained, the method of calculations follows exactly as for the loop case. The only difference is that the coupling constant can be defined simply as $\sin \phi$, and other simplifications are possible. Appendix 3 also gives these, and the result is:-

$$\text{Sin } \phi = \sqrt{\frac{R_s \pi}{4Z_o Q_L}}$$

Under optimum match conditions.

3.4 Spurious Responses

The fundamental resonant frequency of the cavity will be given by:-

$$f_o = \frac{1}{2\pi C \tan \theta_o}$$

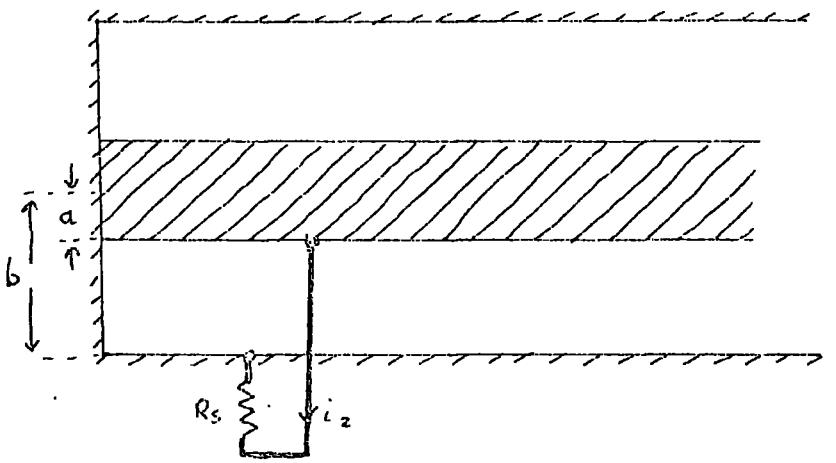

Fig. 10a Direct coupled cavity

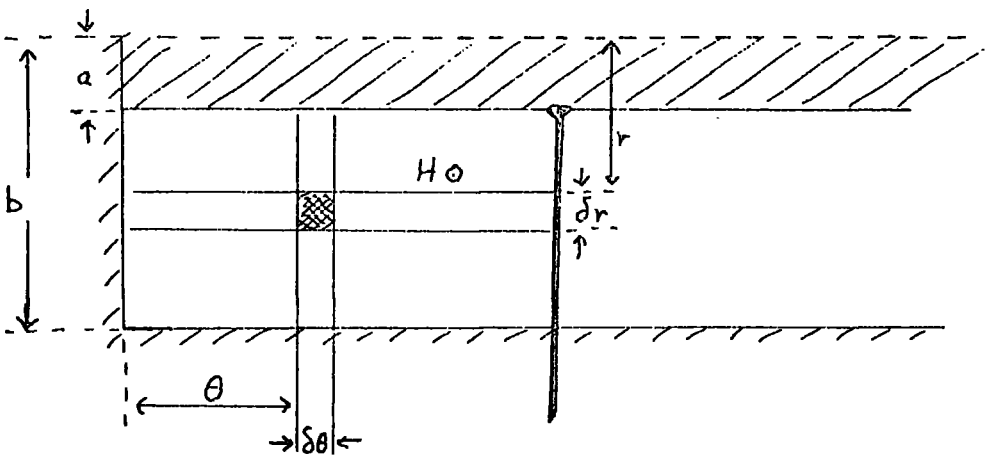

Fig. 10b Showing the magnetic flux density integration

from the transmission line equations. The addition of the second coupling will introduce a small error (δf_o) in f_o due to perturbations of the normal cavity field distribution:-

$$\frac{\delta f_o}{f_o} = + \sqrt{\frac{X_m^3}{X_{L_o} (R_s^2 - X_m^2)}}$$

i.e. upwards in frequency.

This effect is small except for low values of Q_L, where the deviation is of less importance anyway. In most practical cases stray reactance will have a greater effect.

The second resonance of the cavity will occur when the length is approximately $\frac{3\lambda_o}{4}$. The energy stored (eqn.4) will be three times as great as for the fundamental, but the Q_L will be about one third of the fundamental value, due to the modified value of $\omega_o C$. In the case of the loop and direct couplings, this will cause a mismatch between input and output, the extent of which is generally increased by the coupling parameters which also vary with frequency. It is, in fact, theoretically possible to physically arrange these couplings so that no coupling will occur for a selected higher resonance. This could be arranged, for instance, by positioning a loop coupling at a current antinode of the higher resonance.

This type of cavity, then, offers a certain degree of control over the spurious higher resonances, and since the lowest of these occurs at nearly three times the fundamental frequency, they may be ignored in many practical cases.

4.0 Practical End Loaded Cavity

4.1 Basic Design and Construction

The cavity drawn in Fig.11 was built to test the practical accuracy of the end loaded system. The characteristic impedance (Z_o)

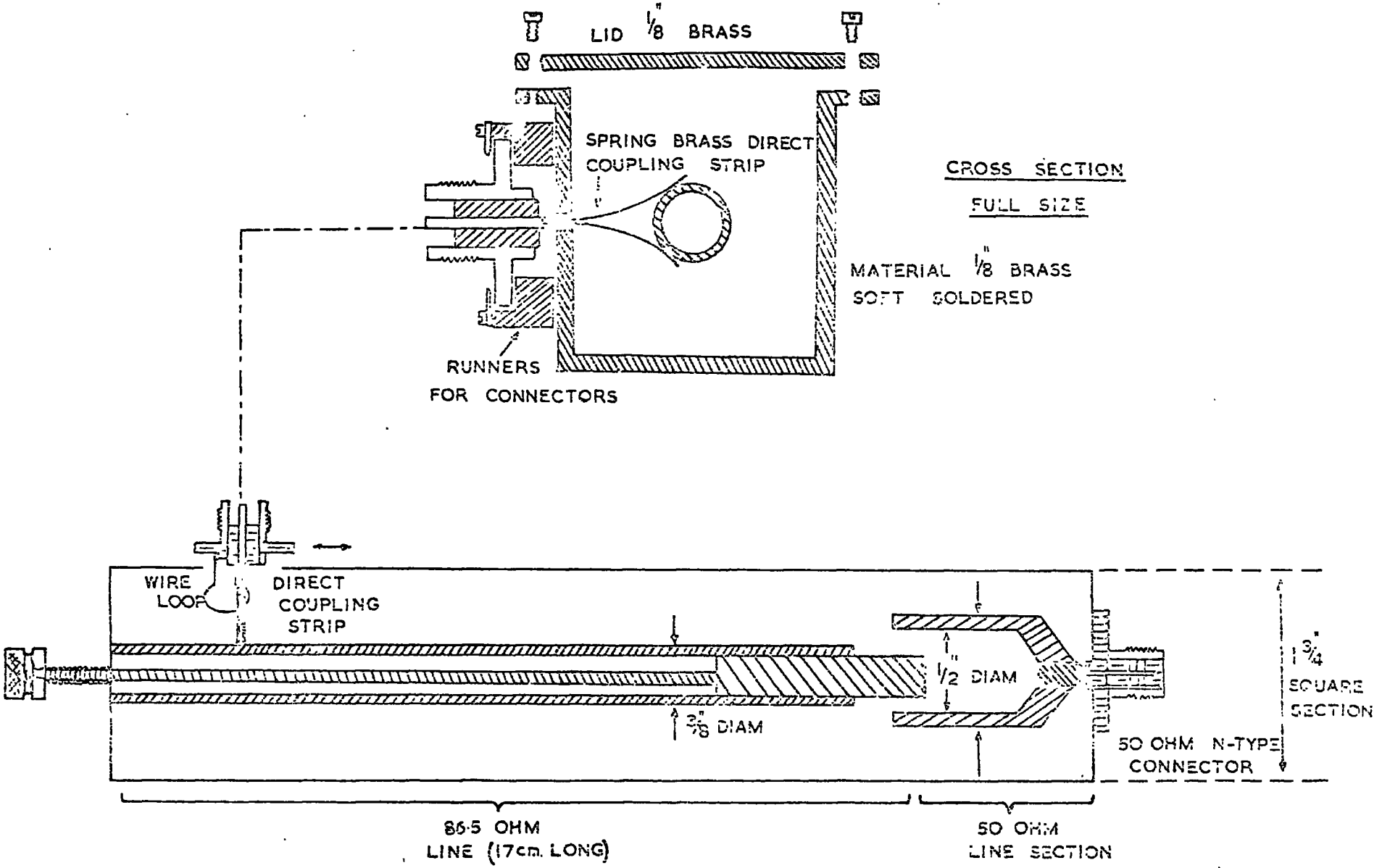
LID 1/8" BRASS
SPRING BRASS DIRECT COUPLING STRIP
CROSS SECTION
FULL SIZE
MATERIAL 1/8" BRASS SOFT SOLDERED
RUNNERS FOR CONNECTORS
WIRE LOOP
DIRECT COUPLING STRIP
1/2" DIAM
3/8" DIAM
1 3/4" SQUARE SECTION
50 OHM N-TYPE CONNECTOR
86·5 OHM LINE (17cm. LONG)
50 OHM LINE SECTION

FIG 11A.

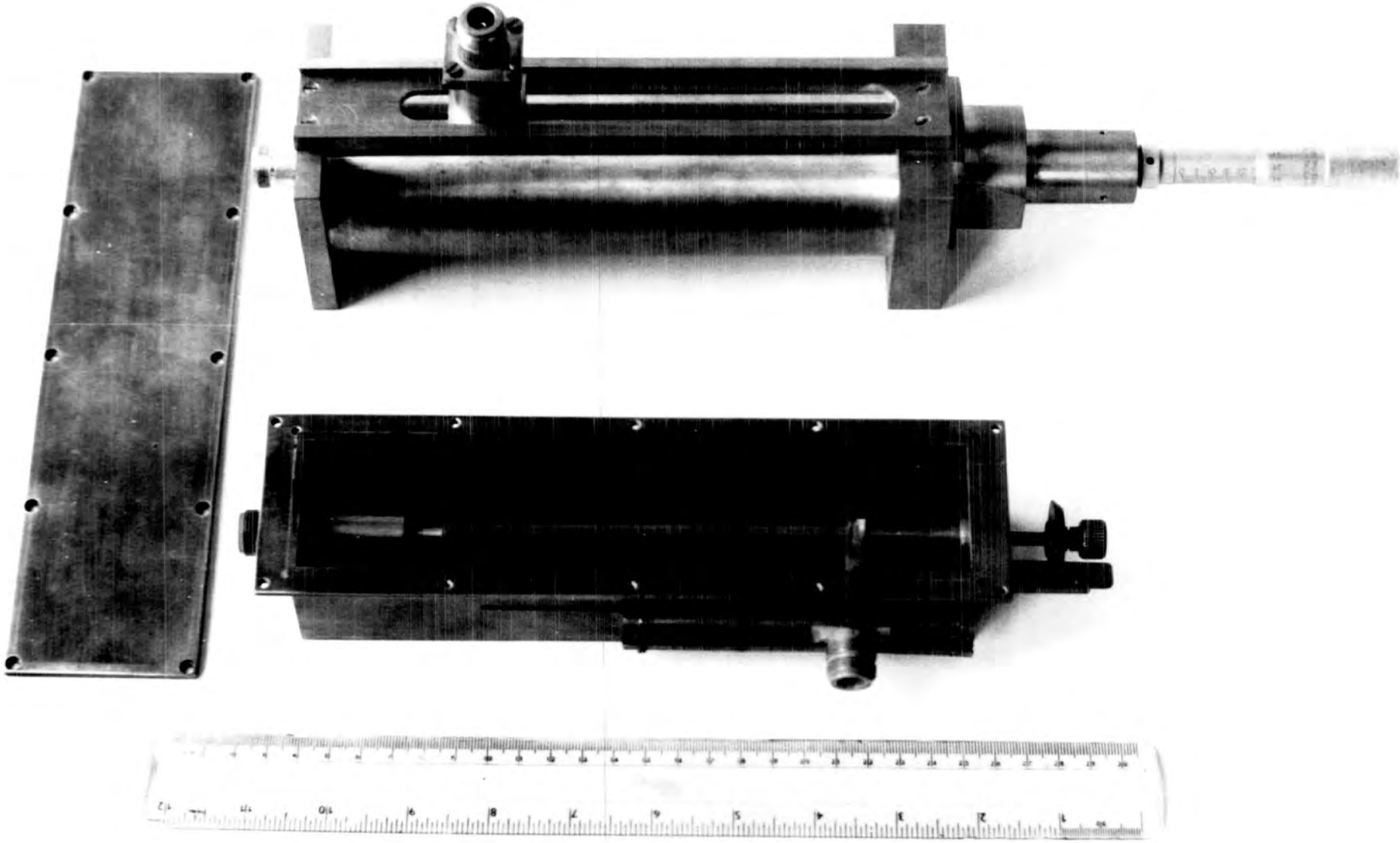

Fig. 11b Two xperimental 400 MHz Cavities

was 86.5 ohms, chosen for low loss and dimensional convenience.

The length of the inner conductor was 17 cm giving an approximate resonant frequency of 400 MHz. The end capacity C was adjustable between 0.35 and 10 picofarads and could be set to an accuracy of 0.05 p.f. using a dial on the plunger adjusting screw. While R_L and R_S values were limited to 50 ohms by the ancilliary coaxial equipment available, the value of θ_o (the electrical cavity length at resonance) could be varied by changing the frequency used. The coupling was inserted into the cavity through a longitudinal slot. This slot was placed where it lay parallel to the circulation currents flowing along the inside walls of the cavity. In this position it caused no appreciable energy leakage from the cavity, whilst the coupling could be easily moved along the length of the slot.

4.2 Measuring Techniques

Apart from physical dimensions the chief measurements to be made are those of frequency and attenuation. The circuit Q may be found by the half-power-points method, and the optimum match conditions determined by finding the point of minimum insertion loss of the filter arrangement. This minimum value of insertion loss, in conjunction with the loaded Q, gives the unloaded Q of the cavity, which is a measure of the internal cavity loss:-

$$\text{Min Insertion loss} = 20 \log_{10} \left(1 - \frac{Q_L'}{Q_o} \right) \text{ (in dB)}$$

The attenuation is derived from power measurements made in a 50 ohm system using a thermistor type of power meter.

By measuring the centre conductor length in the cavity with the plunger fully withdrawn, a value can be obtained from the resonance

relationship for the residual value of the end capacity C:-

$$C = \frac{1}{\omega_o Z_o \tan \theta_o}$$

where ω_o is the resonant angular frequency. The accuracy of this resonant frequency was checked using a cavity frequency meter on the harmonics produced by the source, enabling a large degree of accuracy to be obtained.

With a value for the residual and capacity, the capacitor can be fully calibrated (Fig.12) using a low frequency bridge method. The value of θ_o, the electrical length of resonance, can then be found from the value of C at resonance and the frequency. This method of finding θ_o eliminates errors that could occur in estimating the actual physical length of the inner conductor when part of it is forming the end capacitor. Since θ_o occurs in the Q_L equation as $\tan^2 \theta_o$ errors in this near to 90^o are quite important. A plot of $\omega_o C$ against θ_o is given in Fig.13 for several values of Z_o.

4.3 Experimental Results

4.3.1 Loop Coupling

Initially the cavity loaded Q was measured in terms of θ_o at resonance. The input coupling was very light, consisting of a loop which was small enough for its loading effect on the cavity to be ignored (except at very high Q values). The Q_L value was then measured by the half power points method, for values of $\omega_o C$ corresponding to values of θ_o from 74 to 84 degrees, giving Q_L values from 20 to 300. Since the input coupling was very light, the theoretical values of equation (7) should be closely followed. Fig.14 is a theoretical plot of Q_L against θ_o for several values of $\frac{Z_o}{R_L}$, and Fig.15 gives this plot for the experimental cavity and results for seven experimental loops are given in Fig.16.

Figure 12

End Capacity vs Dial Setting
For Experimental Cavity

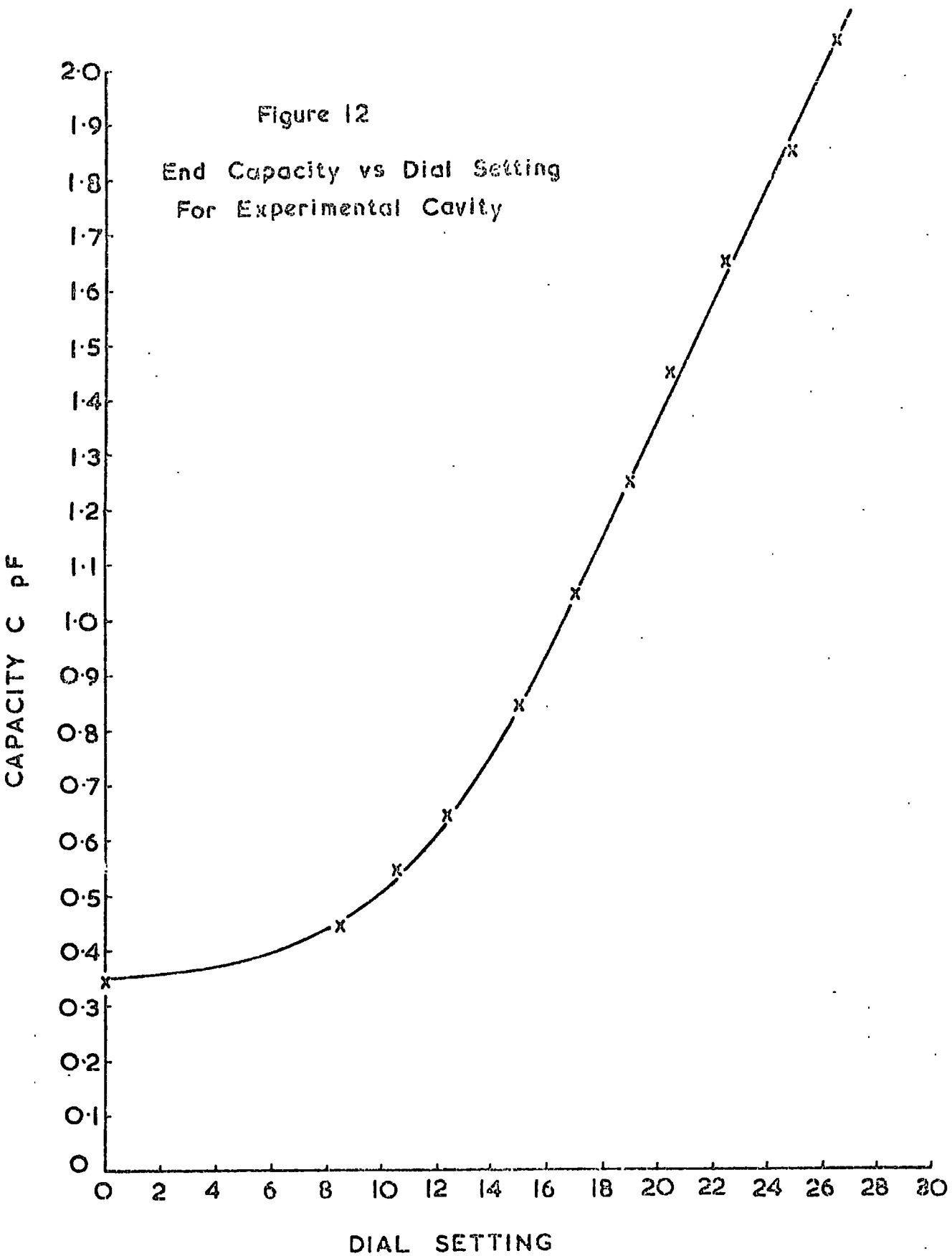

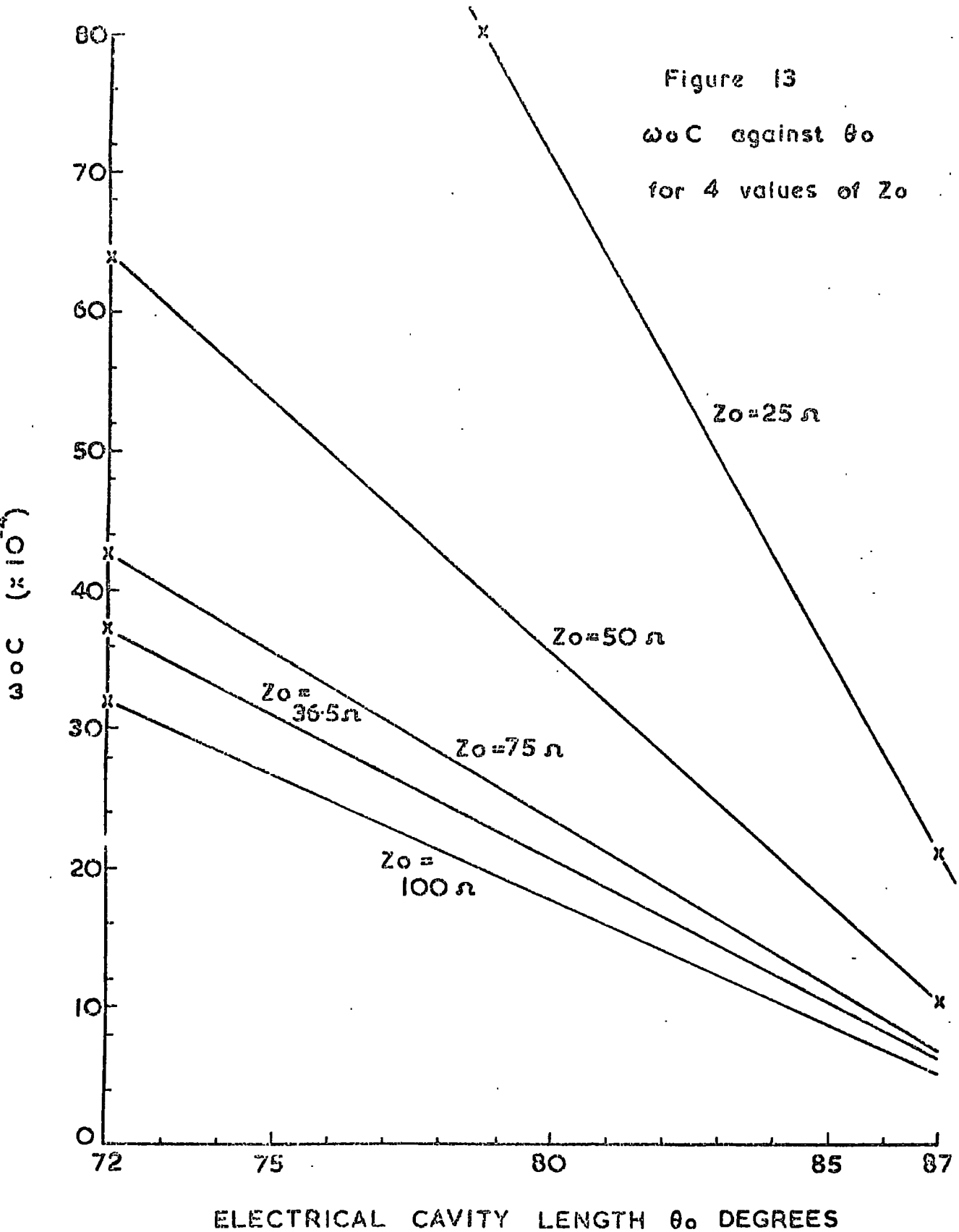

Figure 13

ωoC against θo

for 4 values of Zo

Figure 14

Q_L vs θ_o FOR 3 VALUES OF $\frac{Z_o}{R_L}$

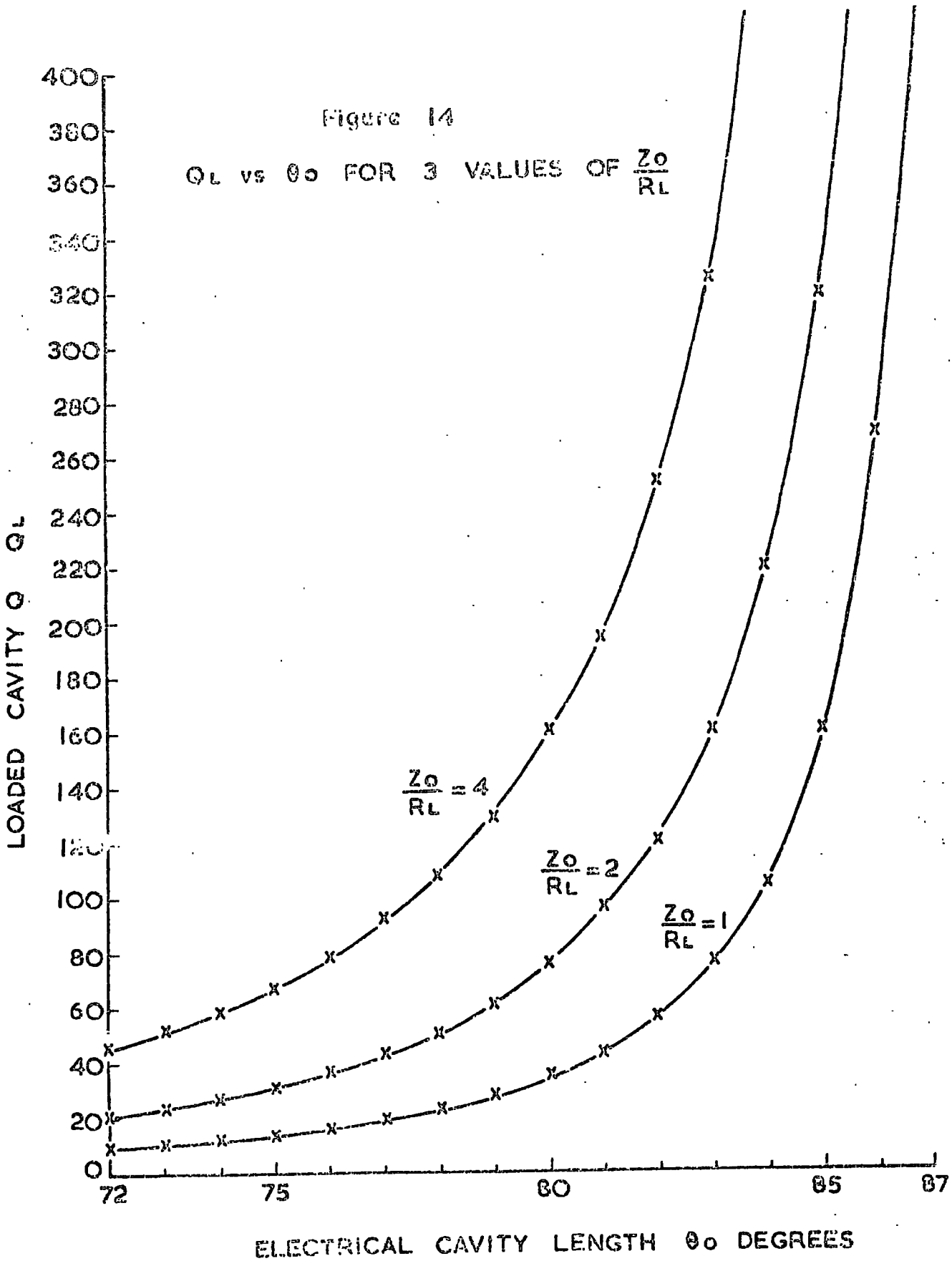

Figure 15

Theoretical Q_L and Experimental points

for Experimental Cavity $Z_o = 66.5\,\Omega$ $R_L = 50$

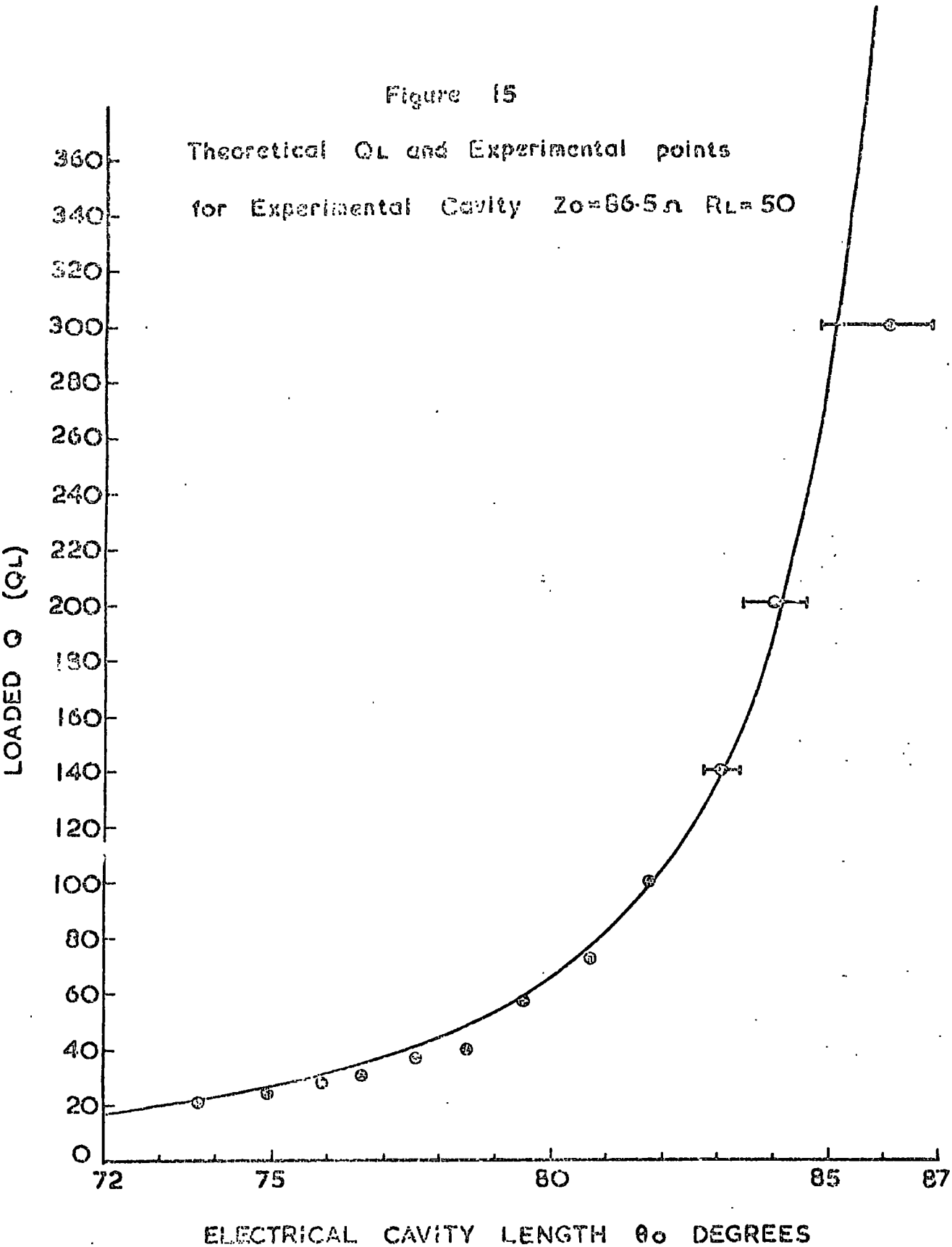

Figure 16

Q_L Against Loop Constant $\frac{A \cos \phi}{V}$

(For $R_L = R_S = 50\,\Omega$, $Z_o = 86{\cdot}5$, $\omega_o = 2{\cdot}5 \times 10^9$)

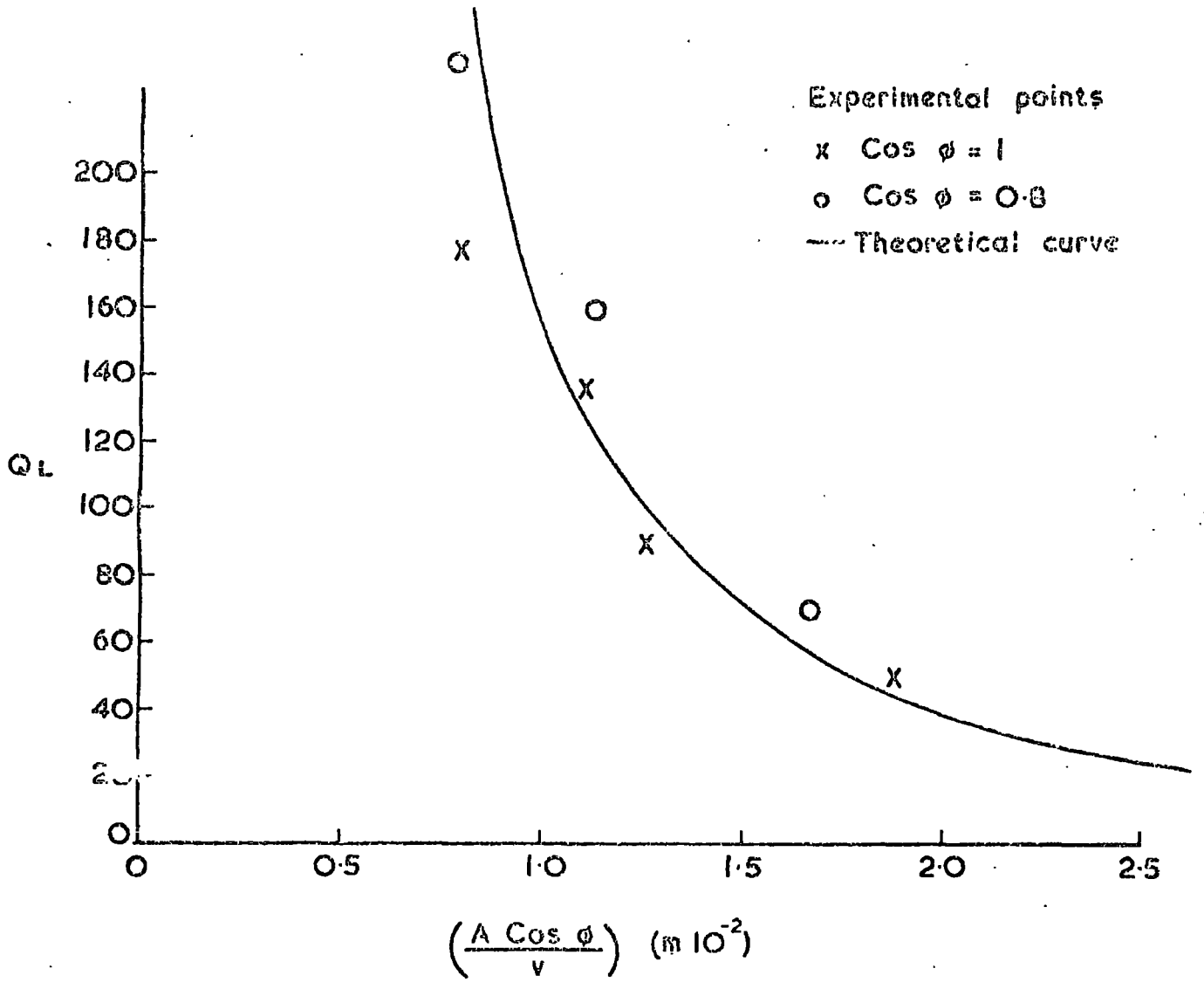

4.3.2 Probe Coupling

The experimental cavity used was not designed for probe coupling, since it proved difficult to use two variable end capacities without stray reactances and undesirable coupling being introduced directly between input and output. However, results already obtained (Fig.15) correspond to those that would be produced for a combined input, output branch as described in Section 3.3.2.

4.3.3 Direct coupling

In the experimental model the coupling consisted of a radial link to the inner conductor, positioned at an electrical distance ϕ degrees from the short circuited end of the cavity. This angle is the only value needed to define the coupling parameter, and a graph is plotted in Fig.17 of Q_L against ϕ for the fixed values of Z_o, Rs and R_L used. Experimental points are compared to the theoretical curve for values of from 2.5^o to 12^o, the lower values being associated with increasing measurement uncertainty due to the finite size of the coupling link.

5.0 Evolution of the Balanced Double Cavity System

5.1 Balanced System

Two identical end loaded cavities can be used in a balanced system if the currents flowing in the centre conductors are in anti-phase. This infers identical input couplings fed in antiphase. The usual way of introducing this condition at the input ports is to use a difference in line length to the two inputs of $\lambda/2$ electrical length at the resonant frequency of the system. The phase shift introduced is therefore frequency dependent, so that inphase components

Figure 17

Q_L Against ϕ (Direct Coupled Case)

For $R_L = R_s = 50\,\Omega$ $Z_o = 86{\cdot}5\,\Omega$

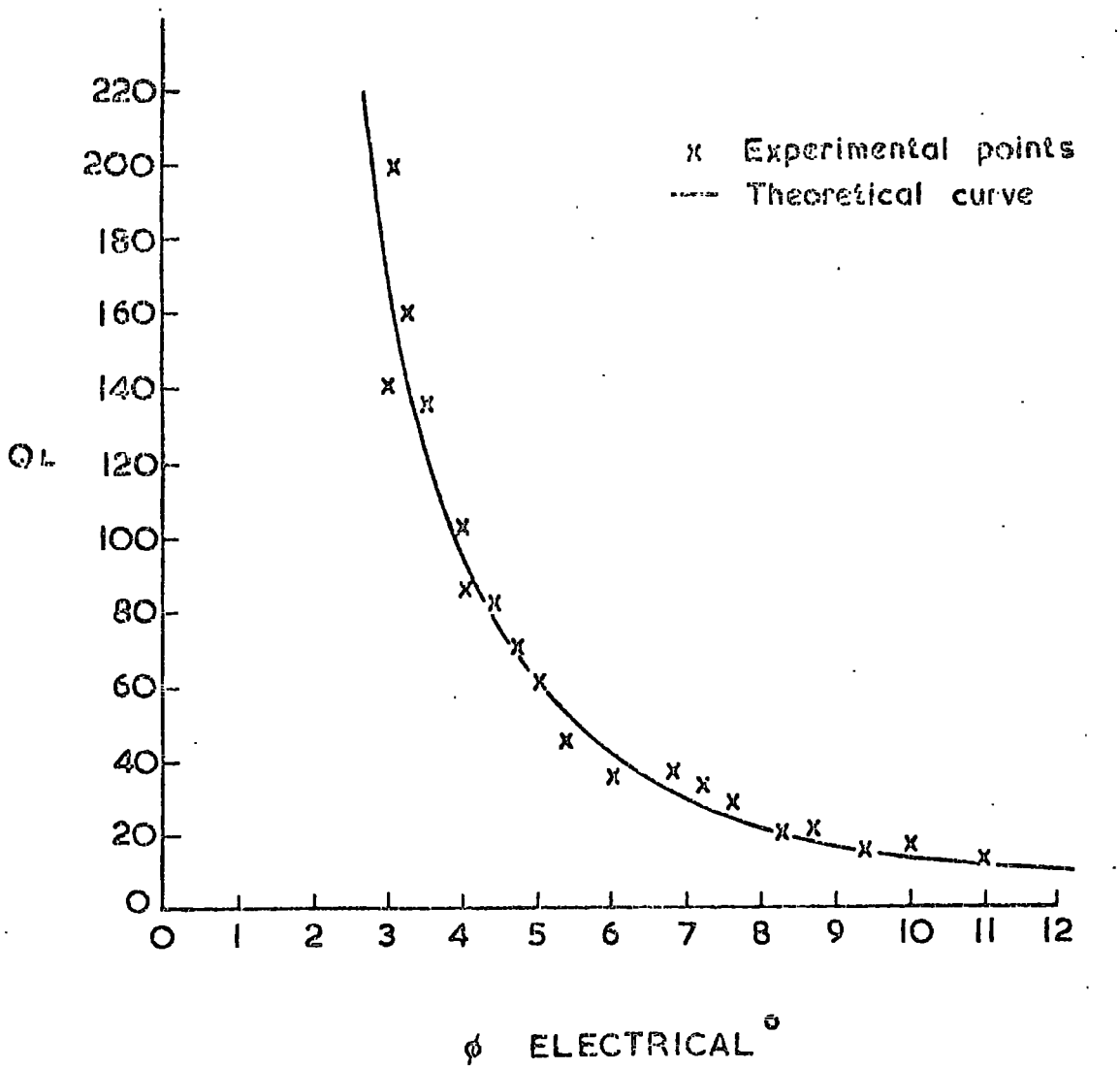

introduced from the cavities will only cancel if the frequency happens to be an odd multiple of the input frequency.

This is not good enough for application to devices such as balanced mixers, where a frequency independent method of cancellation is often required.

Study of Fig.7 indicates a possible solution to the problem of creating a frequency independent phase reversal at the input of an end loaded cavity. If the coupling loop has its sense of rotation reversed, the phase of i_2 is reversed, producing the correct phase reversal of i_o which is required. The final arrangement of this system is shown in Fig.18. The two identical cavities lie side by side and the input coupling consists of a symmetrical figure of eight loop, the actual input being at the centre of the "8" created. Theoretically, the dividing wall between the cavities is not needed, as examination of the current flow will indicate. In practice, of course, slight differences in manufacture give varying stray reactance values which cause unbalance. A useful adjustment to correct this unbalance is provided by the variable tuning capacitance. As an example, the response of a pair of cavities is superimposed in Fig.19. Here the passband at 4.48 GHz is little affected by mistuning to provide a null rejection at 4.55 GHz.

5.2 Application to a 4.5 GHz Mixer

The type of mixer under consideration required three main functions of the input passive circuit. They are:-

(1) Unbalanced to balanced transformation of the signal input, also balanced at the local oscillator frequency.

(2) Impedance matching between signal source and the input impedance of the mixer.

(3) Image rejection.

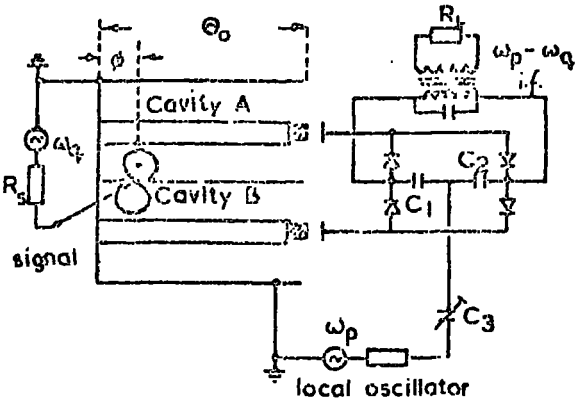

Fig. 18 Diagrammatic Representation of a 4·5 GHz Lattice Mixer.

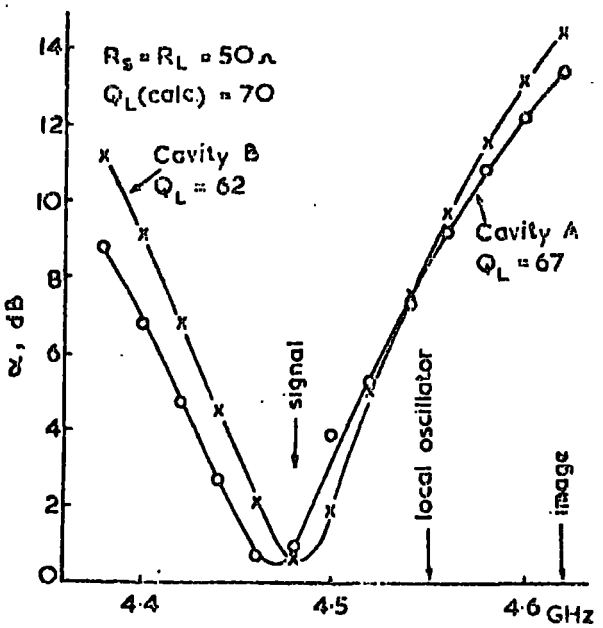

Fig.19. Transfer Charac's of Cavities

In Fig.20 a lumped component solution is shown, but with conventional techniques, the losses inherent in this type of circuit increase greatly above 1 GHz, due partly to radiation from the components which approach the size of the operational wavelengths. A conventional microwave solution using stripline or coaxial techniques would consist of:-

(1) A Rat-race; (2) Two filters; (3) Two matching sections. Although the loss of each component would be quite low, the combined loss would be high. More important would be the difficulty of adjustment of such parameters as impedance matching and the balance of the system. These adjustments are necessary because of diode production spreads, which are not as extreme with Schottky-barrier diodes as with point-contact, but nevertheless trimming adjustments are essential for peak performance. The balance of the Rat-race component depends on phase cancellation at the input port, this in turn is decided by physical lengths which are difficult to adjust and are frequency dependent, as mentioned in the previous section. Another problem with this type of input circuit is size. Whereas a lumped component version should be smaller than a tenth of a wavelength, the distributed transmission system has to be several wavelengths long in total. Even using high dielectric constant substrates to reduce the effective guide wavelength, the result may be too large for some applications, especially at low frequencies.

The end loaded cavity is a composite structure which combines several functions and easy adjustments. The semi-distributed circuit is best analysed from lumped equivalent circuits rather than Maxwell's theorems and boundary conditions as would be used for waveguide cavities. Appendix 2 obtains the reactance response of an end loaded cavity, valid for frequencies in the region of the primary resonance

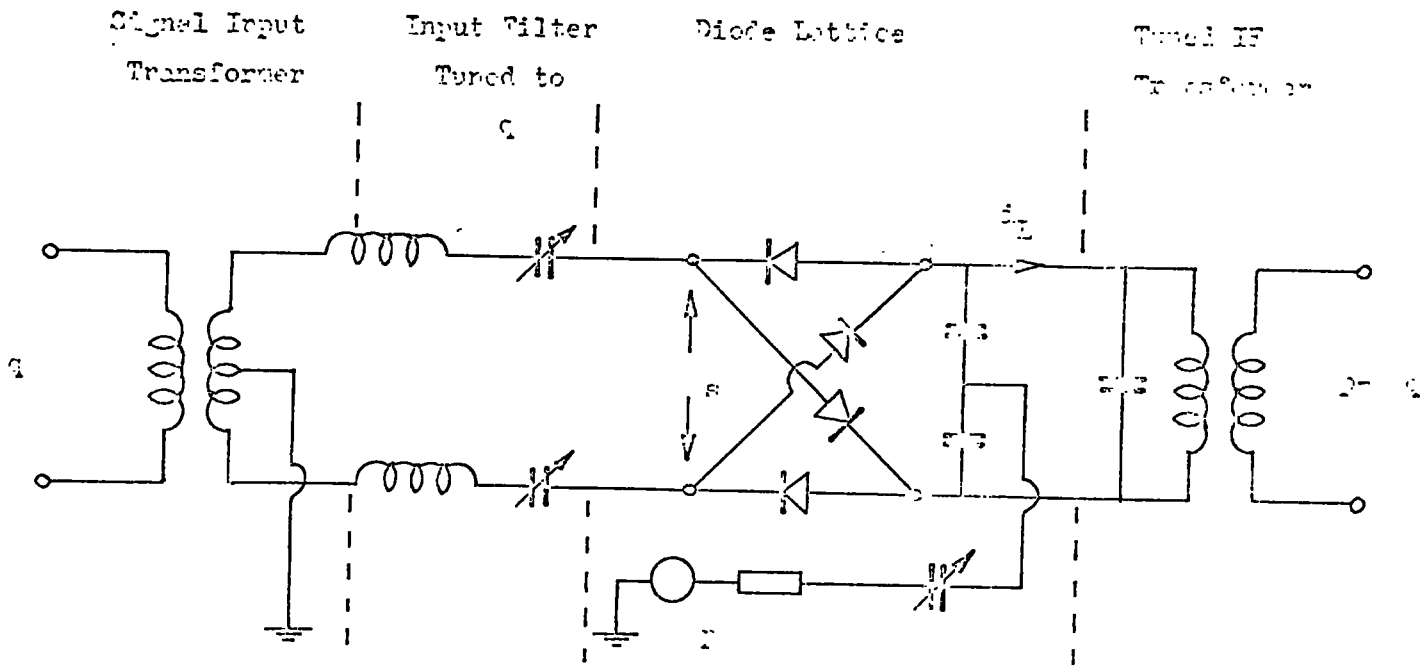

Series Tuned
Local Oscillator Source

Fig 20 Basic Lumped Component Lattice Mixer Circuit

which is used. The reactance response, as shown in Fig.21, is suited to the image rejection mixer. The image rejection is controlled by the loaded Q value, whilst input matching to the diode quad depends on the coupling values used. Three dimensional mixer symmetry can be arranged as shown diagramatically in Figs. 22 and 23, and in prototype form, Figs. 24 - 28. The cavity is designed to be assembled with joints along current flow lines wherever possible, thus performance should be unaffected by tightness of screws etc. For similar reasons the coupling loop is assembled as one piece, and there is no current flow between it and the cavity block. The usual machining precautions and silver plating are applied in order to reduce the losses; full details are given in Ref.20.

5.3 Results

Figs. 22 and 23 show dimensional drawings of the cavity block and the diode/I.F. substrate. Instead of this diode substrate, a dummy test substrate (Fig.29) can be fitted in order to simulate a 100 ohm balanced load. Using a typical test circuit shown in Fig.30, cavity performance may be carried out. The results given in Fig.19 were obtained using this test arrangement and gross unbalanced or assembly faults easily detected before mixer assembly. As a guide to cavity performance, losses of 0.4 dB per cavity are normally obtained at 4.5 GHz with an image rejection of 10 dB, 140 MHz away from resonance. The loss formulae given in Section 4.2 hold for the cavity just as for a lumped resonant circuit. The loss obtained with this formula, should have a small excess added, to account for the attenuation caused by the connections. It was decided to obtain an estimate of the total cavity loss in preparation for possibly

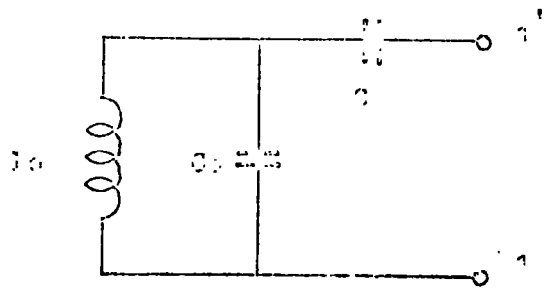

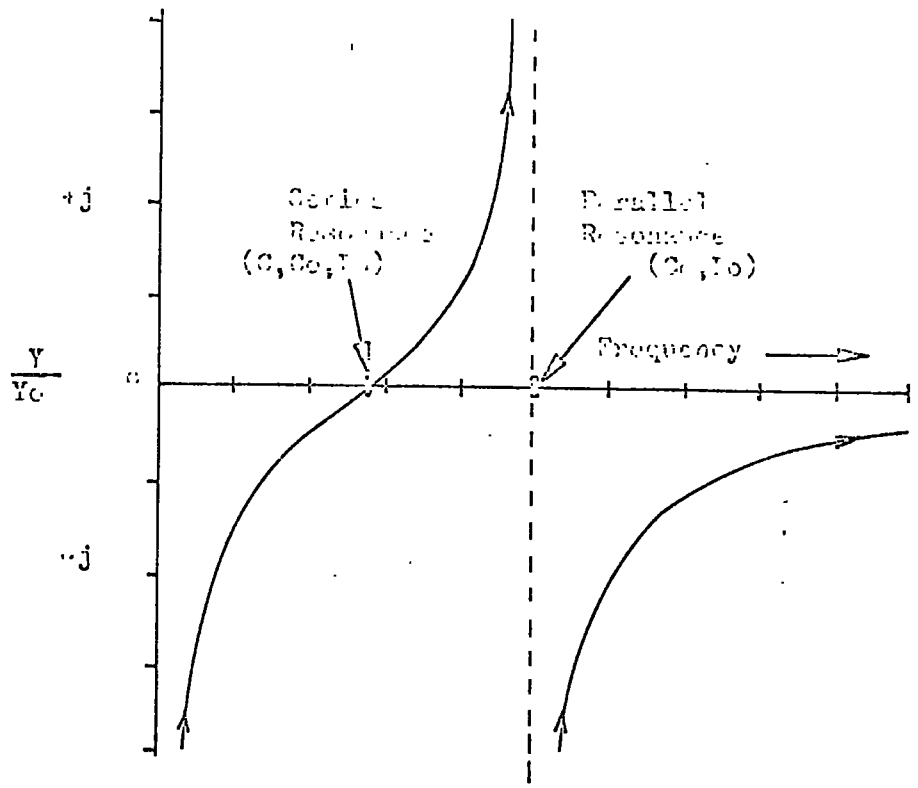

Fig 21 Cavity Reactance Response

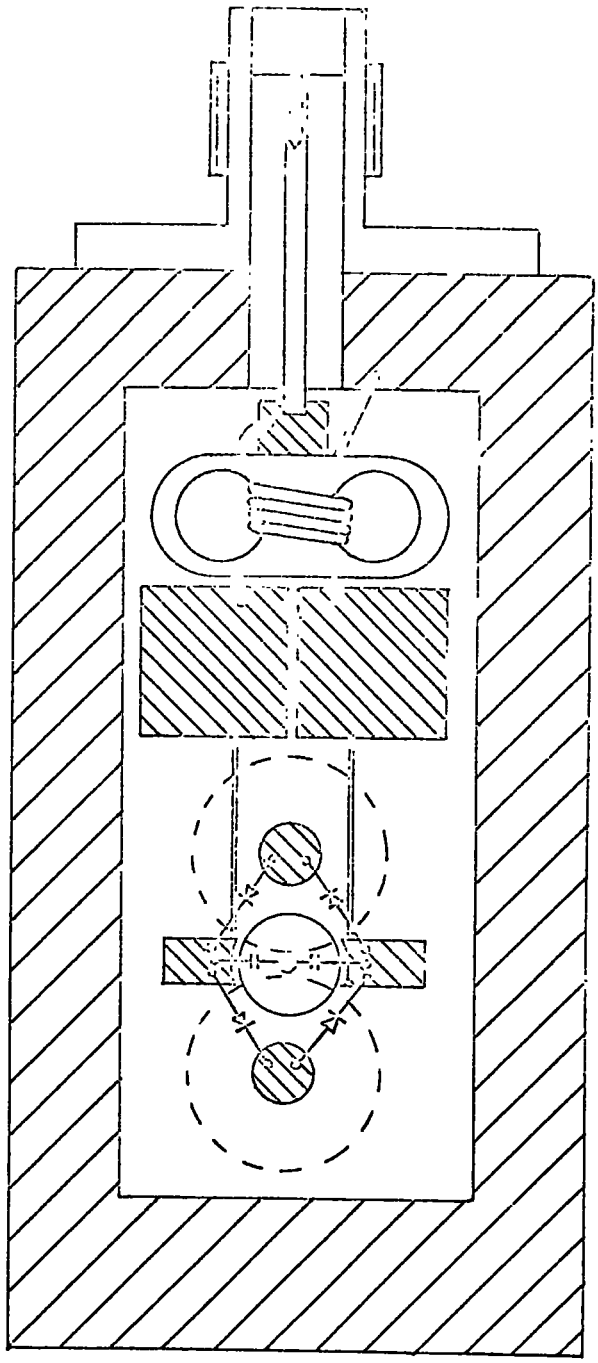

Fig. 22 To View 5.5 GHz Mixer Cavity

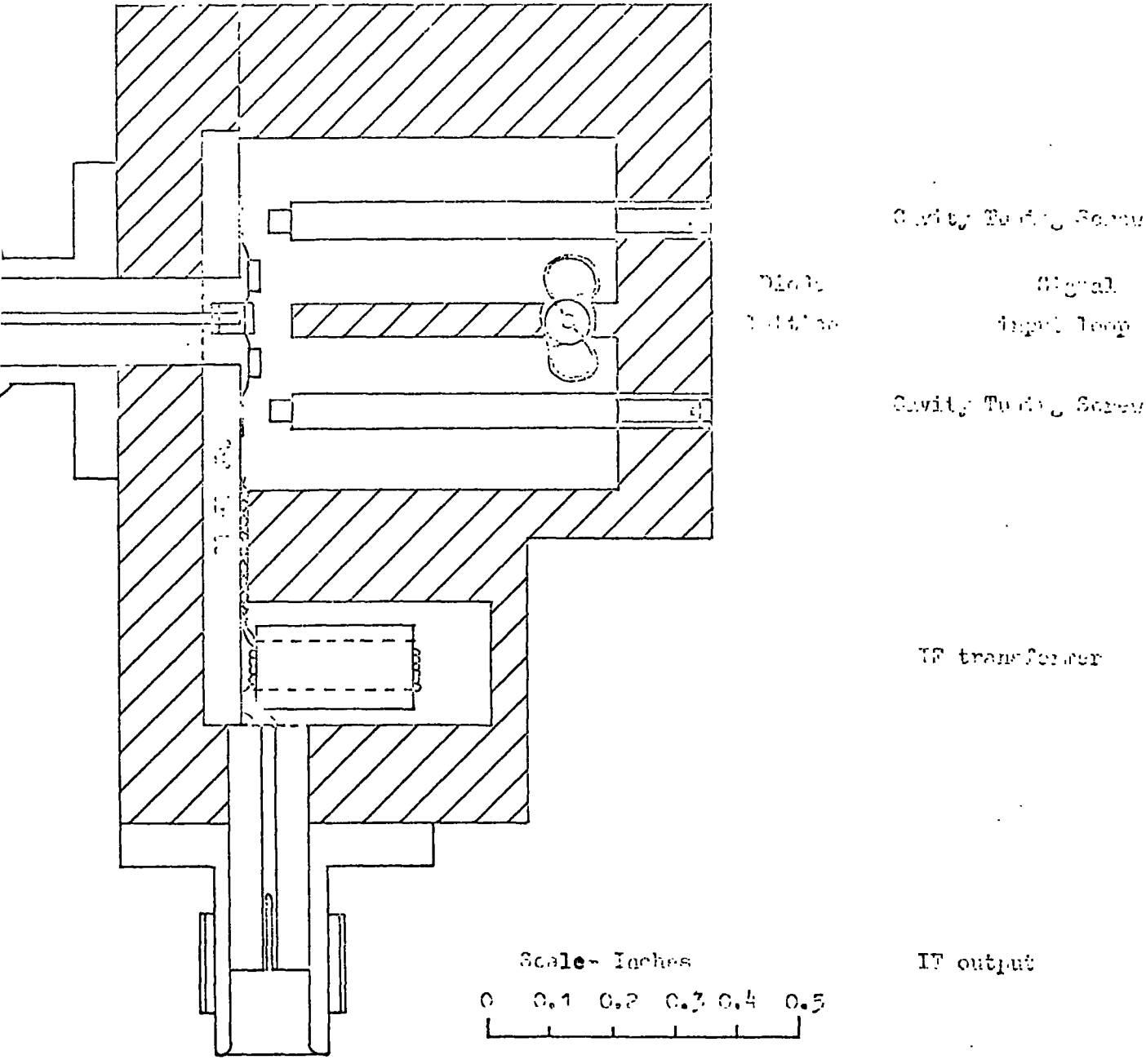

Fig 23 Side View of 4.5 CM. Mixer

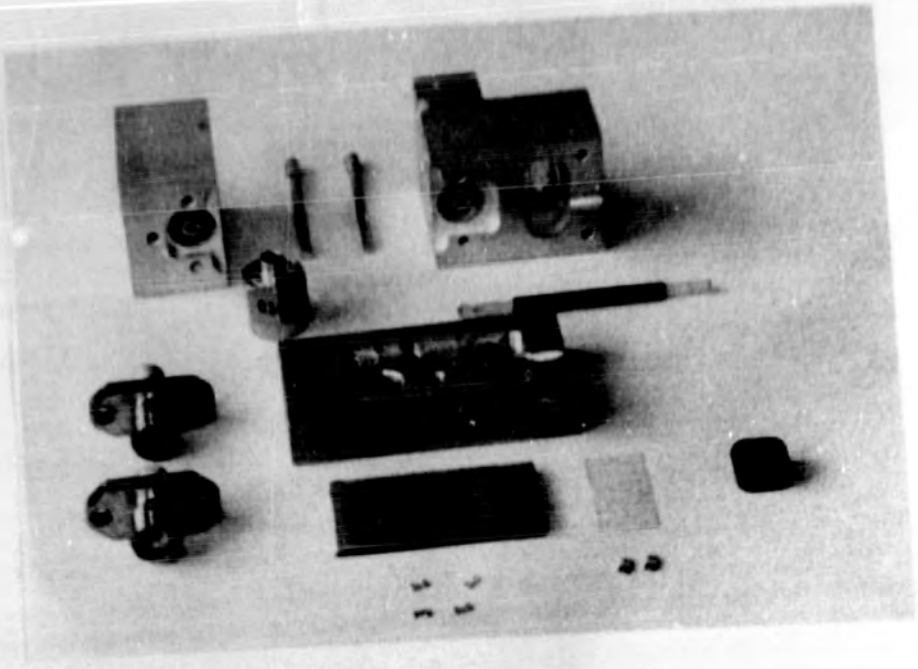

Fig. 24 Mixer Parts (Mixer 4)

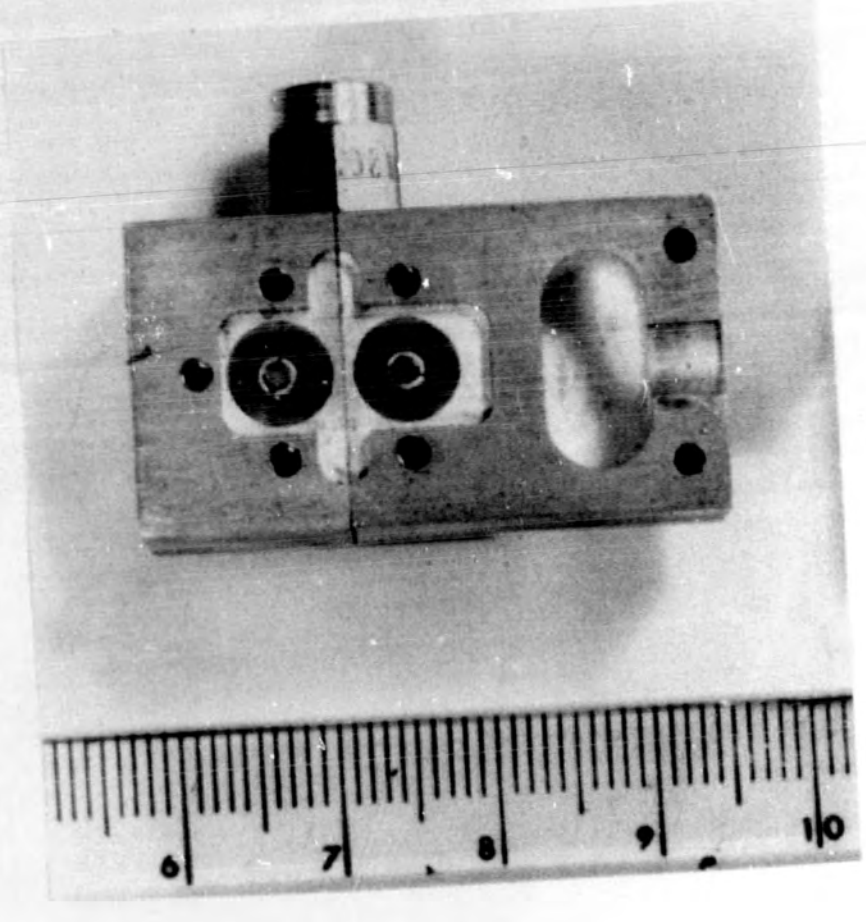

Fig. 25 Cavities (Mixers 3 - 6)

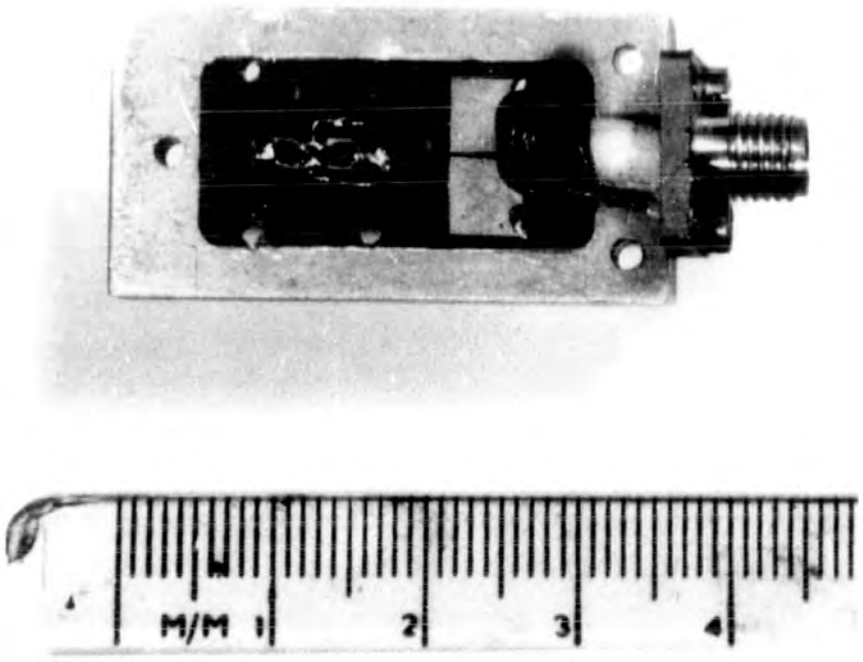

Fig. 26 Mixer Diode Substrate (Mixer 3)

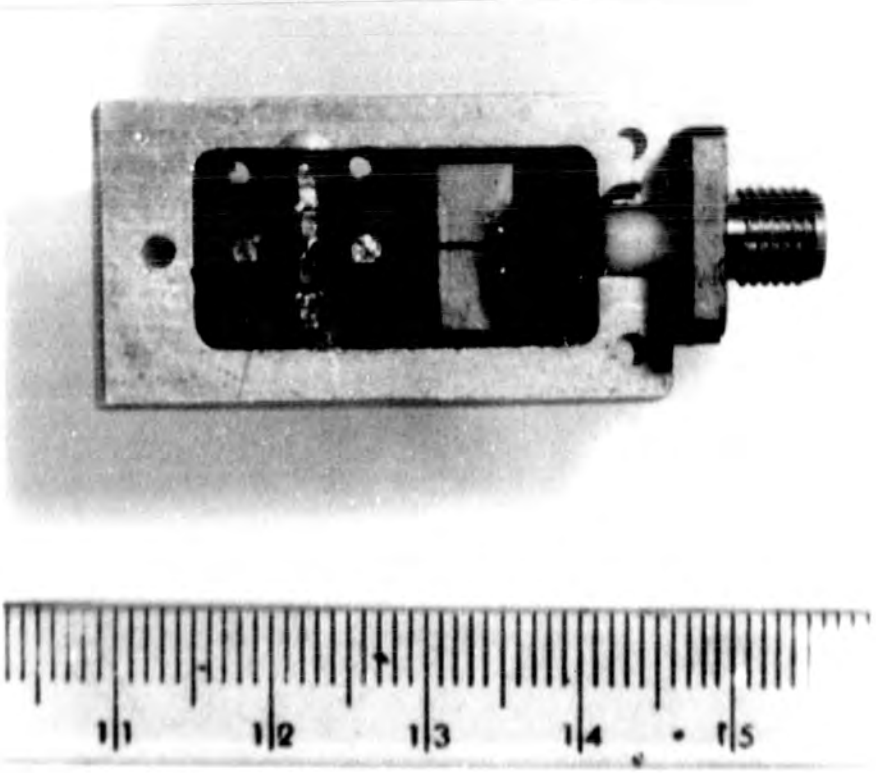

Fig. 27 Mixer Diode Substrate (Mixer 4)

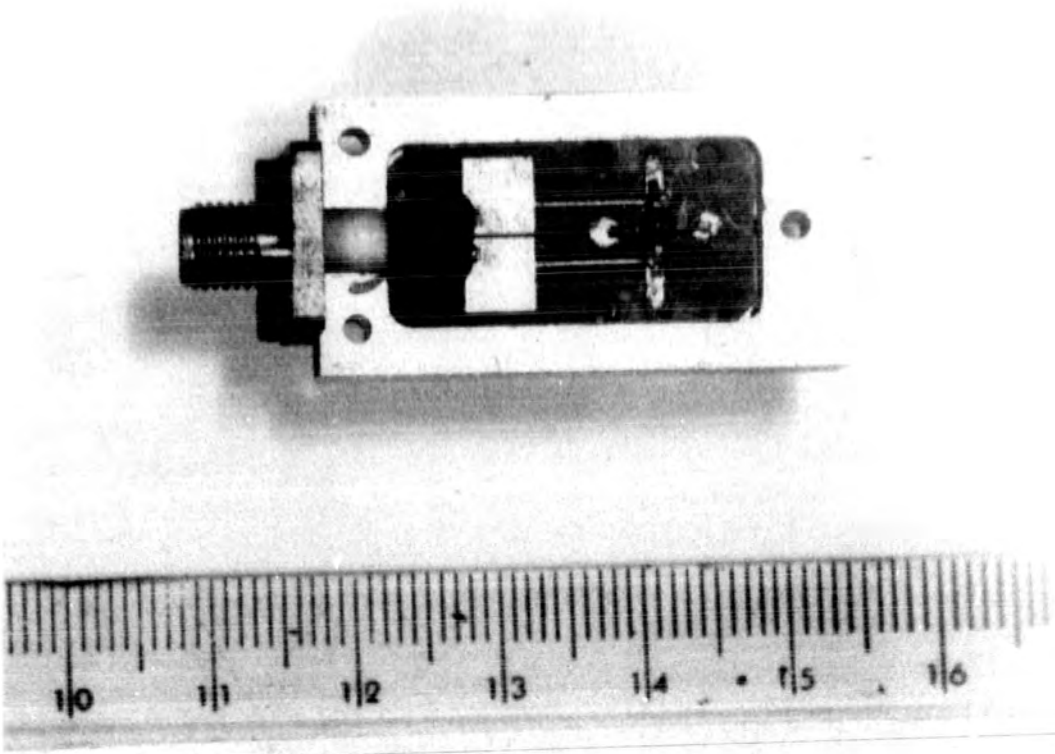

Fig. 28 Mixer Diode Substrate (Mixers 5 and 6)

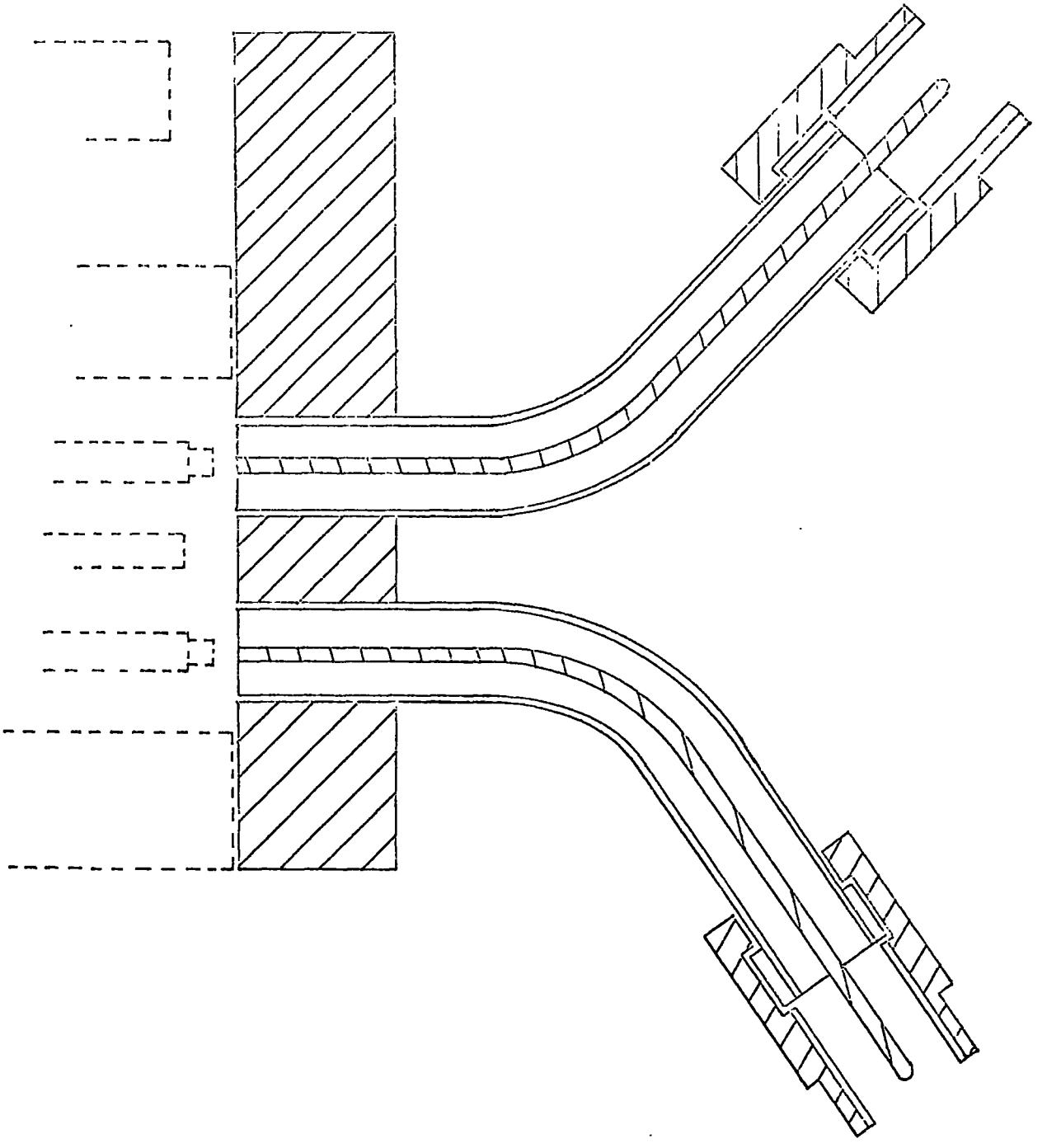

Fig 29 a

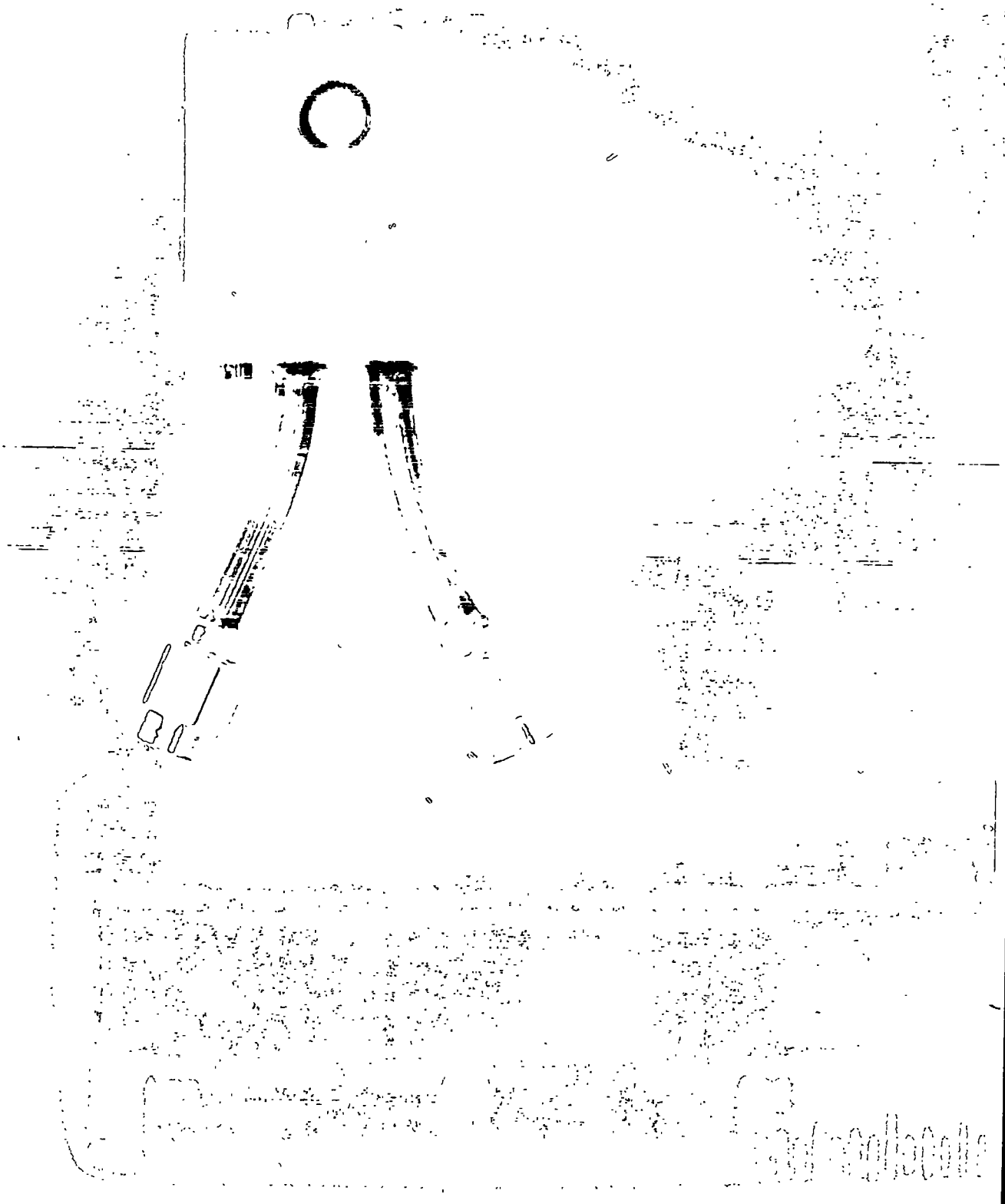

Fig. 29 Test Substrate with Cantilever attached

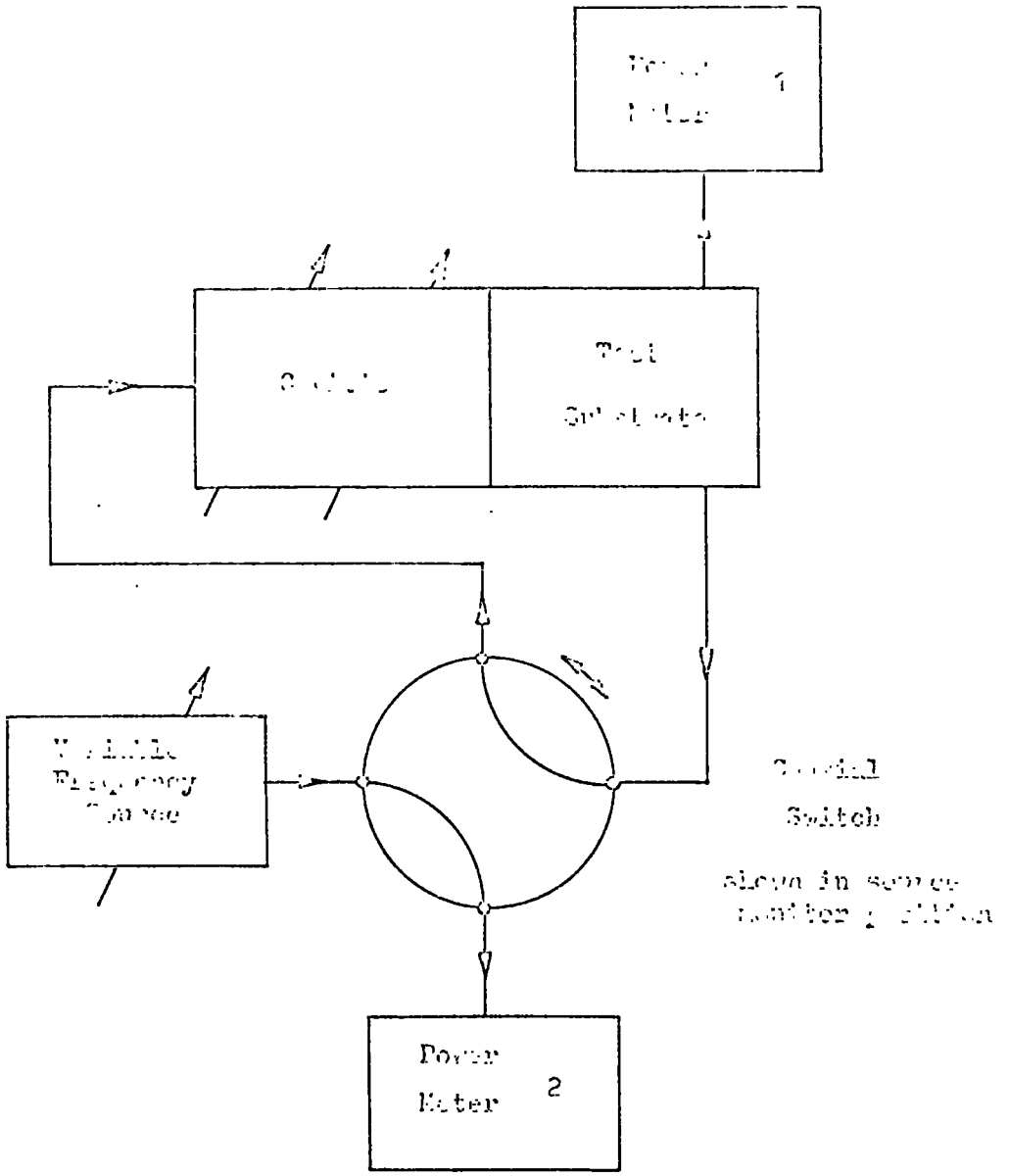

Fig 30

obtaining an optimum value of Q_L, knowing the effect on mixer conversion power loss of such factors as image rejection and total cavity loss. Using the circuit given in Fig.30, the electrical cavity length (and hence Q_L) may be varied by changing the input frequency and returning to resonance by adjusting Co. The value of Q_L may be measured by the half-power-points method, in which the cavity transmission falls by 3 dB at a frequency δf from the resonant value f such that:-

$$Q_L = \frac{f}{2\delta f}$$

The image rejection can be calculated from this, as can the unloaded Q value Q_o, knowing the cavity loss which is measured by optimally matching the output power meters to the cavity outputs. The loss of the stub tuners is subtracted from the result. The results are given graphically in Fig.31; a plot of total cavity loss against image rejection for the conditions given. A theoretical plot of cavity loss with an unloaded Q value of 950 is also shown. This is almost parallel to and about 0.2 dB under the measured total loss curve, a practical unloaded Q of around 950 from the gradient, with indicating connections losses of around 0.2 dB. Incidentally, this unloaded Q value is about ten times higher than that which could be obtained using lumped tuned circuits at this frequency.

6.0 Conclusions and Discussion

In this section we have looked at a fairly simple coaxial cavity, from the point of view of its use as a practical device. The analysis is therefore biased towards obtaining fairly accurate mechanical data which can be easily used to construct such a cavity. At the frequencies at which this type of cavity is most useful

Figure 31 Cavity loss against image rejection.

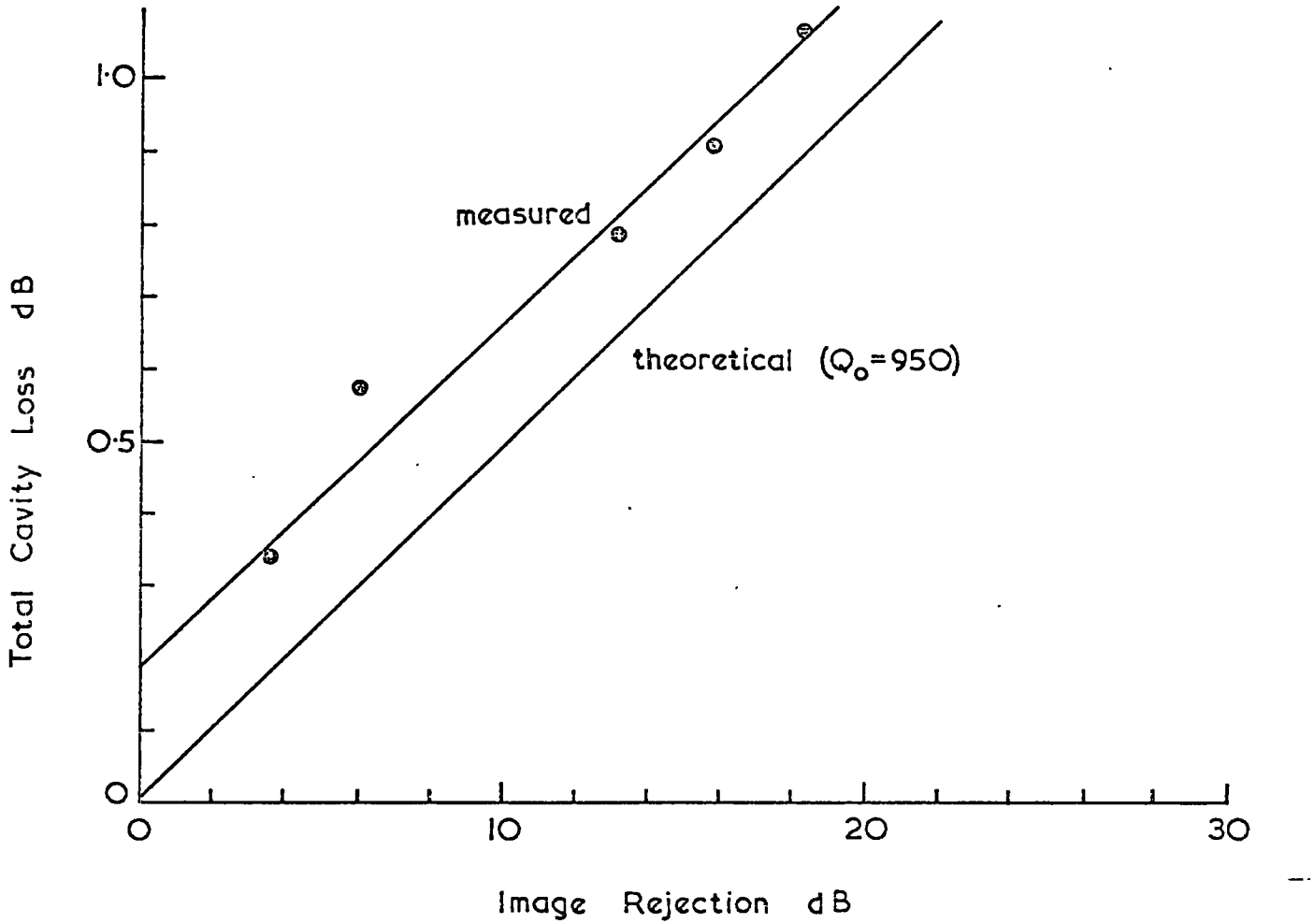

(i.e. 1 to 10 GHz), the construction involves a list of skilled processes, involving turning, boring, plating and general fabrication of metalwork. Today, in this country at least, such processes prove time consuming and expensive in industry, and printed techniques based on stripline transmission lines would be preferred.

It is worth considering, therefore, why stripline was not used for this project. After all, the principles of stripline have been laid down since the early 1950's, and any analysis done here would be simplified somewhat due to the two dimensional nature of the stripline technique. The disadvantages lie mostly with the technology, which is, of course, rapidly changing in this field. However certain disadvantages are basic to the two dimensional system and cannot be easily overcome. Briefly, the difficulties lie in two categories. Firstly there is an incompatibility with fitting active devices, which for years has limited the range of stripline to signal distribution systems. Partly this is due to the active component packaging, which is essentially three dimensional even if planar devices are involved; partly ground plane connection difficulties are involved with many types of stripline. The main trouble seems to be the difficulty of trimming or adjusting the passive circuit to match the spread of active device parameters.

Secondly, in stripline, resonator construction is restricted to distributed transmission line systems by excessive losses of lumped components, especially inductors produced in the medium. Also, the unreliable ground plane (earth) connections restrict the use of resonators with high current flow to earth. For the type of mixer under consideration, the limits imposed produce a stripline system of the following characteristics:-

(1) It may be larger than the cavity system despite the use of high dielectric constant substrate.

(2) It cannot be mechanically balanced (i.e. symmetrical) in three dimensions (signal, local oscillator and I.F.).

(3) Signal bandwidth and balancing range are narrower, due to phase changes in the large (in wavelengths) passive circuit.

The result is to produce a particular "breed" of single balanced mixer suited to stripline use. As we shall see in the next section (and Appendix 5), this does not have the low theoretical loss that is associated with the double balanced system.

PART II - 4.5 GHz LATTICE MIXERS

7.0 Introduction

Receiving systems at microwave frequencies normally employs a low noise radio frequency amplifier stage, followed by a mixer and an intermediate frequency amplifier. Friis[21] showed that the noise figure of the mixer/I.F. amplifier combination is proportional to the conversion power loss of the mixer. Using a low loss mixer and an I.F. amplifier, therefore, it may be possible to obtain as good a noise performance as that obtained using an additional R.F. amplifier. Apart from the physical advantage of having no R.F. amplifier, electrical specifications on such items as cross modulation and bandwidth may be more easily met using a mixer as the first stage in the receiving system.

At present, diode mixers offer the best noise performance at microwave frequencies, so to produce a practical mixer, a theoretical analysis using a close approximation to practical diode parameters is needed. The problem here is to produce a diode model, which has a sufficiently accurate solution, without being so complex that the mathematics are unmanageable. Several people have produced adequate analyses, mainly for restricted conditions, under which very low losses are possible. The problem lies in realising these low diode losses in a practical circuit, not so much because practical diode losses are higher than theory would indicate, but because imbedding network losses are so high. The passive network in which the diode(s) operate has many functions, including matching, filtering and supplying the correct local oscillator drive. Under some theoretically desirable operating conditions, the loss involved in providing the functions outlined above would outweigh the gain in diode performance obtained. The conditions for low diode loss obtained in the analysis used, must therefore be realisable with low loss at microwave frequencies.

This part is therefore concerned with the practical realisation of a mixer at 4.5 GHz using the range of diodes commercially available at the time of writing. The first chapters are a simplified theoretical survey, justifying the use of the image rejection lattice arranged with current drive[32]. The passive circuit is then considered and final results are presented with a chapter on measurements. Finally, an attempt is made to see the effect of mixer improvements on low noise receiving systems in general, and the influence on either components in the system is studied.

8. Mixer Circuits

8.1 Historical

The first methods of radio wave detection used a physical side effect of reception, such as sparking across an air gap in a resonant circuit. This works well with a very high field strength, which is proportional to the size of receiving and transmitting aerials, the transmitter power, and the frequency. The low frequency communication networks, therefore, required a signal "detector" of much greater sensitivity, and various solid-state rectifiers were used until about 1925, when the thermionic value was introduced. The chief disadvantage of the solid-state rectifiers was their unreliable nature, as a result of a lack of understanding of the conduction processes involved.

The non-linear resistance characteristic of both solid state and thermionic detectors, was essentially a square law at low signal levels. The detecting effect was to square mathematically the current, or voltage, flowing in the device. If this current was a carrier wave with information carrying sidebands, the result contained a small coefficient of the required information, amongst other components. It was soon noticed that interfering signals close to the one being received

were not impressed upon, but modulated by the received signal. This mixing process was used for rendering carrier wave morse signals audibly, by means of producing an audio beat note or heterodyne. The interfering signal was replaced by a "local" oscillator in the receiver, which could be a self-oscillating detector or amplifier. The heterodyne signal could be selectively amplified to improve the signal to noise ratio, and the supersonic heterodyne or "superhet" system was born.

The advantage of the superhet system was to do the majority of the amplification at a fixed frequency and hence simplify tuning and keep a fixed bandwidth throughout the tuning range. A second detector was used at the end of the intermediate frequency amplifier for its original purpose, while the first detector was now a true mixer.

In the middle 1930's, the demands on the mixer were for high efficiency with the minimum of valves, in addition to isolation of signal and local oscillator circuits. A family of multigrid valves was developed to amplify the signal and "gate" it at the frequency of the local oscillator. This was efficient, but needed at least five grids (including the screen grids used for isolation), and these introduced a good deal of shot noise. At low frequencies, the atmospheric noise received was higher than this internal noise, but at high frequencies the noise, and the transit time of electrons across a valve, was a limiting factor to its use.

Interest in high frequencies for Radar use in the early 1940's, brought a new effort into production of solid-state mixers and detectors. These were constructed normally of silicon with a tungsten or molybdenum wire "cats-whisker" contact. The junction capacitance of this point contact was low, and the high frequency performance good, but there was a large element of "black magic" in production[23]. Semiconductor technology and understanding developed to a great extent when transistor production demanded it in the 1950's. The use of photo-lithography and

materials such as Gallium Arsenide, has enabled the Schottky barrier diode to be produced with a good high frequency performance, and consistent reliable characteristics. The latter is important because the use of matched pairs or quads of diodes in balanced and double-balanced mixers, has many advantages[24].

At the same time as these diodes have been developed, other useful non-linear phenomena have been exploited and useful devices produced. These can be sub-divided into: variable capacitance types, negative resistance types and three terminal devices (transistors and F.E.T's.). All of these are usable in mixer circuits, with varying advantages of gain and convenience in circuit design. However, at present, the Schottky barrier diode still seems to offer the best performance combinations, especially at frequencies in excess of 1 GHz.

8.2 Basic Principles

A frequency converter normally consists of a frequency source called the "local oscillator" or "pump", and a network containing one or more non-linear devices. There must also be means to couple the input and output signals, as well as the local oscillator. The complete network is often called a "mixer" necause the input signal (which will be called simply the signal) is mixed with the local oscillator in a non-linear device to produce product frequencies.

One (or sometimes more) of these products is the required output signal. In a receiving system the output frequency is known as the intermediate frequency or I.F., because of its place in the receiving chain between the ratio frequency and the desired modulation frequency. The I.F. usually lies between 10^6 - 10^9 Hertz. The bandwidth must be sufficient to carry all the information transferred from the signal, yet a low enough frequency is required for low-noise, high-gain amplification.

The non-linear device used can be predominantly non-linear reactance or resistance. Normally the two cases are called parametric frequency converters and mixers, respectively. The parametric converter[25] of a negative resistance mixer[26] can provide conversion gain, which is attractive at first sight. However, apart from the stability and bandwidth problems in this type of converter when frequency translation is in a downward direction[27], the devices at present available give a noise figure which is much worse than the perfect device theory would indicate.

Although the mechanism of mixing has been stated as being non-linearity in some characteristic of a device, strictly it is the time variation of this characteristic (which is normally periodic) in conjunction with the local oscillator, which does the conversion. This introduces a new family of possible devices, which although not strictly non-linear (or not used in a non-linear mode of operation) can be time varying. Relays and associated devices are good examples, as are transistors and F.E.T's., some of which can be used at microwave frequencies.

The most important disadvantage of transistors and F.E.T's. at present is the excess noise they introduce into the mixing process, although for circuit convenience they are often used successfully up to 1 GHz.

The positive resistive diode mixer will always exhibit a conversion loss, low though this may be. The advantages in the microwave region of such a mixer are:-

(1) Wide bandwidth and no stability problems.

(2) Good, repeatable performance due to accurate modelling of Schottky barrier diode characteristics, even at microwave frequencies.

(3) The theoretical treatment of a purely resistive case, although incomplete, is better at predicting practical results than in the reactive case.

The last two points are important to this report because of the need to define what constitutes a good mixer, and to establish the fundamental limits of its performance using practical devices.

8.3 Diode Arrangements

Practical mixers may use one, two or four diodes. Two or more diodes allow the circuit to be "balanced". In the case of two diode mixers, the balancing is done with respect to the local oscillator frequency. Local oscillator leakage from both the signal and output ports is then prevented, and any noise present in the local oscillator (which may be considerable compared to the signal power) should ideally cancel out at the output terminals. This occurs only under perfect conditions, and any practical circuit must use matched diodes, and possibly incorporate balance trimming adjustments as well.

The four diode mixer may be of the series, shunt, or ring (lattice) type. The lattice type is widely used since it is double-balanced, with respect to both signal and oscillator. Historically, lattice mixers have been ignored at microwave frequencies for two reasons. Firstly, the early point contact diodes were hard to select into properly matched pairs, let alone matched quads, and the match could easily have been influence under working conditions by the variation of diode parameters which was prone to occur, apparently at random or as a function of environment, age, or input power[23].

The second reason is that the theoretical improvement in noise figure afforded by such an arrangement would have brought little overall improvement due to noise contributions elsewhere in the system. For these two reasons, then, the recent availability of single package matched quads of Schottky barrier diodes, cannot be underestimated in terms of its influence on future mixer design.

8.4 Terminations

Correct termination of mixer ports is extremely important. The output products do not just consist of the desired intermediate frequency component. The actual frequency and magnitude distribution is determined by the diode non-linearity law and the arrangement used. If the system is considered as one in which all the signal power is converted without loss into all the output components present (no gain is possible in the resistive case), the power converted into the desired output component depends on correctly terminating all the other unwanted components. If this can be done for all the unwanted components, (and this is not always possible in some configurations), all the output power is channelled into the intermediate frequency component, and a theoretical conversion loss of zero is obtained. This is obviously impossible in practice due to termination losses and the infinite number of output components. However, unwanted products of magnitude approaching that of the desired output must be dealt with in order to obtain resonable results. The second termination condition that must be observed is, of course, that the signal and output ports must be conjugately terminated in order to obtain maximum power transfer.

It may be noted that the termination for the local oscillator port has not been mentioned. This is because, provided that the correct drive waveform and power is supplied, the local oscillator plays no part in the process directly, merely providing the periodic variations of diode resistance. In practice, however, especially with mixer configurations which demand high drive levels, there is rarely local oscillator power to spare at microwave frequencies, and efficient coupling is necessary.

8.5 Classification and Performance

The combination of diode arrangements in a mixer, and the possible terminations to unwanted components seems endless. In fact four basic families (Fig.32) can be extracted, depending on the input and output port terminations of unwanted frequency components[28]. Fig.33 shows the seven diode arrangements possible using one, two, or four diodes, either in shunt or series with the signal path. Combining the diode arrangements with the terminations gives a group of 28 mixers.

The decision on which of these 28 circuits to use, rests on the theoretical performance possible and the ease of realising the conditions imposed by the theory at microwave frequencies. In general, the higher the degree of balance of a mixer, the lower the number of unwanted components produced, and therefore the easier the filtering processes become, and the higher the efficiency of the system. Against this, the extra complexity involved must be placed, but for the present application the double-balanced mixer would seem to be the optimum. The two diode balanced mixers (8 in number) and the four diode balanced mixers (8 in number) have much in common, the extra diodes allowing the normal input and output balun transformers to be eliminated. The four double balanced mixers all use the "ring" configuration of diodes, so called because they are connected in a series ring of four of the same polarity. Of course, the double-balanced arrangement is only one possible higher arrangement, which can be considered as two balanced mixers connected in parallel with the inputs out of phase (Fig.34). Another higher arrangement would consist of three balanced mixers, connected with the inputs 120° out of phase[29]. This would use six diodes and cancel a lot of unwanted frequency components. There is, however, the problems of producing an accurate wideband 120° phase shift. The output components produced by several types of mixer are discussed in Appendix 5.

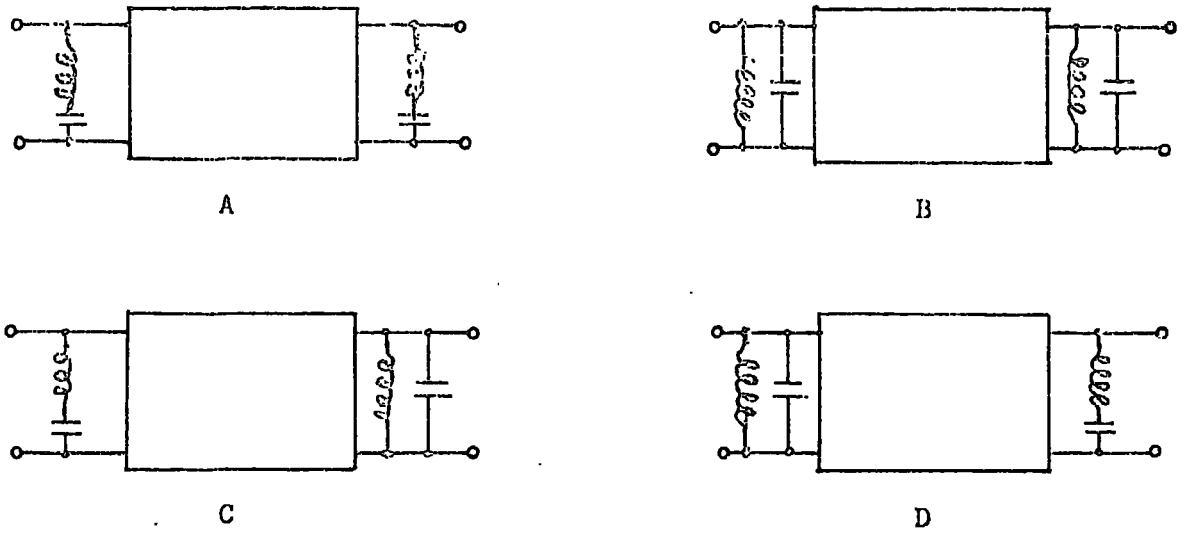

Fig 32 Input and Output Conditions for Mixers

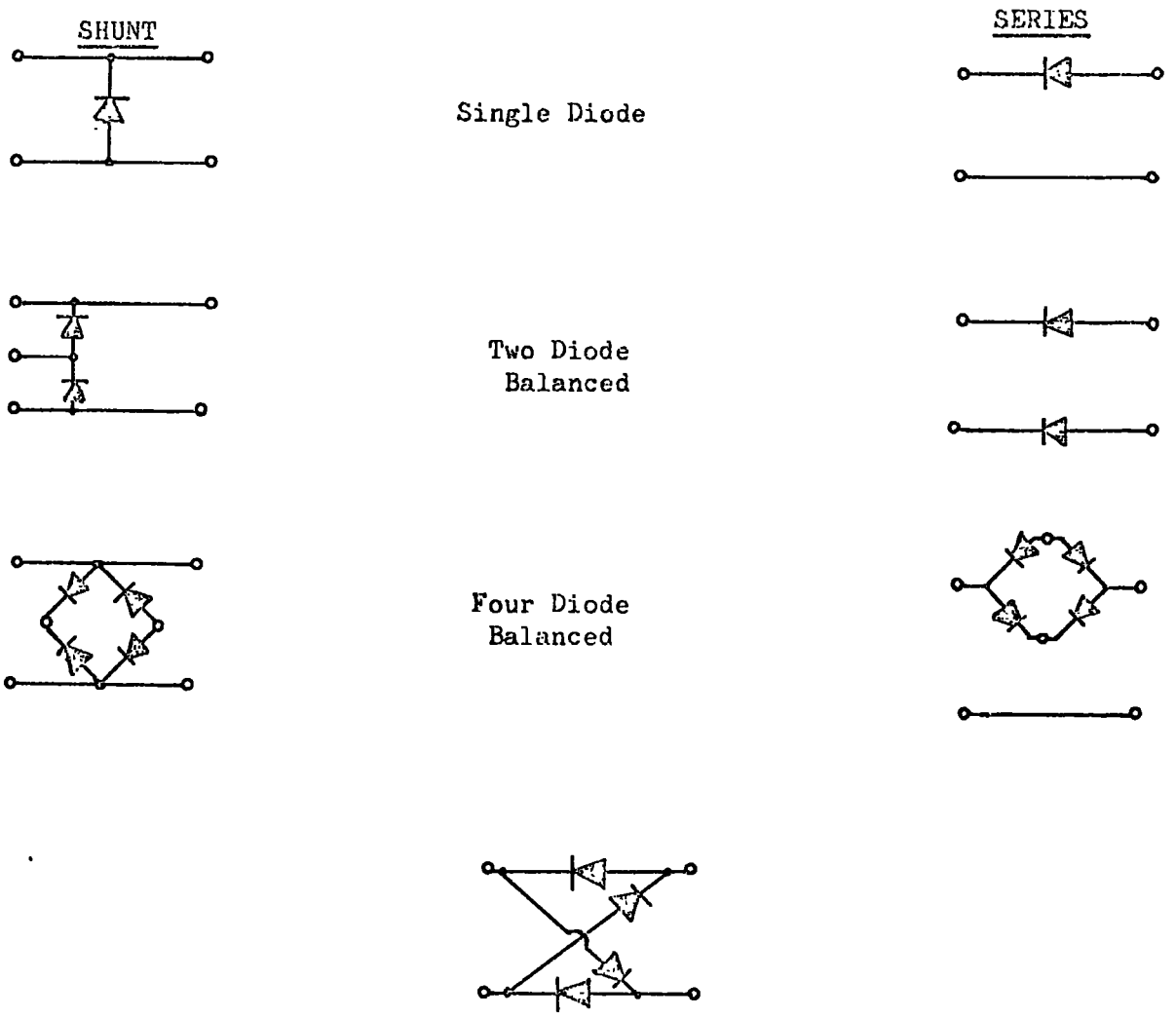

Fig 33 Seven Diode Arrangements using one to four diodes

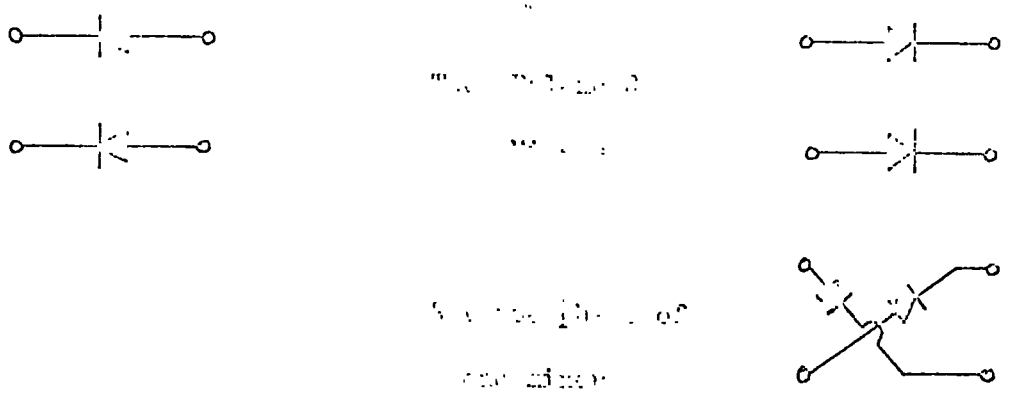

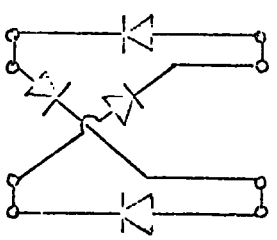

Fig 34

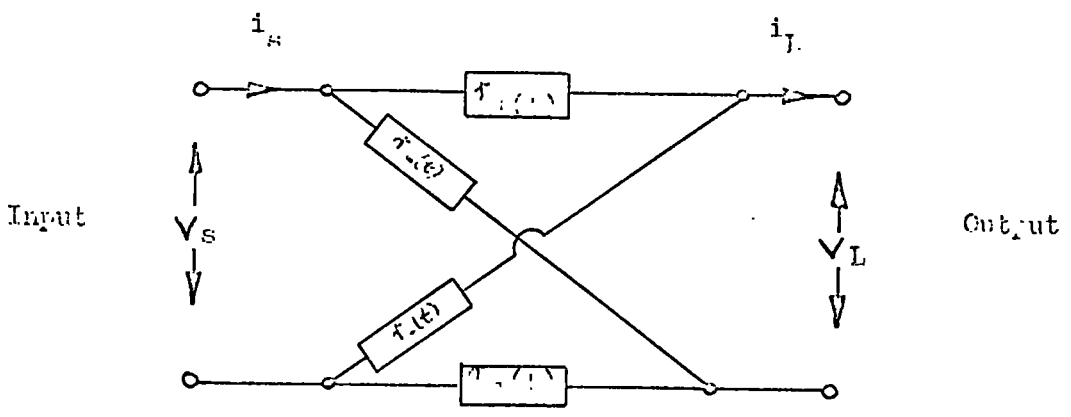

Fig 35

9. Summary of the Theory of Lattice Mixers

9.1 General Theory

Appendix 5 gives a mathematical treatment of the operation of a lattice mixer. The assumption made is that each diode acts as a perfect switch, the resultant switching function is a squarewave which can be considered as an odd order Fourier series. A more accurate approach would have been to treat the diode as a time varying linear resistance, with a law such as:-

$$\sum r_m \cos m\omega_p t,$$

where ω_p is the pump or local oscillator frequency. Small signal analysis laws can then be used on the circuit.

In the case of point contact and hot carrier diodes, the variable barrier resistance is largely explained using Schottky's model of a p-n junction, from which is deduced the theoretical law:-

$$V = \frac{kT}{q} \ln \left(1 + \frac{I}{I_s}\right) \quad .. \quad .. \quad .. \quad .. \quad (1)$$

A totally different law is required for diodes which operate with different current flow mechanisms, such as backward diodes and thermionic devices. Even this law does not hold too well in practice, and several modifications have been proposed with reference to specific devices, or specific parts of the characteristic curve. For the forward characteristics, a reasonable agreement in both slope and magnitude may be obtained by adding a term Ir_s to the right hand side of the expression. This series resistance r_s, known as the spreading resistance can be measured in practice by a pulse technique. Although the value obtained is not necessarily constant over the whole characteristic, it causes the greatest effect in the high forward current region where it is measured fairly accurately by this technique.

The pumping waveform applied to the diode is of considerable importance, although at microwave frequencies it is fairly difficult in practice, to employ waveforms other than sinusoidal because of the bandwidth required. The approach here is to use sinusoidal current drive and express the mixer relationships in terms of the current, drive level and diode characteristics. (Fig 41).

If we take equation (1) (including the Ir_s term) and consider I as the half wave rectified waveform of the sinusoidal current drive, we can differentiate with respect to I and obtain the diode resistance expressions:-

$$r_+(t) = r_s + r_b \frac{1}{1 + X(t) - X(t)\ S(t)} \quad .. \quad .. \quad (2)$$

$$r_-(t) = r_s + r_b \frac{1}{1 - X(t) + X(t)\ S(t)} \quad .. \quad .. \quad (3)$$

where:-

$$S(t) = \frac{4}{\pi} \left\{ \cos \omega pt - 1/3 \cos 3\omega pt + 1/5 \cos 5\omega pt \ldots \right\}$$

$X(t) = X \cos \omega pt \qquad X = \frac{ip}{2I_s}$ Normalised current drive level.

The lattice arrangement of time varying resistances thus formed is illustrated in Fig.35. By short circuiting the output terminals, we can obtain general expressions for the output currents (i_L) and input voltage (V_s) which contain all possible frequency products generated within the lattice. These expressions may be given in the form:-

$$v_s = i_s r_b \sum^{even} A_n \cos n\ \omega pt + v_L \sum^{odd} A_n \cos \omega pt \quad .. \quad .. \quad (4)$$

and

$$i_L = i_s \sum^{odd} A_n \cos n\ \omega pt + \frac{vL}{r_b} \sum^{even} A_n' \cos n\ \omega pt \quad .. \quad .. \quad (5)$$

r_b is the diode slope resistance at the origin.

Introducing frequency selective terminations to the lattice we finally obtain two equations which contain only input and output quantities:-

$$\text{(Signal voltage)} \quad v_q = i_q r_b K_1 + v_1 K_3^{\frac{1}{2}} \quad .. \quad .. \quad .. \quad .. \quad (6)$$

$$\text{(I.F. Current)} \quad i_{-1} = i_q K_3^{\frac{1}{2}} - v_{-1} K_2 \quad .. \quad .. \quad .. \quad .. \quad (7)$$

The K parameters[22] are in general complex and are functions of the image termination, diode quality factor $r_s' (=\frac{r_s}{r_b})$ and local oscillator drive level.

The conversions power loss under matched conditions is simply:-

$$\frac{\mathrm{Re}(v_q i_q^*)}{\mathrm{Re}(v_{-1} i_{-1}^*)} \quad .. \quad .. \quad .. \quad .. \quad .. \quad .. \quad (8)$$

Real parts are required because (6) and (7) use phasor quantities.

9.2 Solution of the Resistive Cases

9.2.1 Introduction

For correct operation the output of the lattice requires a voltage restriction to the desired intermediate frequency component. The input however is open to variations. The largest, and therefore most important parasitic voltage appearing at the input terminals is the "image" ($2\omega p - \omega q$). Figs. 36 and 37 illustrate the input and output components graphically, from which it can be seen that the image magnitude is comparable to that of the signal, so roughly ± 3dB difference in conversion power loss, can be produced by termination of this component alone. Terminations may be divided into, open-circuit, short-circuit and the value of the signal source impedance. The first two cases are often called narrow band conditions and produce the best results. The last condition is often known as the broad band case,

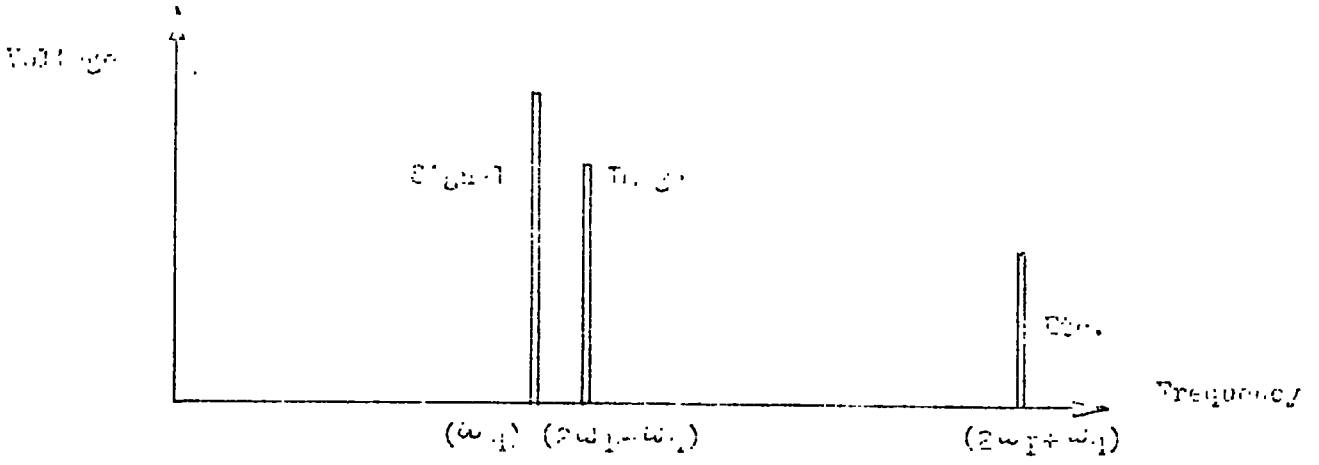

Fig 36 Voltages appearing at the Terminals

Of the form $m\omega_p \pm \omega_q$, m is an even integer

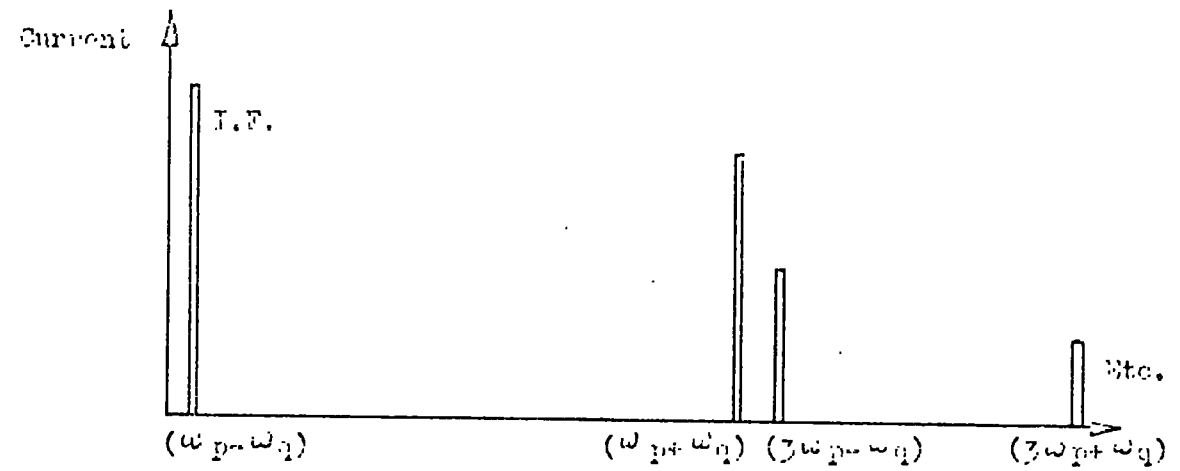

Fig 37 Output Components

Of the form $n\omega_p \pm \omega_q$, n is an odd integer

and a conversion power loss of 3dB is the theoretical lower limit, whilst 0dB is the theoretical limit of both narrow band cases. At first sight both open and short-circuit cases would appear to give similar results, since in neither case is any image power dissipated in the termination. However, in the short circuit case, image currents flow in the lattice itself through the termination, and losses will therefore be higher than those of the open-circuit version.

Figs. 38, 39 and 40 show typical calculated results for the three cases, the conversion power loss (cpl) being plotted in dB against X for various values of the diode quality factor $r'_s = \frac{r_s}{r_b}$. Knowing the local oscillator drive current required, and considering the effective lattice circuit as seen by the local oscillator (Fig.41), the local oscillator power (Po) required can be calculated. If the terminations are purely resistive, equations 6 and 7 are real and:-

$$Cpl_{(min)} = \frac{1 + k^{\frac{1}{2}}}{1 - k^{\frac{1}{2}}} \quad \text{where } k = \frac{K_1 K_2}{K_3 + K_1 K_2}$$

The optimum input and output impedances of the lattice can then be expressed as:-

$$Ri_{(opt)} = \frac{k^{\frac{1}{2}}}{K_2} r_b \quad \text{and} \quad R_{L(opt)} = \frac{K_1}{k^{\frac{1}{2}}} v_b$$

For purely resistive terminations and operation the K parameters are real and positive, but may be different for each type of mixer due to the different image terminations.

9.2.2 Narrow-band Open-circuit Mixers

Fig.38 shows a cpl approaching zero for high drive levels and perfect diodes. Unfortunately, under these conditions the optimum terminations approach zero as well.

Fig 38

NARROW-BAND OPEN-CIRCUIT MIXER

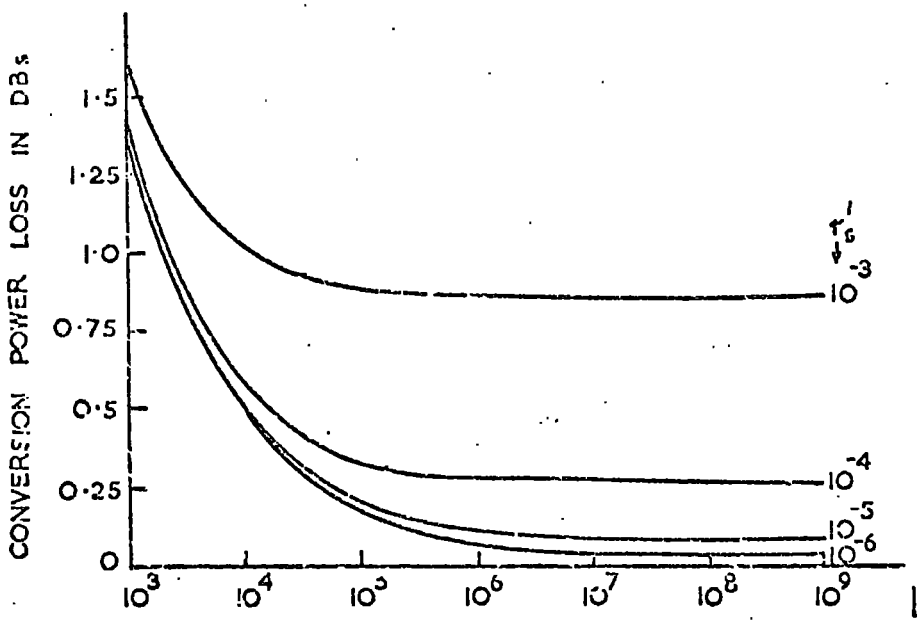

Fig 39

NARROW-BAND SHORT-CIRCUIT MIXER

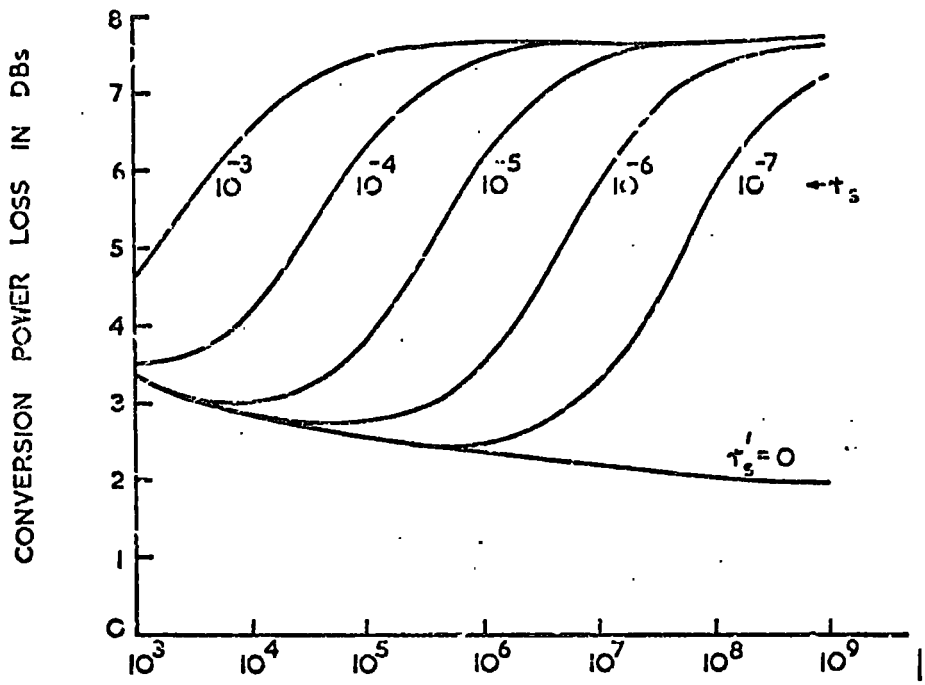

Fig 40

BROAD-BAND MIXER

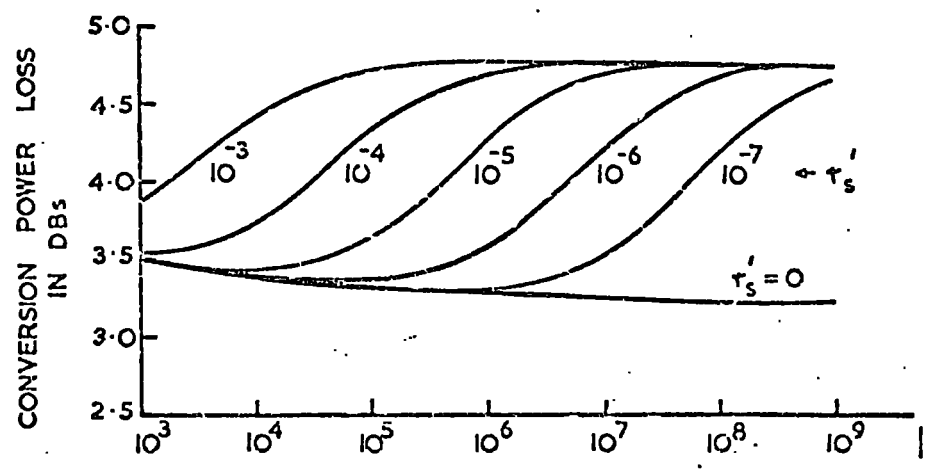

MINIMUM CONVERSION POWER LOSS AS A FUNCTION OF THE L.O. DRIVE AND THE QUALITY OF THE DIODES.

Normal conditions of use still allow a very good performance to be obtained. At a drive level of 10^7 for instance, a mixer using diodes with I_s = 10 mA $r'_s = 10^{-6}$, needs 90 mW of local oscillator power, and a cpl of less than 0.1 dB should be obtained with an infinite image termination.

9.2.3 Narrow-band Short Circuit Mixers

The extra loss produced by the image current flowing through the diode lattice is apparent from Fig.39. In addition, except for perfect diodes, there will be a minimum value of cpl as the drive increases. For infinite drive levels, the value of the cpl approaches 7.65 dB for all practical diodes and, as would be expected, zero for perfect diodes.

9.2.4 Broad Band Mixers

In a practical mixer, especially if the ratio of signal to I.F. frequency is high, the image termination may be almost identical to that of the signal since it is so close in frequency. However, ideally all the higher order products should be rejected, although these will normally be at such a low power as to have no significant effect on the cpl. Fig.40 illustrates this case, minimum conversion power losses of 3 to 3.5 dB can be obtained using practical diodes, provided the optimum drive level is used. At infinite drive levels, ideal diodes would give a cpl of 3.0 dB as expected, and for all practical devices the cpl levels off at 4.771 dB.

9.3 Practical Performance

The narrow-band open circuit mixer would seem to be the best arrangement to use in a practical circuit, but the image frequency

termination cannot then be considered ideal. In general it can be expressed as $R_{-2} + jX_{-2}$ and with most filter networks it will be mainly reactive with R_{-2} similar to the signal source impedance.

The K factors used in the last section for calculation of cpl and optimum input/output impedances, will therefore, now be complex. Apart from an increase in minimum cpl, this will give rise to complex input and output impedances, which will have to be conjugately matched. Luckily it turns out that a degradation in cpl of only 1 dB will be produced if the image rejection is at least 10 dB[22], a value which is fairly easily obtainable. Also the output impedance, which is very high in the ideal case, is reduced to a level which can be matched with less loss to the I.F. amplifier input. This is important practically, because the signal is at its lowest level in the receiving system at this point, and therefore most vunerable to noise.

9.4 The Effect of Diode Parasitics

Up to now the diodes have been considered as pure time varying resistances for ease of theoretical treatment. To this extent the effect of parasitics in the lattice itself is totally different to the effect of non-ideal terminations, since the basic lattice equations are now no longer valid. In any practical case, however, even at high frequencies, the parasitic reactances (Fig.42) are small compared to the time-varying resistance of the diodes, and indeed are chiefly due to the packaging and assembly of the quad of diodes.

Returning to Section 9.1, equations (2) and (3), for the time varying resistance of the diodes, we can insert a complex term to cater for the parasitics. The values can then be used in the original analysis, introducing the simplifications which result from a restriction to realistic value of parasitic reactances. P.W. Wright

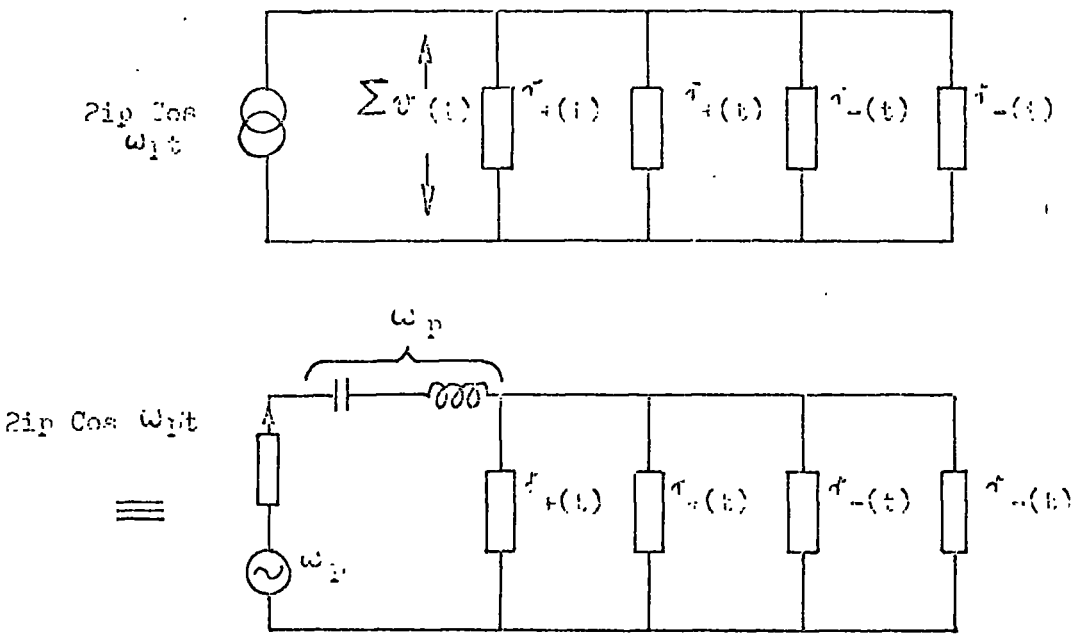

Fig 41 Local Oscillator Circuit

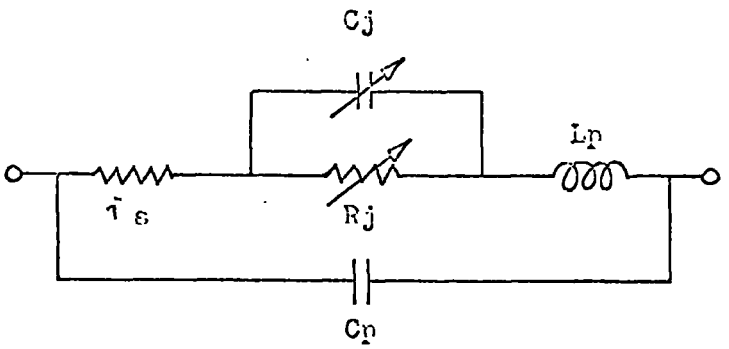

Fig 42 Diode Parasitic Equivalent Circuit

has done these calculations[30], and an example of the effects produced in a practical case is illustrated below for a mixer with ωq = 4490 MHz and ωp = 4560 MHz.

A. Parallel Capacity

For r_s = 15 ohms and Lp = 1.5 nH, the conversion power loss increases by 1.4 dB for each 0.1 pf of capacity. This does not appear to vary much with drive conditions, although assumptions used appear to break down at very low (and largely unrealistic) levels. Both depletion capacity (Cj) and package capacity (Cp) are lumped into one time-invariant value for this calculation. This assumes that the time-variable part of Cj is small compared to the whole combination, and that rs << Rj, both of which are normally true to a good degree of accuracy. In Fig.43 experimental values obtained by Gregory are given. These confirm the values given if one assumes the effect of the diode capacitance is three times more at 4.5 GHz as it is at 1.5 GHz.

B. Series Inductance

For r_s = 15 ohm and a fixed value of (Cp + Cj) of 0.13 pf, the conversion power loss increases by about 1.2 dB for each 1 nH of inductance.

The effects of resistance inductance and capacity are not directly cumulative. Calculations for a mixer using diodes:- r_s = 15 ohms L = 2 nH C = 0.13 pf gave a loss of 2.2 dB. The effect of the parasitics on input and output impedances is also of some importance. The fixed ratio of $\frac{4}{\pi^2}$ between input and output impedances which comes out of the lattice calculations, is preserved, but the actual magnitudes are much reduced by parasitics. Again, this can turn out to be of advantage practically, because the impedances are reduced to a value which can be easily matched into, without the usual loss involved in matching very high impedances to transmission line levels.

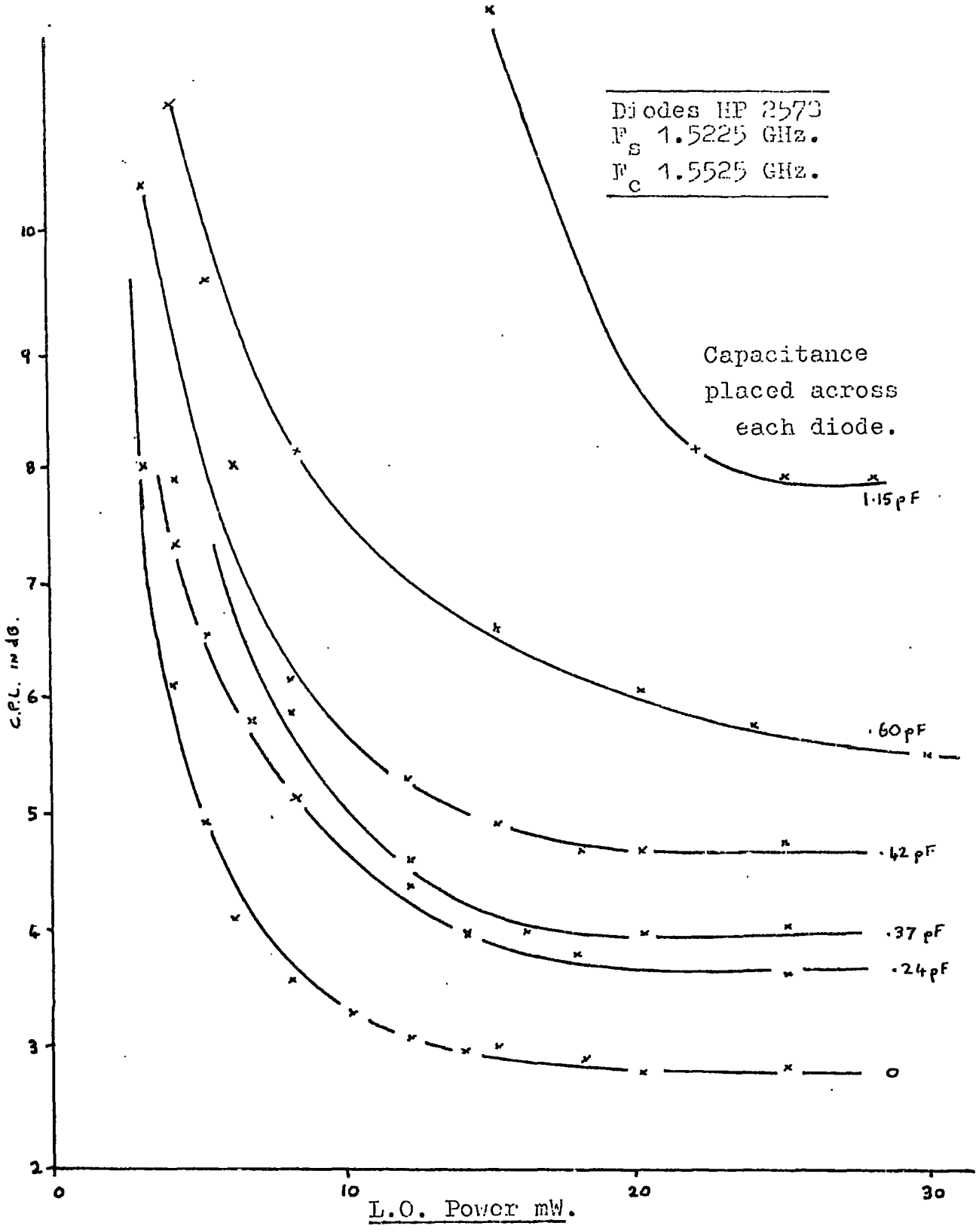

Fig.43 The effect of Diode Parasitic Capacitance on an Experimental Mixer. (J.Gregory)

10. Microwave Mixers

10.1 Introduction

Because of the huge information bandwidth it can carry, the microwave frequency range is very important in communications. Another point is the small size of high gain directional aerials at these frequencies, whilst the low intrinsic atmospheric noise and extra-terrestrial range enable very low noise receivers to be used to advantage. In such a system the mixer is an important item, more so if it has no R.F. amplifier in front of it in the receiving chain. Indeed, a mixer can theoretically out-perform an R.F. amplifier for many purposes.

Point contact diodes were used extensively for early microwave mixers. Since these were often used in Radar sets, where the diode was often subject to pulses of R.F. energy as well as vibration, the point contact diode was considered unreliable in maintaining its electrical parameters for any period of time. The use of mixers with matched pairs or quads of diodes was therefore ignored. With the advent of microwave-communications links, balanced arrangements were used in order to reduce the noise contribution of the klystron local oscillator then in use. These mixers used waveguide techniques, which are still employed for the frequency range above 10 GHz. At low frequencies, however, the reduction in size (but not losses) offered by microstrip and stripline systems is attractive, whilst lumped component mixers are used up to 1 GHz. Schottky barrier diodes are nearly universally used in mixers today, although backward diodes are coming into use for low level detector where their considerable non-linearity at the origin gives a high efficiency.

10.2 Practical Circuits

10.2.1 Signal and Local Oscillator Coupling Methods

There are a number of ways of coupling the signal and local oscillator into a diode lattice. The circuit employed here is best illustrated by the lumped component version in Fig.44. The signal (ωq) is coupled in via an unbalanced to balanced matching transformer. The two series tuned circuits between this transformer and the diode lattice, present a pass band for the signal and a mainly reactive termination to the image and higher components. In practice neither the input transformer nor the series tuned circuits can be lossless. Ignoring for the moment the transformer losses, the higher the loaded Q value of the series tuned circuits, the greater the rejection of the image, but also the greater the signal loss in the pass band. This pass band loss L, directly affects the cpl since it represents a signal attenuation and it can be related to the tuned circuit Q by the well known formula:-

$$L(db) = 20 \log_{10} \left(1 - \frac{Q_L}{Q_o}\right) \quad .. \quad .. \quad .. \quad (9)$$

where Q_L is the working Q and Q_o the unloaded Q of the tuned circuit.

The image rejection depends on Q_L and $\frac{\omega q}{(2\omega p - 2\omega q)}$, so for the lowest cpl, the intermediate frequency ($\omega p - \omega q$) should be as high as possible, to allow a low value of Q_L and a high value of image rejection to be obtained at the same time. It must however be practicable to amplify the intermediate frequency with as low as noise figure as possible, in order to obtain a good system performance[21].

The result is, therefore, a three way compromise which must be solved for each individual application, especially with due regard to bandwidth considerations.

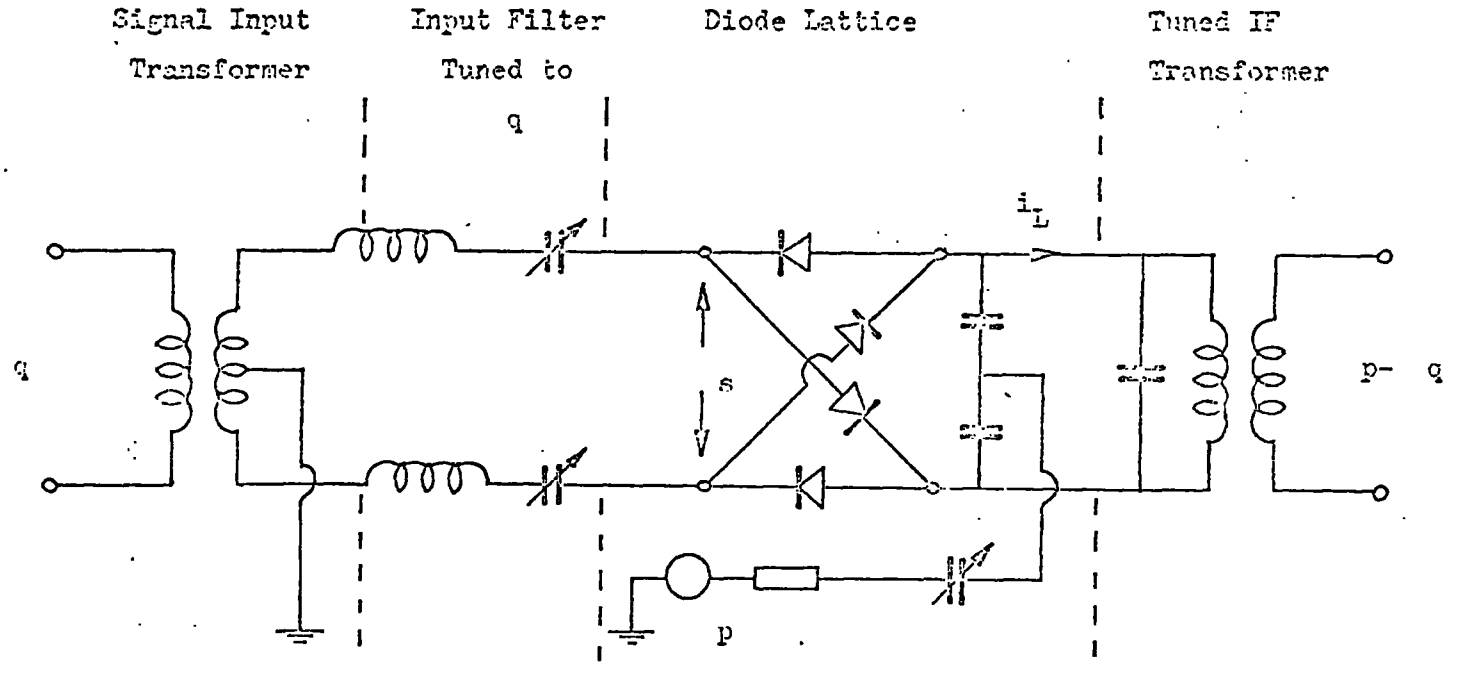

Fig. 44 Open - Circuit narrow band lattice Mixer Circuit.

In the case of the local oscillator circuit, however, power loss is less important than balancing of the drive current. Fig.44 illustrates the sinusoidal current drive circuit, which may be arranged at low frequencies using a series tuned circuit involving the whole lattice arrangement, or at microwave frequencies with tuning stubs. At high microwave frequencies, there may be some concern with minimising L.O. losses, in order to obtain high drive levels using the low power sources available.

10.2.2 The Diode Quad

The diode quad is wired in a ring configuration. The parameters of the actual diodes used are generally governed by commercial availability, and a balance has to be generally struck between those with high parasitic capacity and low r_s, and the opposite combination. Packaging is most important at microwave frequencies from the point of view of parasitics, and matching of diode characteristics is also of concern for best results. From the constructional point of view, the most important point is that the ring of diodes and associated capacitors should be considerably smaller than the wavelength at the frequencies used. For balanced conditions to prevail, the ring must be electrically symmetrical with respect to the signal I.F. and local oscillator circuits. At microwave frequencies this implies mechanical symmetry as well, due to the effect of stray reactances. The three degrees of symmetry required mean that a three dimensional layout is needed.

10.2.3 Intermediate Frequency Extraction

It may seem that because the intermediate frequency is usually the lowest frequency involved in a mixer, it therefore ought to be easiest to handle. However, the I.F. output of a mixer is at the lowest signal level of the entire receiving system, and losses here are probably more serious than at the signal input, due to the possibility of the I.F.

amplifier noise figure increasing when its input is mismatched. At present, in the experimental models built, the I.F. section consists of a wideband 70 MHz balanced to unbalanced transformer, to convert from the high lattice output impedance down to the standard 50 ohm measuring system. Choke lines are provided from the lattice to the transformer to reduce local oscillator leakage from the I.F. port. A conventional 70 MHz low noise amplifier is used for test purposes using bipolar transistors. It is hoped to develop a balanced I.F. amplifier arrangement, able to be directly connected to the diode lattice, in order to take advantage of the lower loss and noise figure possible with this arrangement. Elimination of the I.F. transformer would also pave the way to an integrated system of increased bandwidth.

11.0 4.5 GHz Practical Mixers

11.1 Mixer Measurements at Microwave Frequencies

11.1.1 Introduction

The usefulness of a microwave receiver is limited by its ability to discriminate between weak signals and noise. Associated with the signal, no matter what its source, is a noise power N:-

$$N = k\,T\,B \quad .. \quad .. \quad .. \quad .. \quad .. \quad .. \quad (10)$$

where K = Boltzmann's constant

T = Absolute temperature

B = Bandwidth.

The noise figure F of a receiver (sometimes called the noise factor), expresses its relative ability to amplify without introducing additional noise. It may be given as the ratio between the signal to noise ratio at the input, to that at the output:-

$$F = \frac{\frac{S}{N}}{\frac{S_o}{N_o}}$$

where $\frac{S}{N}$ is the input signal to noise ratio

$\frac{S_o}{N_o}$ is the output signal to noise ratio.

The effective parts of the receiver can be split into two sections as shown in Fig.45. The I.F. amplifier section is specified by the gain and noise figure. In the case of the mixer section, it would appear at first as if only the conversion power loss L would affect the noise performance. This would be so if the diodes introduced only the noise of their passive barrier resistances. Unfortunately, the current flowing in the diodes creates additional sources of noise of three main types:-

1. Noise in the series "spreading" resistance.
2. Shot noise at the barrier.
3. 1/f or "flicker" noise at low frequencies (generally considered to be a surface effect).

The usual way of introducing this additional noise is to define an output noise ratio of the mixer:

$$t = \frac{T_1}{T} \quad .. \quad .. \quad .. \quad .. \quad .. \quad .. \quad (12)$$

where T_1 is the effective absolute noise temperature of the mixer. Normally, using intermediate frequencies in the MHz region, and Schottky barrier diodes made from gallium arsenide, this ratio is very low ($\approx$ 1.1 is quoted).

Returning to formula (11), the input noise of the mixer is simply the thermal noise as given by formula (10). The signal power output of the mixer is:-

$$S_o = \frac{S}{L}$$

and the output noise power is:-

$$N_o = k T_1 B.$$

Substituting into formula (11), the noise figure of the mixer becomes simply:-

$$F_m = Lt.$$

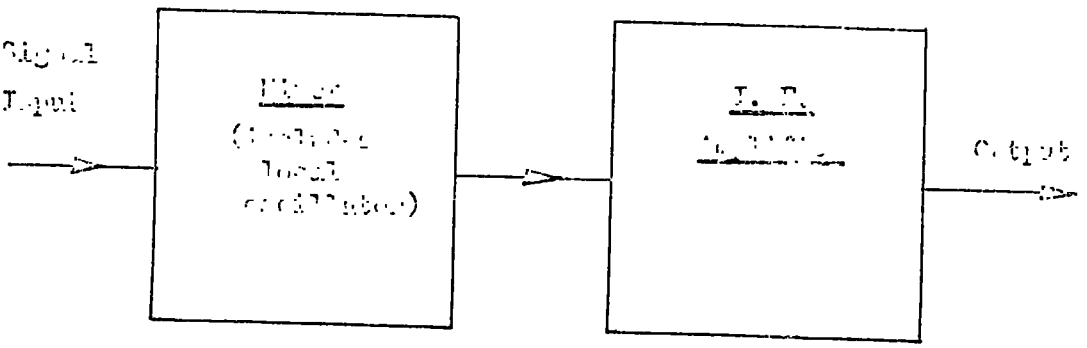

Conversion power
loss = L dB

Noise Figure
= $F_{I.F.}$

Noise temperature
Ratio = t

Gain = $G_{I.F.}$

Fig 45a Simplified Receiver Block Diagram

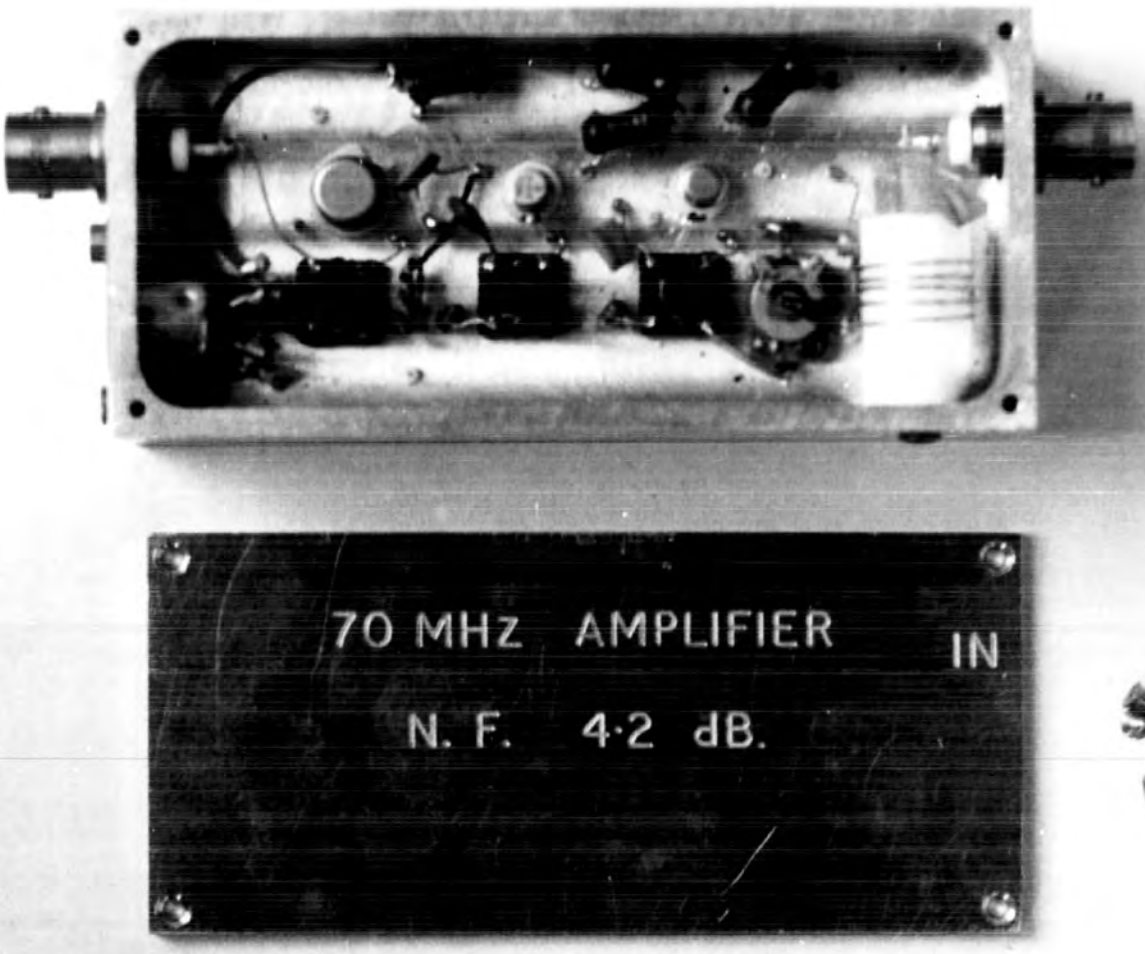

Fig. 45b I.F. Amplifier

The overall receiver noise figure is ascertained by considering the mixer and I.F. amplifier as two networks in cascade[31] (and assuming the noise bandwidth of the mixer exceed that of the I.F. amplifier):-

$$F_{(overall)} = F_m + \frac{F_{IF} - 1}{G_m}$$

Now F_m = Lt and Gm = $\frac{1}{L}$

$$F = L(t - 1 + F_{IF}) \quad .. \quad .. \quad .. \quad .. \quad .. \quad (13)$$

which is the Friis formula as mentioned in Chapter 1.

It is therefore evident that the noise figure of a receiver is determined to a large extent by the conversion power loss of the mixer. The noise temperature ratio t is generally governed by intrinsic device characteristics, although it can be reduced by lowering the current drive flowing in the diodes. This usually increases L and defeats the object of the exercise. Apart from this compromise, the I.F. output impedance of the mixer may enter into the formula to a small extent, which could influence the I.F. noise figure adversely in some cases. The only other point concerning the I.F. amplifier is that the gain (G_{IF}) does not affect the receiver noise figure, although the amplifier noise figure (F_{IF}) is itself normally a value obtained from cascaded stages, and is therefore as complex a subject in its own right, as the receiver noise figure.

To sum up, we need measurement of mixer conversion loss and noise figure to know how well it would perform in a receiver system. These measurements are considered in Section 11.1.2 and 11.1.3. Also it is useful to know how the mixer is performing as regards theoretical predictions. This is covered in Section 11.1.4, so far as these conditions can be measured accurately at microwave frequencies. Finally in Section 11.1.5, optimisation techniques are discussed in order to discover how to best operate a mixer in a given application. This is becoming of some importance, as more demands are made for receiver

systems with special requirements, such as bandwidth or cross-modulation performance. In these cases, optimisation for minimum noise figure as considered here, may not be the best approach.

11.1.2 Diode Measurements

In a mixer, the diodes perform in a complex situation. This situation should follow directly from the theory which assumes a given diode model. In the present case the semiconductor diode is considered to be predominantly a time-varying resistance, and there are three constants which characterise its performance. There are, r_b the incremental resistance at the origin, r_s the spreading resistance, and I_s the reverse saturation current constant. Furthermore, to assess the diodes potential at microwave frequencies, parasitic capacity and lead inductance should be known, as mentioned in Section 9.4. The ratio r_s/r_b denoted by r'_s, is used to describe the quality of the diode and I_s is incorporated in the definition of the local oscillator drive X.

The information supplied by manufacturers of diodes tell little about the diode, because the conditions under which the measurements are made are so restricted and inconsistent between manufacturers. Indeed, in some cases, it is the mounting rather than the diode which is being measured. One trouble with the values specified is that they cannot be measured directly. The resistance r_b cannot be, because any measuring D.C. would shift the operating point of the device from the origin. Similarly for A.C. measurement systems because of the non-linearity of the measured region. To make a direct estimate of r_s requires a high forward current that could destroy the device or heat the junction, thus changing the conditions of measurement. I_s, on the other hand, is usually masked by surface leakage currents (it can be as low as 10^{-14} amps), and quite impossible to measure. If r_b is known, however, the relationship $r_b = \frac{kT}{qIs}$ can be used.

The best estimate of r_h is possibly that obtained by A.C. bridge methods, obtaining a balance whilst successively reducing the bridge excitation voltage. Another method used at Durham is to plot the characteristic V-I curve for the diode, and use a computer to obtain an extrapolation to the origin. A typical value obtained for a GaAs diode is 1.3×10^{11} ohms, whilst point contact diodes have shown values as low as 7.5×10^{3} ohms, both diodes incidentally, were sold for X band (10 GHz) use.

The r_s can be measured using a pulse technique[32], where A.C. or D.C. resistance measurements are used whilst the device is pulsed into the high forward conduction region. Heating effects are reduced directly with the duty cycle of the pulse, but has still to be taken not to damage the device. A computer extrapolation is also useful to obtain a second value of r_s.

Parasitic capacity and inductance is difficult to measure because they depend to such a degree on the mounting geometry used. An estimate can be made numerically knowing the device geometry, and results compared with Smith chart impedance measurements and A.C. bridge values, if these can be obtained.

11.1.3 The Power Meter and its Application

The conversion power loss of a mixer is defined as the ratio of power supplied at the signal frequency to the power output at the intermediate frequency, under matched conditions in both cases. The signal level at which a mixer is fed from an aerial system lies between 10^{-14} to 10^{-3} watts, which is a vast range of which only the top few orders can be used for measurements to any degree of accuracy. Although it may appear to be possible to measure signal level, attenuate it a known amount, and then amplify the I.F. output, poor gain stability of

the amplifier will vastly reduce the accuracy. Considerable negative feedback can give a suitable gain stability in an amplifier, but this technique is not normally employed in low noise amplifiers at frequencies above 1 MHz. The trouble here lies with the magnitude of the loss we wish to measure. An accuracy of 0.2 dB demands 0.1 dB accuracy in both attenuator and amplifier gain.

Since we must measure power levels at two different frequencies, it would seem desirable to use the same method at both frequencies, in order to eliminate differential errors between the microwave power measuring system and the low frequency system. Luckily, power is one of the few fundamental quantities that can be measured directly and conveniently at microwave frequencies. Most of the instruments used are based on power responsive (usually thermal) elements, which can be used at the Intermediate frequency as well as at the signal frequencies.

Normal commercial instruments use one of two thermal effects. Either Calorimetric or Bolometric. Calorimetric types measure the temperature rise of some substance heated by the R.F. energy. Often the temperature rise is measured electrically with a thermocouple. The Bolometric instruments measure the change in electrical characteristics of a wire or thermistor which is heated itself by the R.F. energy, low frequency resistance variations usually being used. A bridge circuit can be employed in both cases, with dummy unheated elements used to balance out ambient temperature effects. Both types of power meter are of approximately equal merit when it comes to measurement of power at the I.F. and signal frequencies in the present application. The one used was the Hewlett - Packard 431C Thermistor type. This was used at a full scale sensitivity of 0.03 milliwatts, and the circuit block diagram used for conversion power loss measurements is given in Fig.46. The ancilliary items used are to minimise error, the main sources of

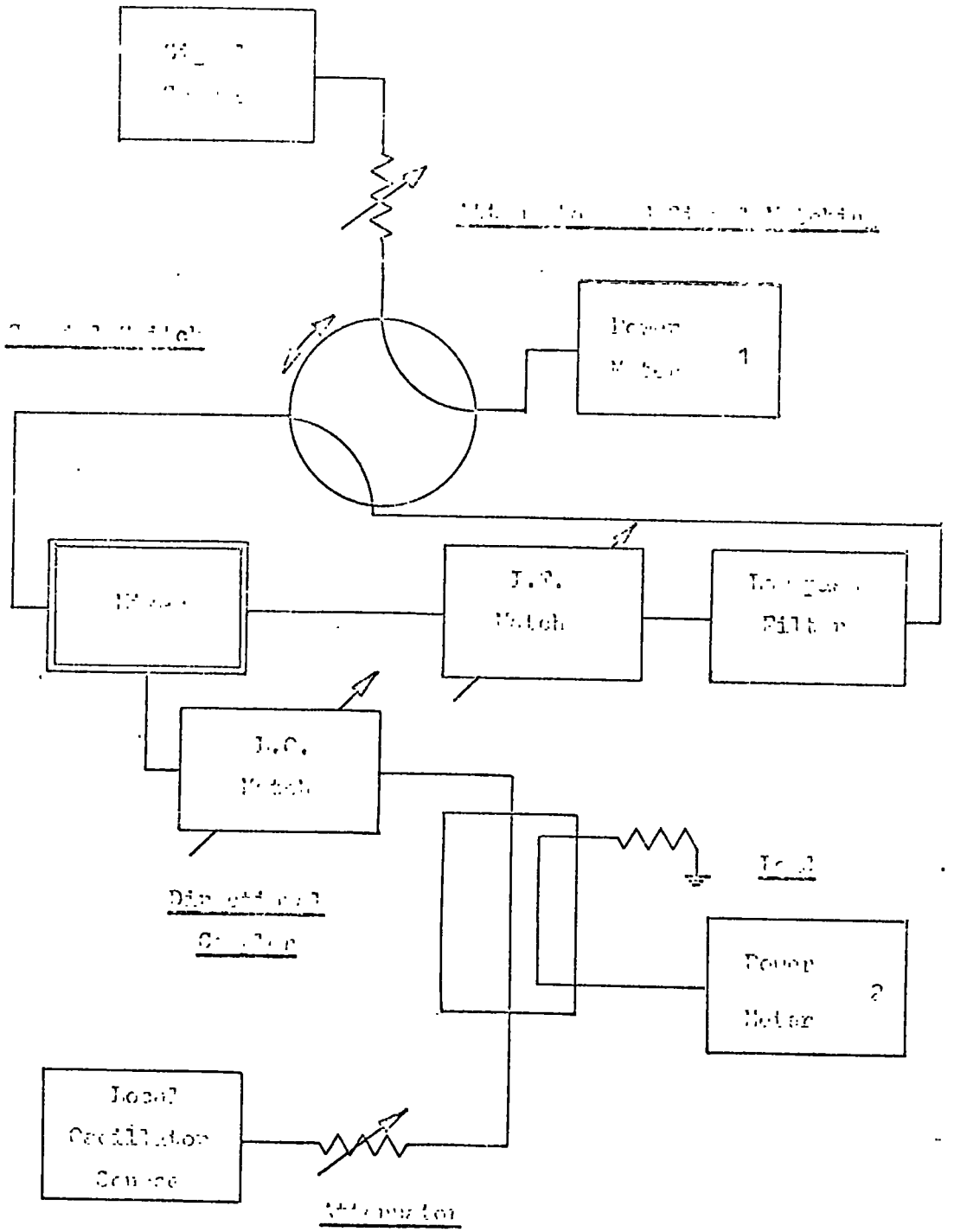

Fig 46a

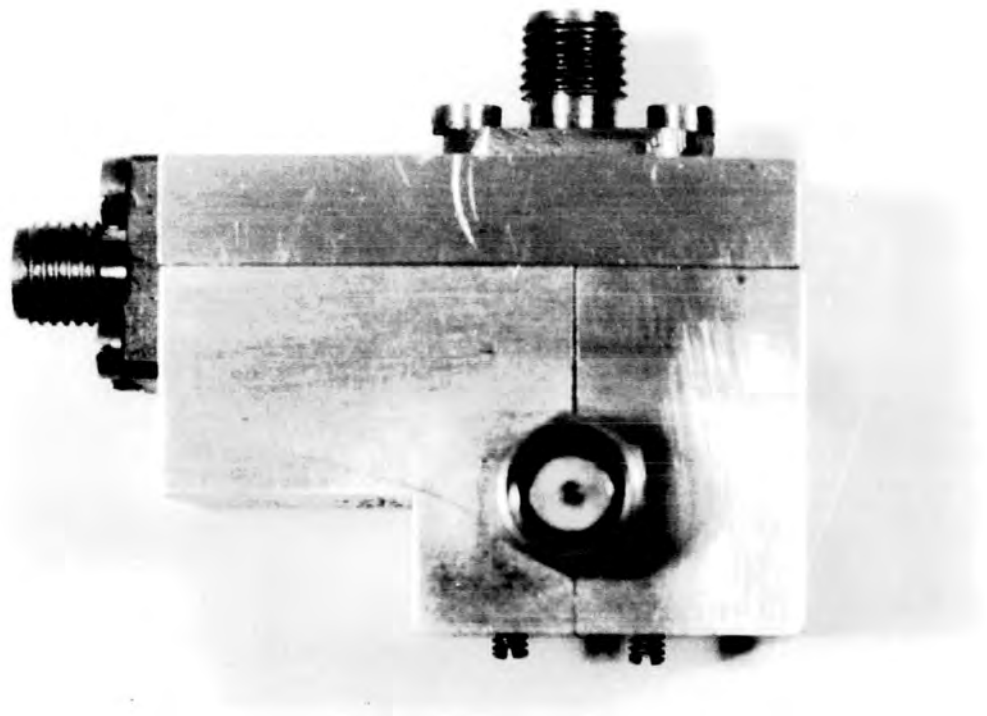

Fig. 46b The Complete Mixer

which are mentioned below.

1. Mismatch Error

Due to a non-conjugate match between power meter and source. In Fig.46 the matching networks minimise this error at the expense of additional loss. This loss was of the order of 0.2 dB and can be measured for a 1:1 match in a transmission line system[33], and this value can be added to the total transmission loss of the measuring system.

2. R.F. Losses and D.C. to Microwave Substitution Error

R.F. losses account for the power loss between the power meter connector and the thermistor lead.

Substitution error is caused by the difference in heating effect at low and high frequencies on the thermistor lead. This occurs due to the different spacial distribution of current and resistance in the leads at high frequencies. These two effects are combined into a frequency calibration factor for the power meter (it is a matter of around 3% at 4.5 GHz).

3. Instrument Error

An error in either meter calibration or zero drift, which is caused by thermal unbalance in the thermistor bridge circuit. In Fig.46 the same meter is used for both signal and I.F. measurements, and the zero drift can be checked between each measurement. With these precautions, the total error should not exceed 0.2 dB using the arrangement given.

11.1.4 Noise Measurements

Noise figure is a term applied to any general four terminal network, which is defined as the ratio of the actual noise power output of the network to the output that would exist if the network were

noiseless; i.e. the noise originated only from the source connected to its input terminals.

Other ways of describing receiver noise performance, such as tangential sensitivity, and minimum discernible signal, are mostly subjective rather than objective. This is especially true of receiver systems working at frequencies above 30 MHz, where the atmospheric noise fed to the system by the aerial is likely to be below that created by the receiver itself. Similarly the signal to noise ratio of a receiver is a worthless term since it is dependent on bandwidth as well as noise performance.

The basic technique for obtaining noise figure is to measure the output power of the network for two input power conditions. Input power changes can be produced in two ways. The first method involves a change in the operating conditions of the source, such as varying the current or voltage supplied. The second method uses a precision attenuator to reduce source power supplied. In this case, however, the calibration may not be accurate enough and the attenuator itself is a noise producing network so its temperature of operation must be known accurately, a quantity which is by no means easy to discover.

There are three commercial types of noise source suitable for use at 4.5 GHz. The primary standard is the Johnson noise produced by a resistor at a known temperature. It may also be claimed that the thermionic noise diode is also a primary standard, since the noise power of a temperature limited electron stream can be computed. However frequency limitation such as transit time rule this type of source out at 4.5 GHz. The third noise source and the one used in this application is the gas discharge tube. In 1949 Mumford[34] published the results of his work which showed that the positive column of a gas discharge could be used as a simple and precise noise source.

He made the hypothesis that a tube giving a monochromatic light source, gives out noise in the microwave bands that is equal to that which would be produced by a black body with a maximum radiation peak at the frequency of the monochromatic light output. Although this was later disputed qualitatively, the noise output is clearly well in excess of that given by the hot load method, where the maximum temperature limit is often only 500°K. The gas normally used is argon or neon, and the pressure is closely controlled to produce a positive column discharge throughout the tube. The tube is mounted in a transmission line which couples to the plasma of the discharge. This source can then be calibrated against the hot load as a standard, the change of noise output with life being only about 0.05 dB for 2000 hours use.

The actual instrument used was the Magnetic AB type 113 with an argon tube. The system block diagram of this instrument is given in Fig.47. The comparison of noise output of the mixer is made automatically by switching the noise source and measuring system at 500 Hz. The result is displayed on a meter directly in terms of noise figure. The main error from instrumentation inaccuracies, is that caused by the variation of source impedance presented to the mixer with the discharge tube on and off. This error can be minimised by good design and is only of the order of 0.1 dB in the present case.

If we are to assume that instrument errors will always cause an uncertainty in such a measurement, the greatest accuracy will occur when the noise source can provide an excess noise ratio approximately the same as the noise figure of the system being tested. Since the argon discharge tube produces an excess noise of about 15 dB (above that produced by the load resistor at 290°K), the range is somewhat high for the low noise mixer considered here. In fact the hot load

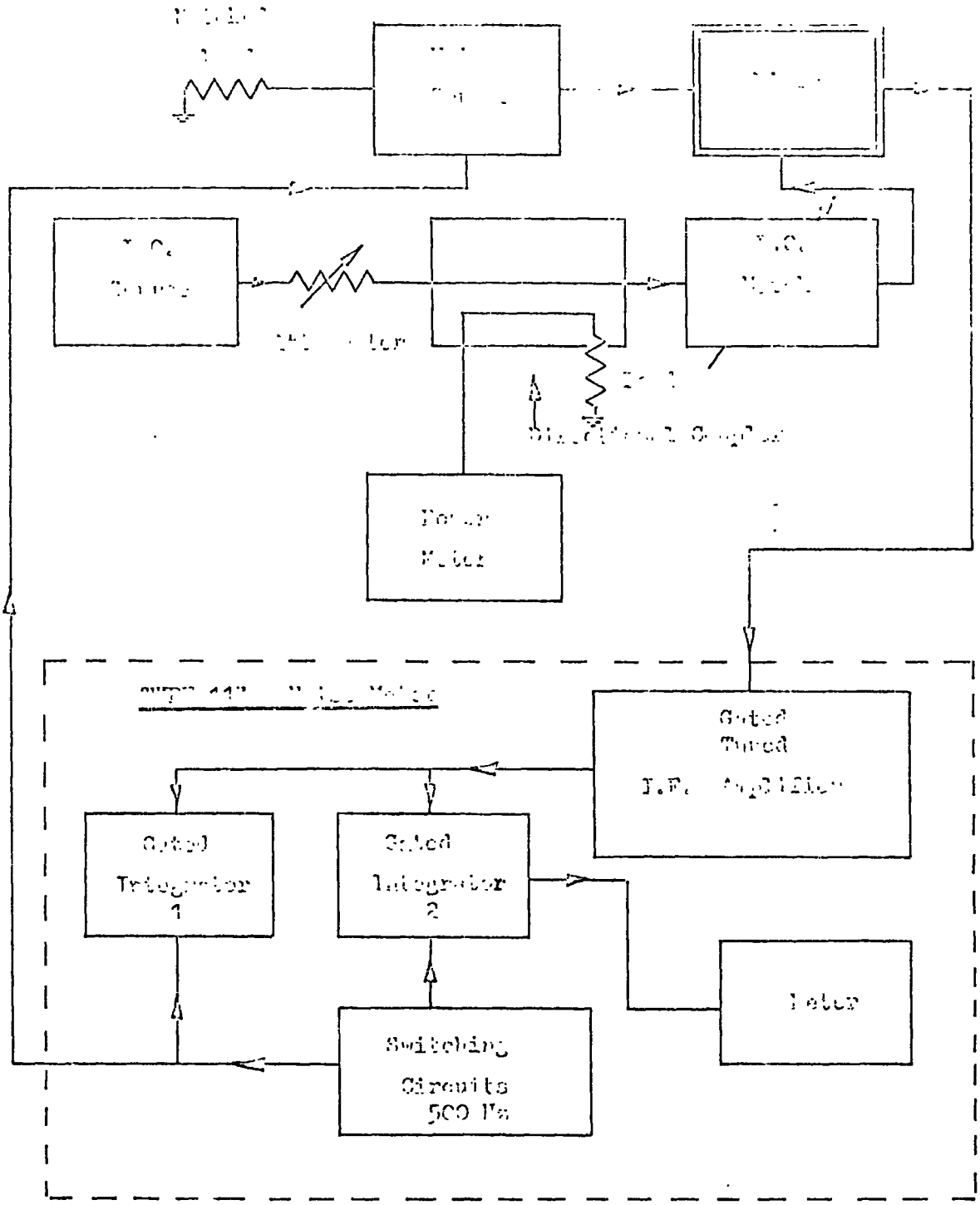
Gated
Tuned
I.F.
Gated
Integrator
1
Gated
Integrator
2
Switching
Circuits
500 Hz

Fig 47 A

Fig. 47b Noise Meter and Tube

would provide a better source except for two severe setbacks. Firstly the resistance of the load must not vary significantly over a very wide range of temperature. Secondly the load resistor, which may be quite large, has to be kept at an even known equilibrium temperature, despite the output coupling which is connected to the outside world. Automatic temperature switching in a similar method to the gas tube is impossible, so instrument drift has to be accounted for while cooling or heating the load, and waiting for equilibrium to be obtained. For these reasons, the accuracy quoted of 1 dB, using the discharge tube and 113 instrument, does seem reasonable, although work is perhaps needed here if lower noise figures were to be measured.

11.1.5 Mixer Operating Conditions

In the present context, the operating conditions involve the voltages and currents flowing in the lattice of diodes and the imbedding circuit. Measuring these quantities allows a comparison with theoretical predictions, and it can also give some insight into possible circuit improvements.

At low frequencies the measurement problems are few. High impedance probes cause little perturbation at the operating conditions, and both magnitude and waveform measurements can be made using an oscilloscope. At higher frequencies probe impedances can cause an appreciable effect on the circuit, and at microwave frequencies, even if a suitable high impedance probe were available, it would be necessary to analyse the information gathered closely. This is because of the finite size of the measuring system in comparison with the wavelength used.

Power and impedance are the two fundamental quantities which can be measured at microwave frequencies. The application of power measurements have already been considered, and it is impedance measurements that have to be used to determine the mixer operating conditions. To see how these measurements can be made, consider a source of internal resistance Ro feeding into a load of magnitude Z. Z can be found in two ways, using power measurements as a basis. Firstly the power transmitted to Z and the power reflected from it can be found by using a directional coupler. This will give a value for $|Z|$ from power transmission equations, which can be obtained by means of finding the VSWR in the transmission line (of characteristic impedance Ro) coupling the source to the load. A slotted line is normally required for this measurement, and if the electrical length from slotted line to the load is known, the phase as well as the magnitude of Z may be obtained. If the mixer under test were the unknown load, the value of Z found would be the input impedance of the cavities. To discover the input impedance of the diodes the cavity transformation ratio is required. This can be found knowing the length of the cavities and the frequency, combined with the coupling dimensions. More practically, the test block as mentioned in Chapter 5 may be used with the known 100 ohm load. As may be noted the transformation ratio depends on frequency, and may be varied this way as an alternative to the three-stub tuner in Fig.46. Both methods have been used and give similar results. Although the tuner may be eliminated by using the variable frequency method, calibration errors and drift of the signal generator still produce overall uncertainties.

The output impedance of the lattice is measured at the I.F. frequency (70 MHz). The balanced output transformer is of known transformer ratio and is connected via a matching unit and a low pass

filter to the power meter. The matching unit is of the Pi type[35] using lumped components, and the general circuit is shown in Fig.48. The component values were chosen for a loaded Q value of about 10 in the prototype in order to obtain the lowest loss of 0.2 dB or less. There are several ways of analysing the circuit operation, one way is to describe the component values by means of three equations. for a working angular frequency ω:-

$$-\frac{1}{\omega C_1} = \frac{R_s}{Q_L}\left(1 + \sqrt{\frac{R_L}{R_s}}\right) \quad .. \quad .. \quad .. \quad .. \quad (14)$$

$$\frac{1}{\omega C_2} = \frac{1}{\omega C_1}\sqrt{\left(\frac{R_L}{R_s}\right)} \quad .. \quad .. \quad .. \quad .. \quad (15)$$

$$L = \frac{R_s}{Q_L}\left(1 + \sqrt{\left(\frac{R_L}{R_s}\right)}\right)^2 \quad .. \quad .. \quad .. \quad (16)$$

where the components are identified in Fig.48.

It can be seen that eqn. (15) can be written:-

$$\frac{R_L}{R_s} = \left(\frac{C_1}{C_2}\right)^2 \quad .. \quad .. \quad .. \quad .. \quad .. \quad .. \quad (17)$$

which is independent of frequency and the Q.

The values of C_1 and C_2 which can be calibrated, give the ratio between R_L and R_s directly.

This network can also be used to tune out reactive parts of the impedance. In the present case these should be tuned out by the input and output transformers when correctly adjusted.

11.2 Experimental Results

11.2.1 Input and Output Impedances

Measurements are available from six separate mixers. Details of these are tabulated in Figs. 49-53 and they will be referred to

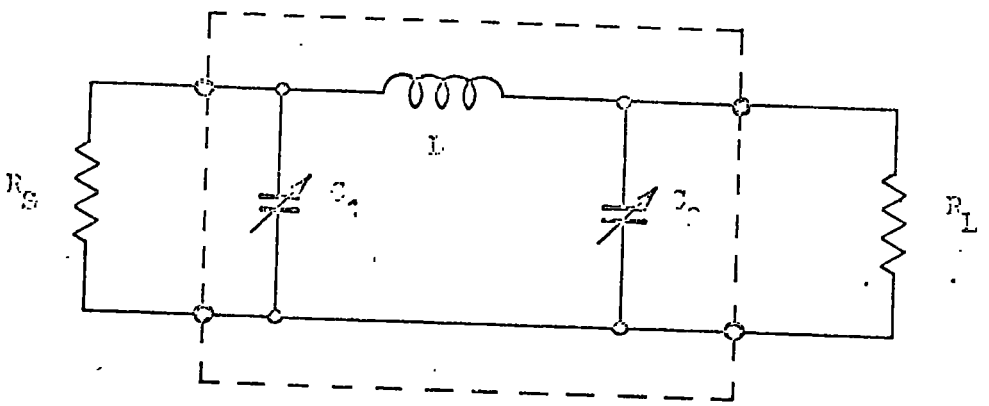

Fig 48 Pi - Network Matching Circuit

by the number given to them in these tables.

Theoretical input impedances are given in Figs.54-56 in the form of normalised input impedance against drive level graphs for the three cases of a purely resistive lattice mixer. Introducing parasitic diode capacitance causes a reduction in the now complex input impedance (Fig.57). It is interesting to relate this graph to the local oscillator level directly as in Fig.58. Here the experimental points are for mixer 2.

Purely experimental input and output impedances are plotted for mixers 3-6 in Figs. 59 and 60, using the methods outlined in Section 11.1.5. The values quoted above 10^3 ohms need treating with care, because of the measurement difficulties (they are measured in a 50 ohm system), and because the image rejection of the mixer suffers for these high values of input impedance. Two other points are worth mentioning from these results. Firstly, the ratio between input and output impedances for any of these mixers at any drive level appears to be a constant. Lattice mixer theory[36] supports this value of $\frac{4}{\pi 2}$, and as indicated in Section 9.4, this should be almost invariant with parasitics or drive level changes. Given the wide variation of diode parasitics and effective drive levels covered by Figs. 59 and 60, this value seems to hold within measurement uncertainty.

The second point is illustrated by the difference in slope between the Gallium Arsenide mixers (3 and 4) and the Silicon diode mixers (5 and 6). This would indicate a better quality factor r'_s $(= \frac{r_s}{r_b})$ for these diodes. Although the r_s value is higher for the GaAs diodes, the calculated r_b value is so much higher than that for the Si diodes, one would expect an even better quality factor. In

Fig. 49a Experimental Mixer Details

Characteristic	Mixed Number					
	1	2	3	4	5	6
Mechanical						
Arrangement Drawings. Figs	50-53	-	22-28	22-28	22-28	22-28
Cavities						
Diameter cm.	0.9	0.9	0.6	0.6	0.6	0.6
Spacing cm.	1.25	1.25	0.8	0.8	0.8	0.8
Characteristic Impedance Zo ohms	86.5	86.5	65	65	65	65
Electrical loss at Resonance dB	1.2	1.4	0.8	0.8	0.8	0.8
Image Rejection (70 MHz I.F. dB)	28	30	15	15	15	15
I.F.						
Centre frequency MHz	75	75	68	68	68	68
Bandwidth (-3 dB) MHz	15	15	12	12	12	12
System loss dB	0.7	0.7	0.4	0.4	0.4	0.4

Fig. 49b Experimental Mixer Details - Contd.

Characteristics	Mixer Number					
	1	2	3	4	5	6
Mechanical						
Arrangement Drawings. Figs	51	-	26	27	28	28
Diodes Mechanical						
Manufacturer	Mullard	H.P.	A.E.I.	A.E.I.	H.P.	H.P.
Type Number	148 CAY/A	2711	DC 1303	DC 1301	2276	2277
Junction type	Schottky	Schottky	Schottky	Schottky	Schottky	Schottky
Material	GaAs	Si	GaAs	GaAs	Si	Si
Package	LID	Ceramic	Stripline Single	LID	Stripline Quad	Stripline Quad
Diodes Electrical (In situ)						
rb Calculated from $\frac{kT}{qIs}$	10^{11}	$5x10^7$	10^{11}	10^{11}	$3x10^7$	$5x10^7$
r_s	15	9	28	20	10	15
Lp nH	,65	1.0	1.0	0.8	0.6	0.6
Cp pF	0.15	0.15	0.2	0.15	0.3-0.6	0.23-0.4
Cj pF (if separable from Cp)	0.1	0.15	-	0.1	0.1	0.1

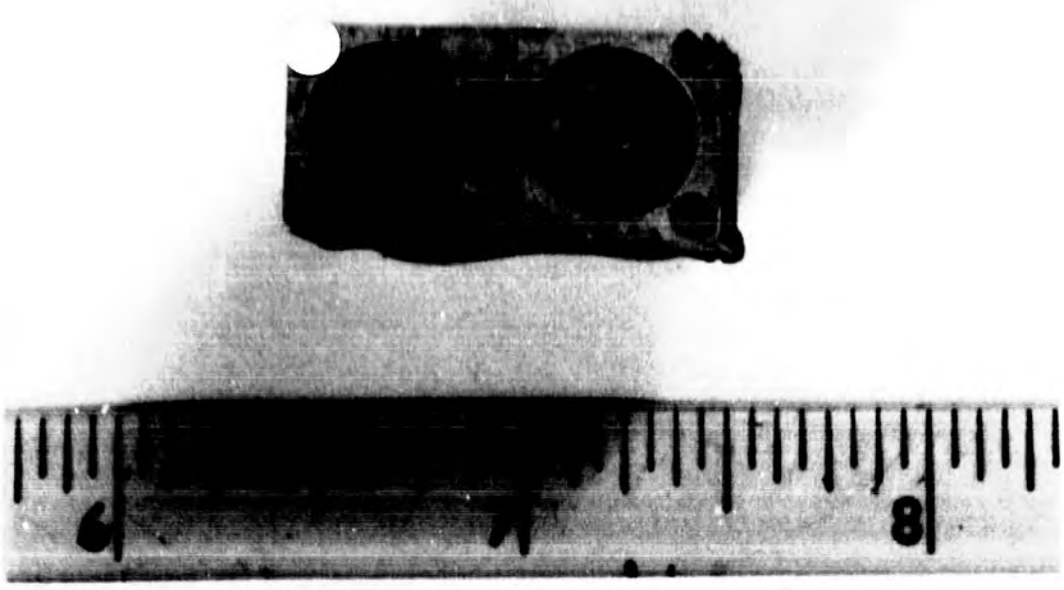

Fig. 50 Mixer Cavities (Mixers 1 and 2)

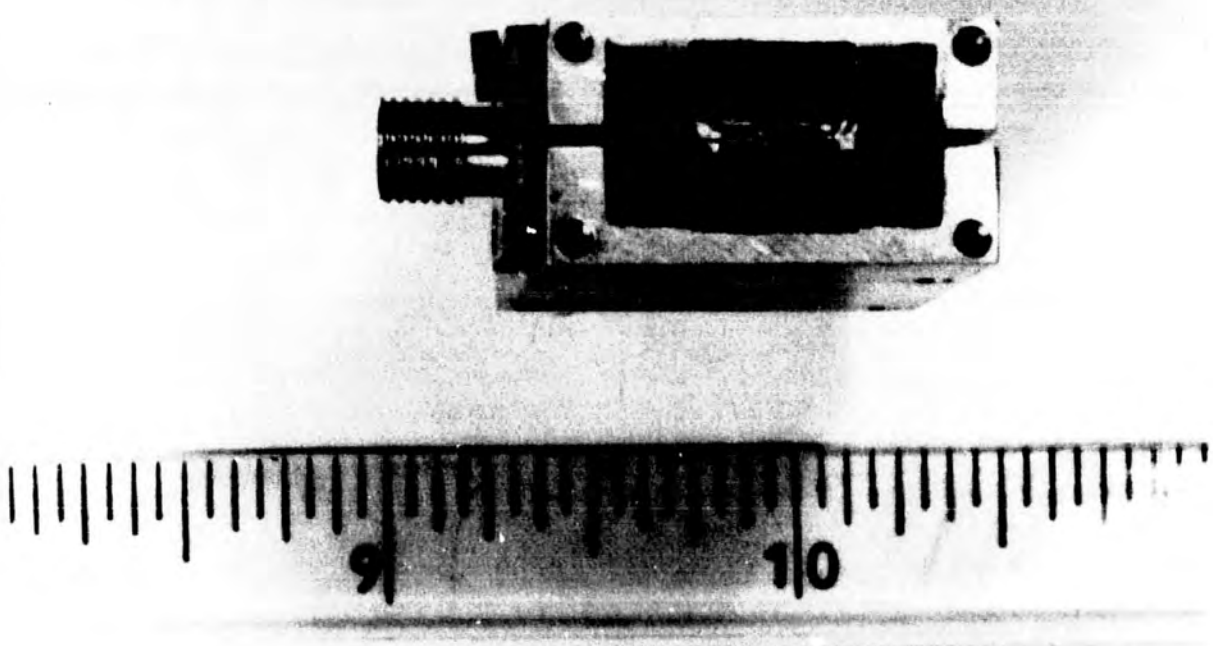

Fig. 51 Diode Substrate (Mixer 1)

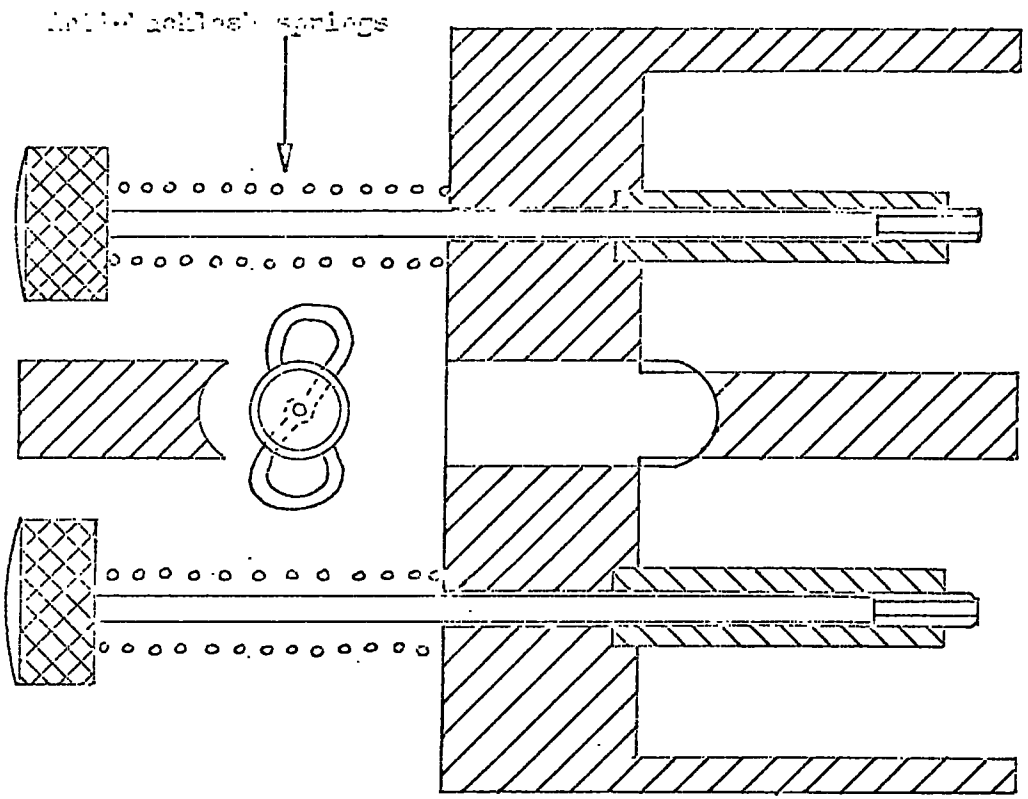

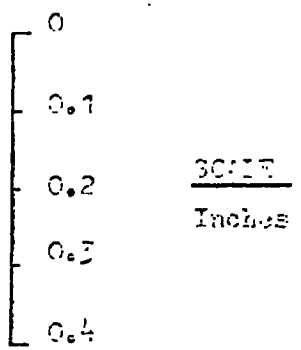

Material:- Brass Silver plated

Fig 52 Cavity Drawing

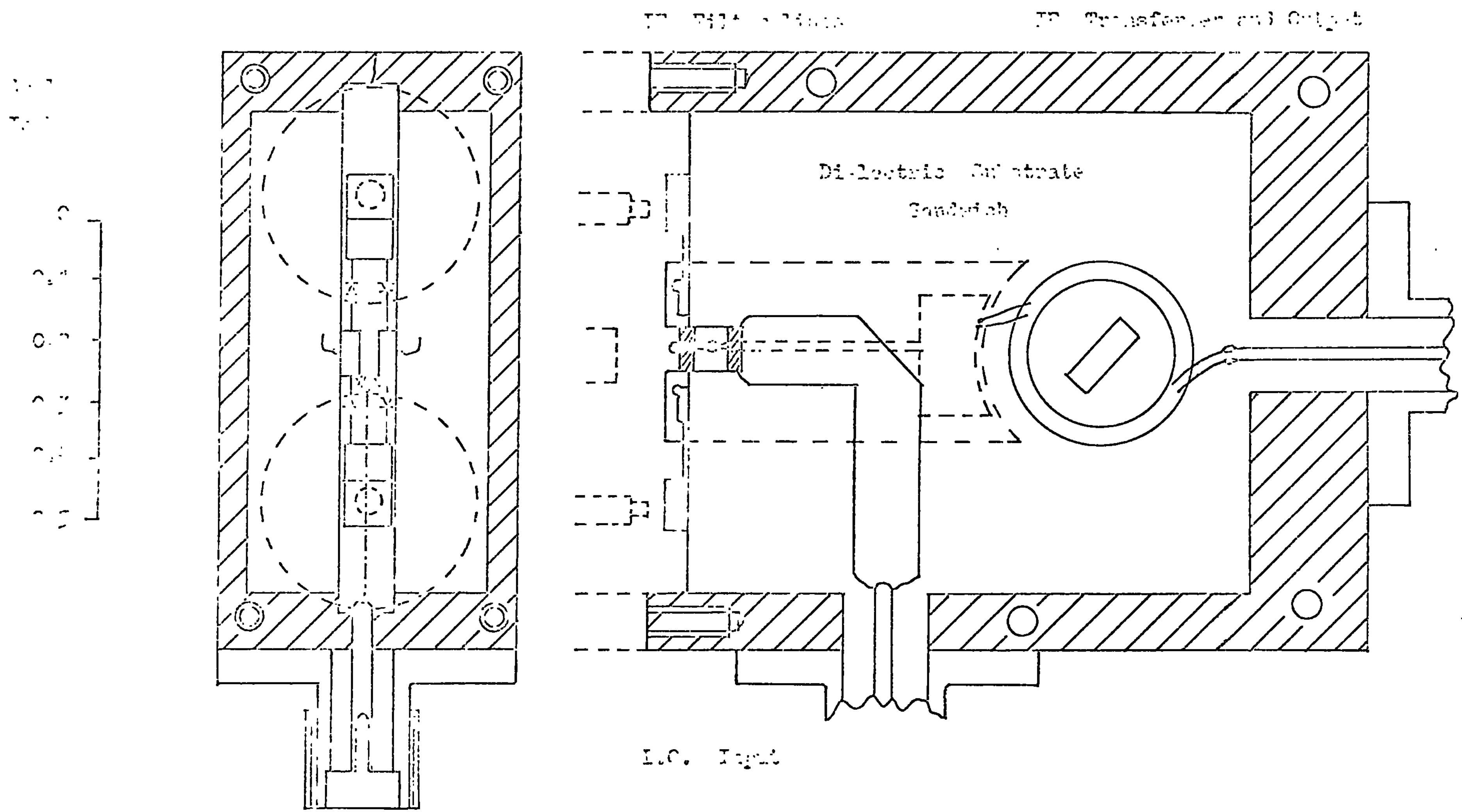

Fig. 53 Mixer Drawing

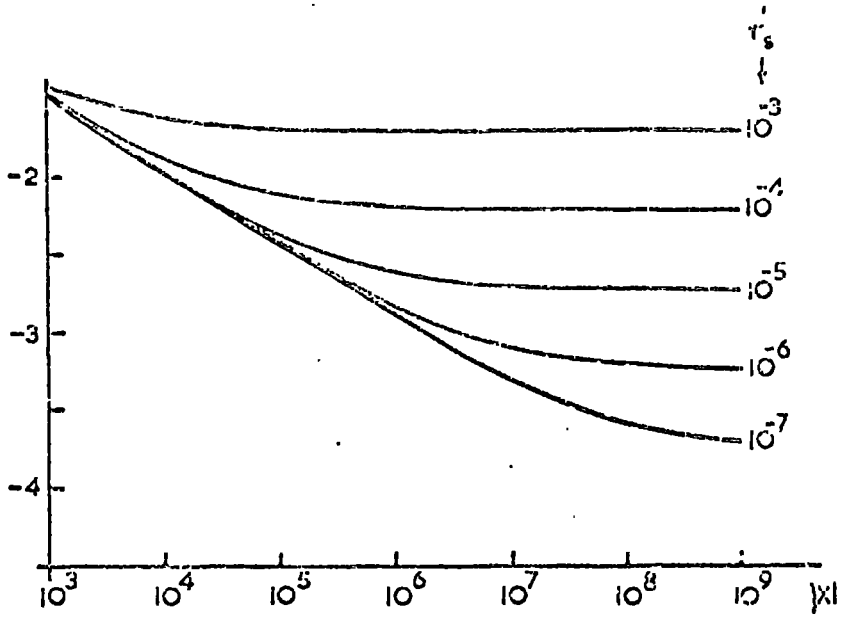

Fig. 54
NARROW-BAND OPEN-CIRCUIT MIXER

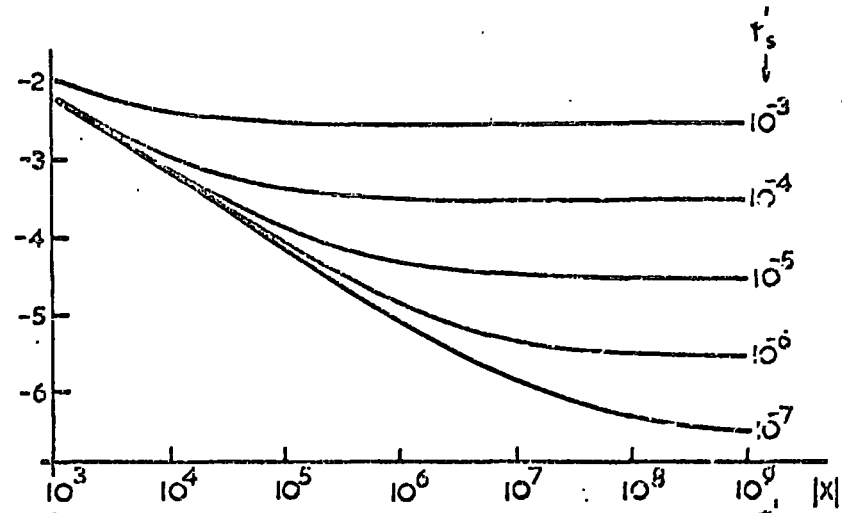

Fig. 55
NARROW-BAND SHORT-CIRCUIT MIXER

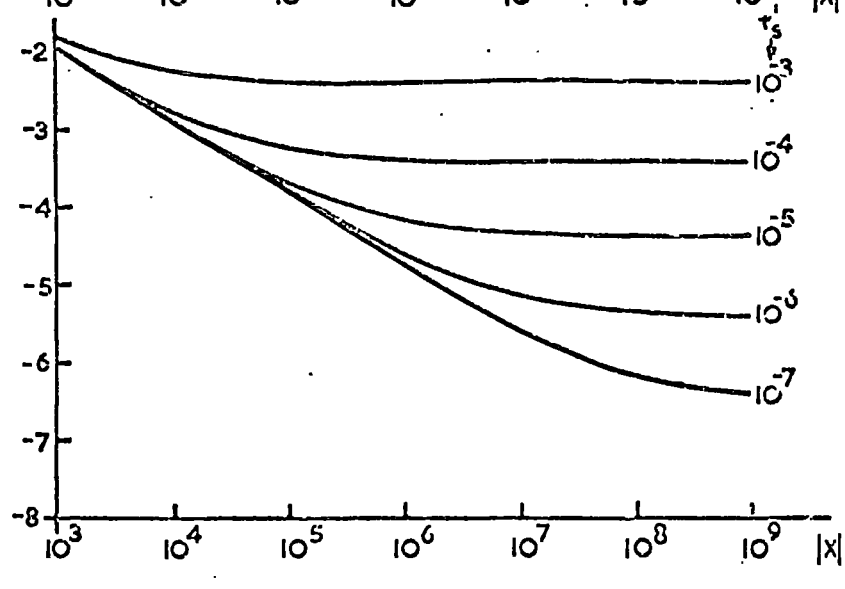

Fig. 56
BROAD-BAND MIXER

OPTIMUM INPUT RESISTANCE AS A FUNCTION OF THE L.O. DRIVE AND QUALITY OF THE DIODES.

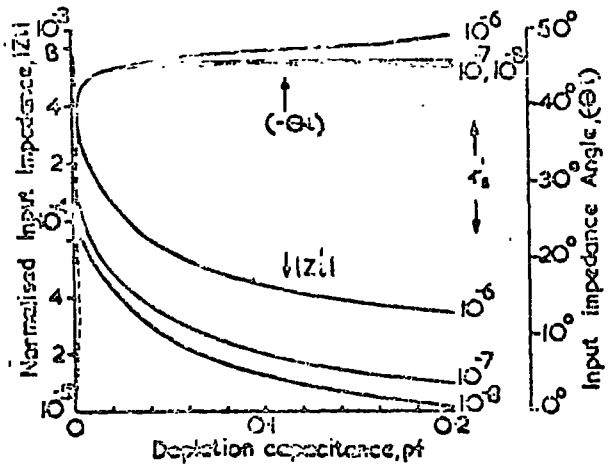

Fig 57 The Effect of Depletion Capacitance on Input Impedance

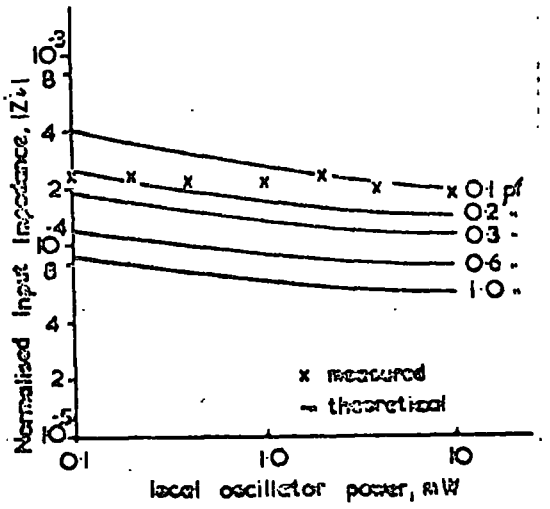

Fig 58 Magnitude of Input Impedance under matched conditions

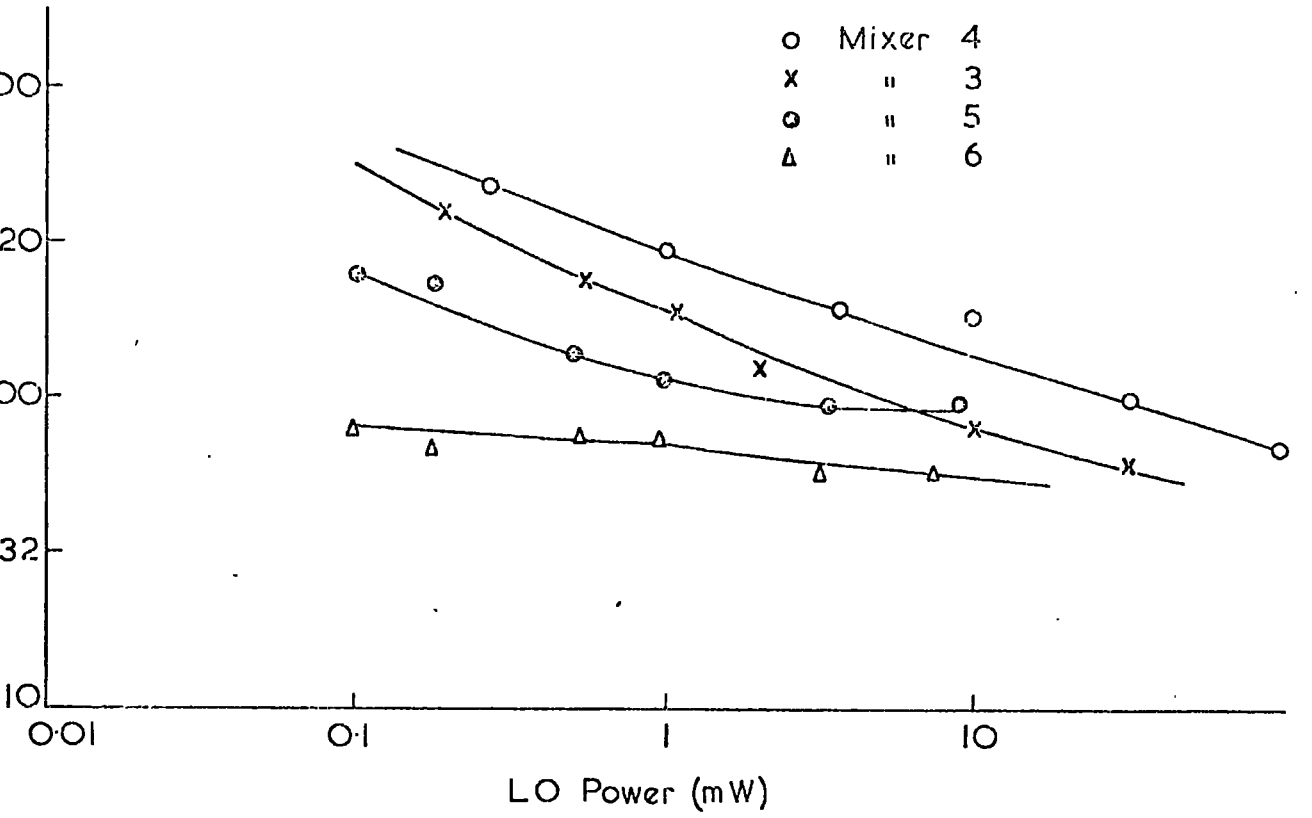

Figure 59 Mixer Input Impedances

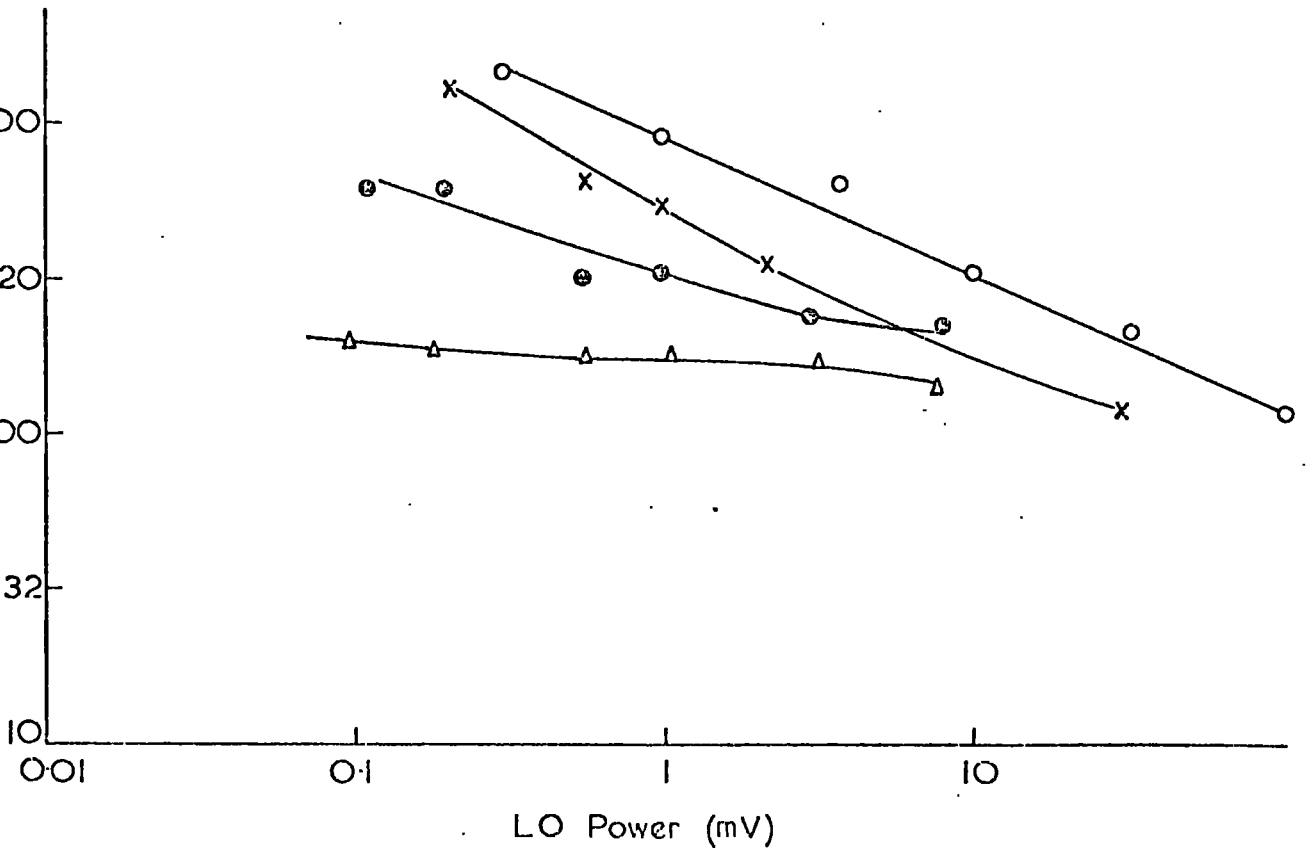

Figure 60 Mixer Output Impedances

practice, the leakage resistance of the GaAs diodes is much higher in proportion to r_b (10^{11} ohms) than it is in the case of the Si diodes where r_b is only 10^7 ohms or so. A significant reason for this is found in studying the junction technology. In the case of silicon, passivation using SiO_2 is obviously more successful than that deposited on the alien surface of GaAs. The better technology of silicon device production also allows better accuracy of junction characteristics, which are critical from the point of view of matching a quad of diodes. This is illustrated in Fig.61, a microscope photograph of a GaAs diode used in mixer 1, the junction area is 1 μm across. The effective value of r_b is therefore much less than that calculated from $\frac{kT}{qIs}$ where Is is obtained from diode forward characteristic measurements. Measuring r_b directly is very difficult, due to the measuring voltage or current changing the operating point of the diode away from the origin, where by definition no current can flow. The best method relies on extrapolation from both forward and reverse characteristics, but due to the rapid change of resistance around the origin this too is inaccurate.

11.2.2 Conversion Power Loss

The theoretical CPL for purely resistive action mixers was shown in Figs. 38, 39 and 40. Taking these values as a basis, we must add a contribution due to the parasitic capacity of the diode. Fig.62 gives these contributions for various capacitance values and two sets of diode parameters which are typical of the types used in practice. The actual experimental values of CPL are given in Figs. 63 and 64 for the Gallium Arsenide and Silicon diode mixers respectively. The conversion power loss is plotted for all six mixers against delivered local oscillator power. This is for

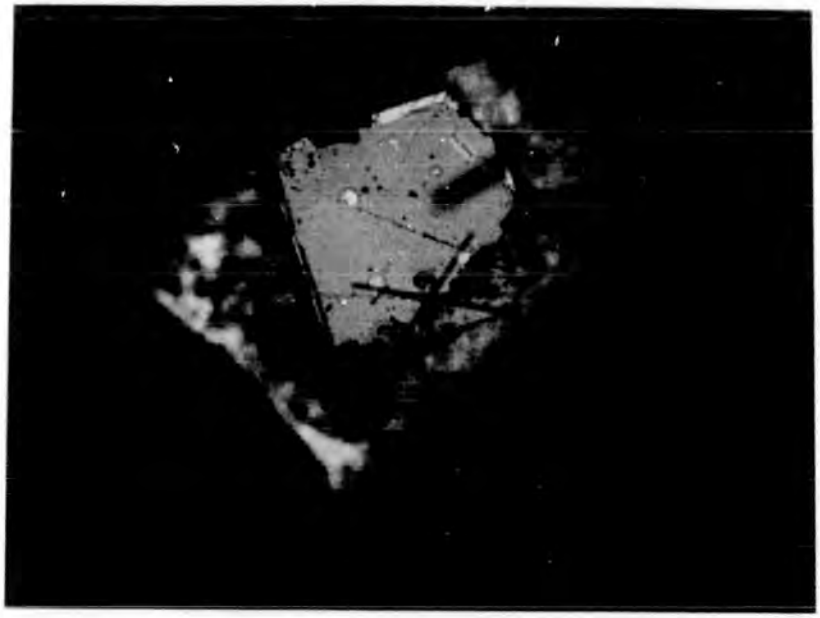

Fig 61 GaAs Diode Chip x 200

Fig 62 Predicted Loss due to Diode Capacitance

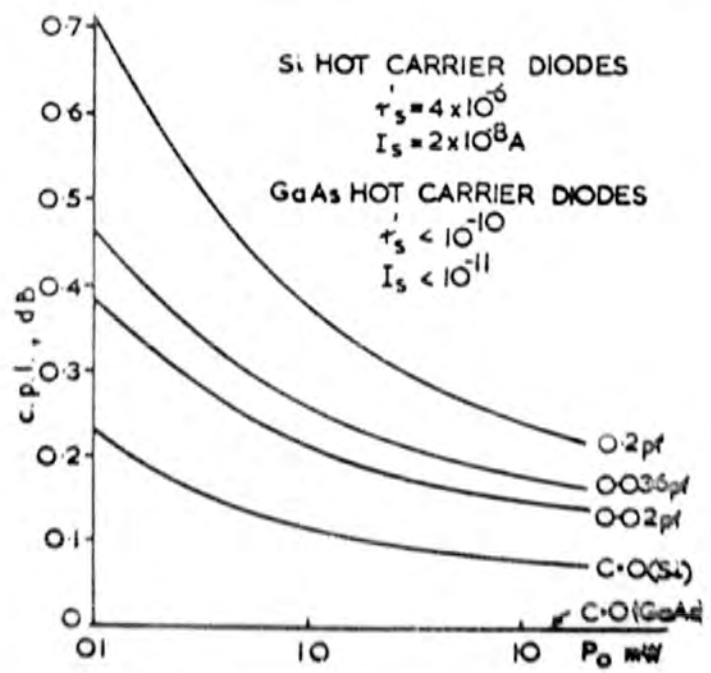

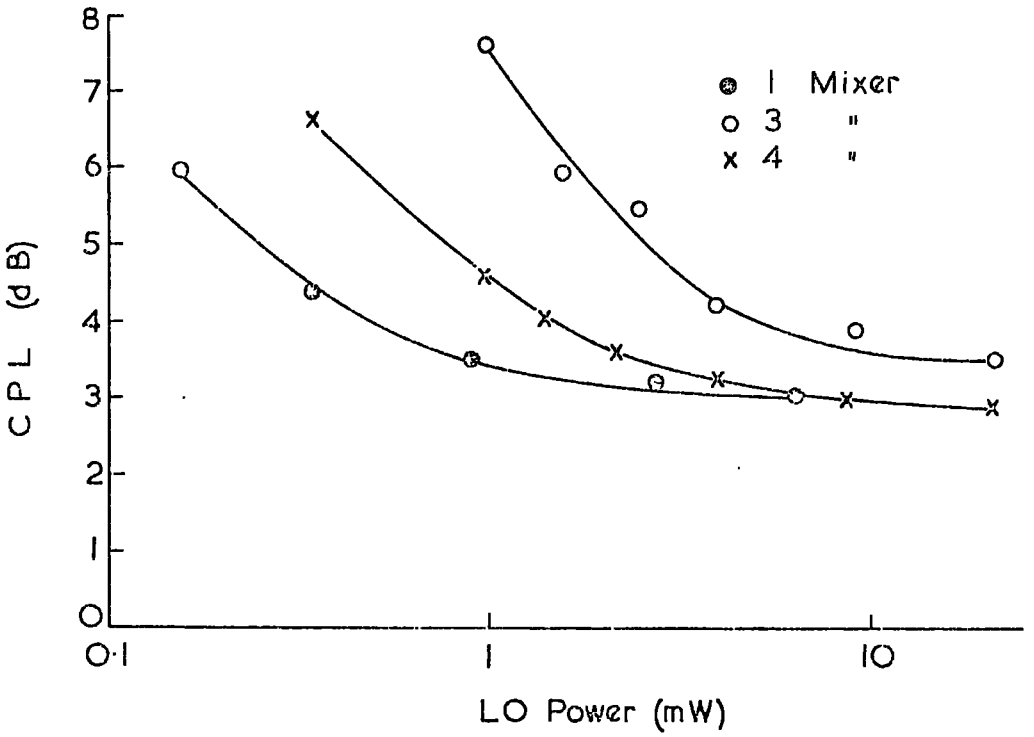

Figure 63 Conversion power loss of mixers using Gallium Arsenide diodes

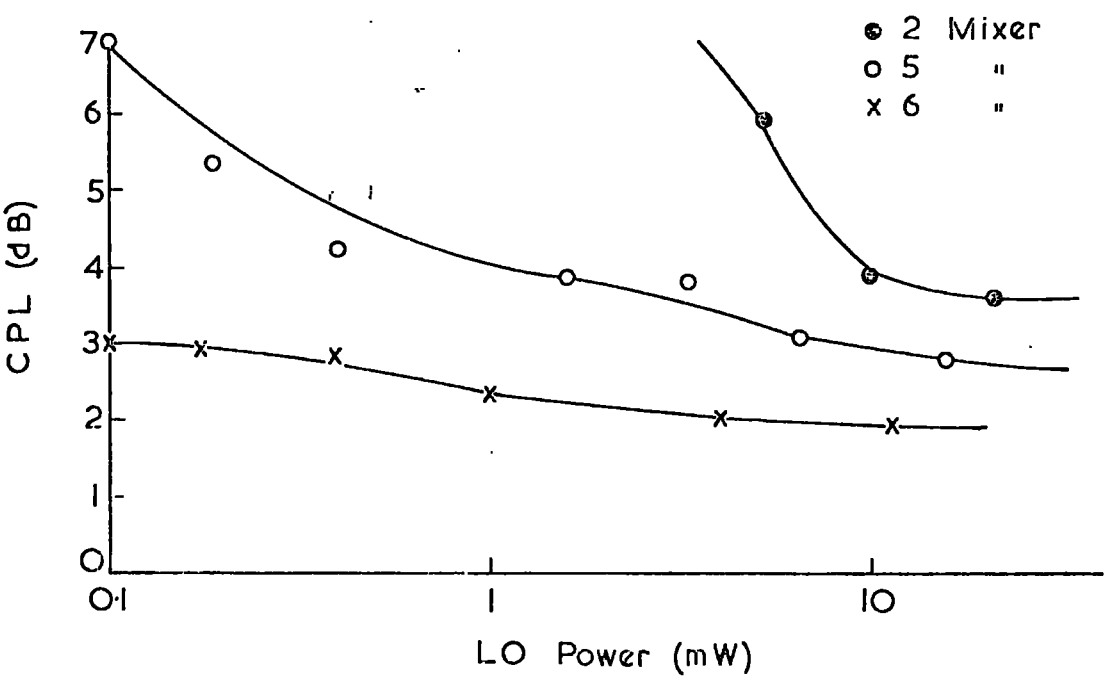

Figure 64 Conversion power loss of mixers using Silicon diodes

practical convenience, and there is no indication of how much of this power is used as current flowing around the diode lattice. Variation of local oscillator power loss would cause a shift in the X axis for each mixer, although those with a similar mechanical arrangement of the local oscillator feed (mixers 3-6), should exhibit little variation. The anomalous result of mixer 2 may be due to this cause, although the diode characteristics showed an inbalance which could also have contributed. These experimental results must then be treated with care. Theoretically the curves are sections of Fig.38, for even though the local oscillator power delivered may be the same between mixers, the X range is different due to the different diode characteristics ($X = \frac{ip}{Is}$). To the theoretical conversion power loss, which is probably around 0.5 dB, the contribution due to diode stray inductance must be added, as also must contributions due to R.F. and I.F. and connector losses in the mixer itself. Finally the imperfect image rejection must be taken into account. The lowest CPL is within 0.5 dB of these estimates in each case.

11.2.3 Noise Figure

The results from the previous section show a reducing conversion power loss with local oscillator drive. It may be considered that an increased drive should have been employed to reduce the CPL further. Partially this was not done because the local oscillator powers available in practical systems rarely exceed 10 mW, and partially because the increased current flow around the lattice causes an increase in noise figure of the mixer. This occurs directly as an increased shot noise contribution (Fig.65), and indirectly as a result of junction heating, which can lead to breakdown of the diodes.

The noise figure of mixer 6 was measured as a function of the local oscillator drive, and is given in Fig.66 which includes a

Figure 65 Noise temperature ratio t of Silicon and Gallium Arsenide diodes against diode rectified current. (Experimental, A.E.I.Ltd.)

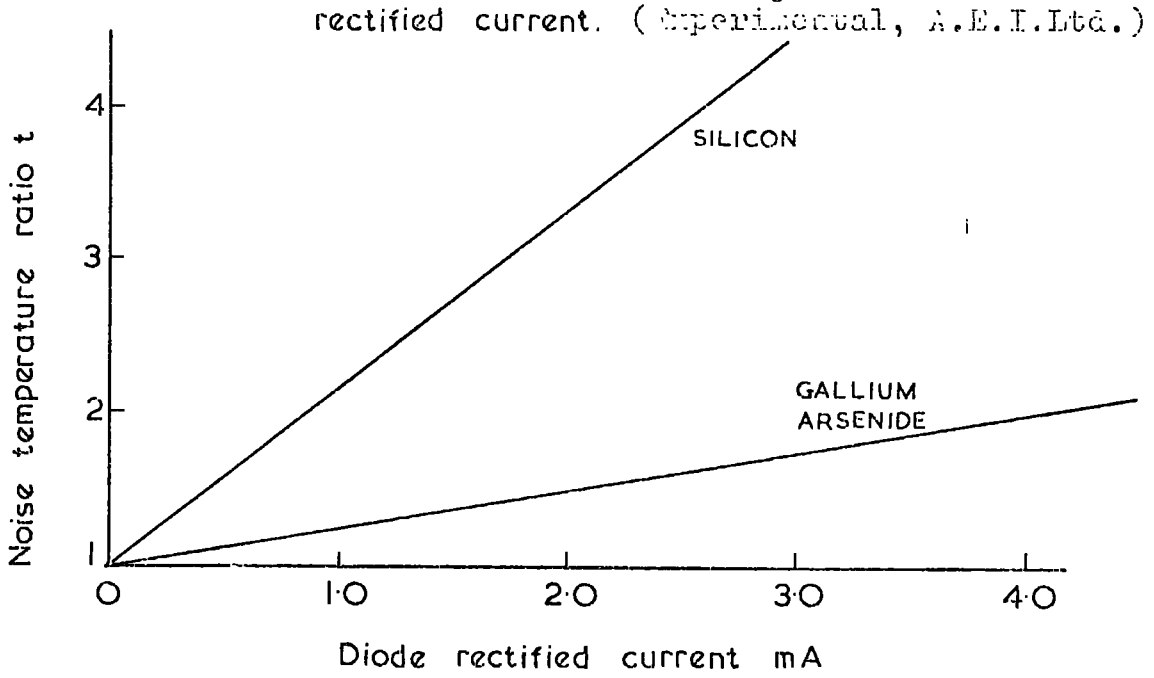

Figure 66 C.P.L. and Noise figure.

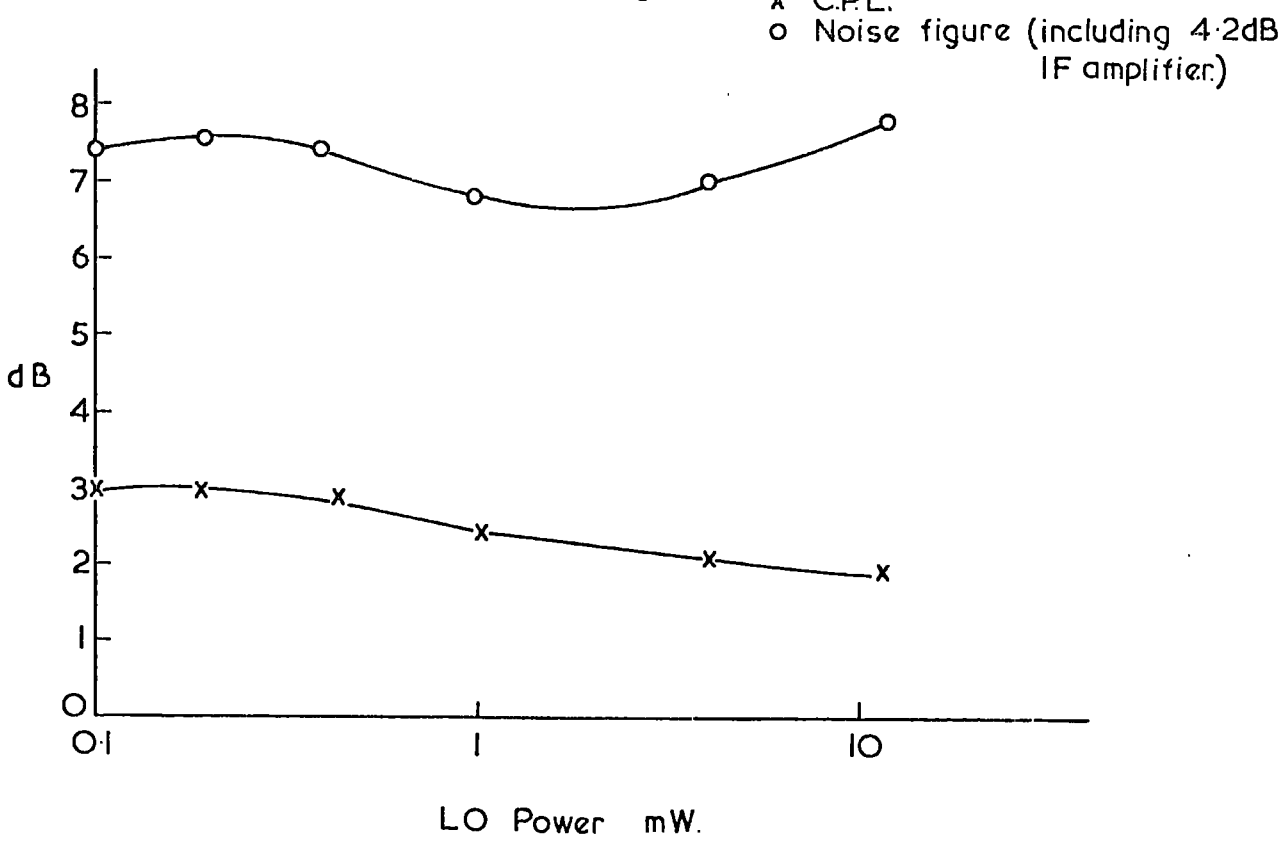

contribution from the I.F. amplifier. The I.F. amplifier noise figure was then measured separately and the noise temperature ratio t of the mixer calculated from:-

$$F_{TOTAL} = CPL\ (F_{IF} + t - 1)$$

The noise temperature ratio (Fig.67) is quite close to that given for the silicon diode in Fig.65, the increase at high local oscillator levels being apparent. This agreement between noise figure and conversion power loss has the important quality of supporting the conversion power loss value. This is important because with some mixers using diodes of variable capacity, parametric gain has been observed, which reduces the conversion power loss without necessarily reducing the noise figure.

12.0 Conclusions and Discussion

12.1 Results

The previous chapters have demonstrated the practical possibilities of producing a microwave mixer of very low and predictable loss. The value of such a mixer as the first stage in a receiver system is illustrated by the noise figure measurements. The overall performance of such an arrangement at microwave frequencies from 5 to 20 GHz using present diodes, would appear to be superior to all present low noise receiver systems, with the exception of those using parametric amplifiers. Even in these cases, bandwidth and complexity requirements may well favour the mixer. It may be asked why this work on a mixer has not been done before. Partially this could be because there was little need for it. At low frequencies atmospheric noise from the aerial makes the use of very low noise mixers pointless, whilst low noise R.F. amplifiers are easy to build anyway. At high frequencies there are three drawbacks with the type of mixer under study. Firstly the passive circuit was hard to design to obtain all the functions

Figure 67 Noise temperature ratio of mixer 6 against local oscillator power.

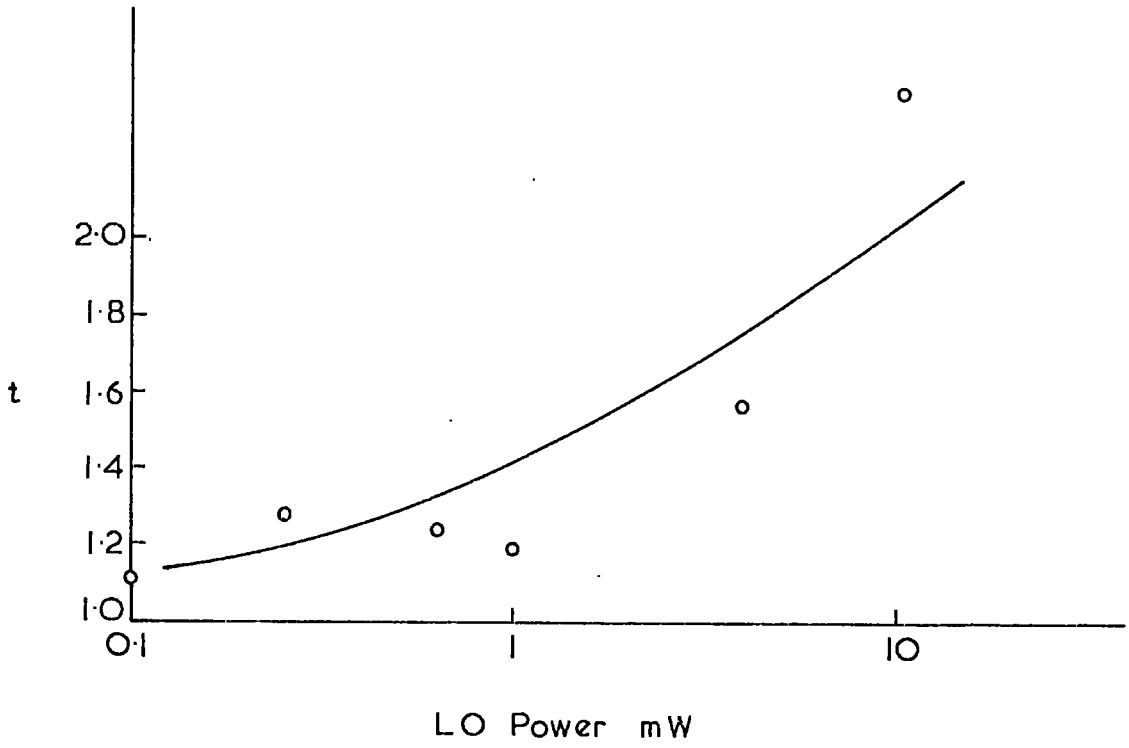

required. Secondly fairly high local oscillator powers are needed, and work is still required to produce sources of good spectral purity and stability in the range above 1 GHz. Thirdly, as mentioned before, only recently have matched diode quads suitable for this frequency range been available. This has probably come about more as a side effect of the use of microstrip techniques for large bandwidths and miniaturisation, than as a direct effort to produce low loss mixer components.

12.2 Future Possibilities

It seems certain that for some time to come the low loss mixer will allow the lowest noise figure and largest receiver bandwidth to be obtained, at any rate at the higher microwave frequencies and at reasonable cost. Present day commercial amplifiers which are uncooled and unpumped, are producing noise figures of 4 dB up to 1 GHz. In the case of transistor amplifiers which show most promise, this frequency limit could be raised to 5 GHz within a few years, but even using field effect types, low noise amplification does not appear to be feasible much above this limit. The mixer considered in this report allows a receiver noise figure of 4 dB or so because the low noise amplification is done at the relatively easy frequency of the I.F. (70 MHz). It could be pointed out that all the mixers used cheap commerical diodes, whereas microwave transistor amplifiers need expensive selected devices to obtain good results.

On the question of commercial possibilities, it would appear desirable to use an entirely integrated or thick film mixer for cheap production. Unfortunately, as mentioned, the present integrated resonators are very poor in comparison with the coaxial air-dielectric cavities used. The extra loss that would be produced would nearly

all occur in the critical R.F. signal path and would certainly increase the overall noise figure by at least 1 dB. It seems then, that a waveguide or coaxial input circuit is desirable, while diodes and associated components could be integrated easily with improved performance, due to the reduction in size and hence reduced reactive parasitics. This improvement is obvious in the case of mixers 5 and 6 where the recently available packaged quads of diodes have been employed. The improvement is due almost entirely to the packaging, the diodes being nearly identical to those used in mixer 2. Because of the inefficient and bandwidth reducing coupling system between the present mixers and I.F. amplifier, it would seem advantageous to incorporate at least the first stage of the amplifier inside the mixer. Advantage could then be taken of the high lattice output impedance at the I.F. frequency in order to make a direct low noise match into field effect or bipolar transistors. A balanced stage at the amplifier input would then eliminate the transformers entirely, which would suit present integration techniques even more.

The loss of the mixer is predictable because the theoretical study uses practical diode characteristics, rather than those based on a theoretical model of the diode. Because the diode law can be expressed in terms of current, it was an obvious choice, for mathematical simplicity, to analyse the lattice mixer action in terms of current rather than voltage. The resultant theoretical results are very close to the practical measurements, especially if contributions due to reactive diode parasitics are taken into account. In this connection, it would be interesting to consider the use of a diode law or characterisation based on the frequency domain rather than on current and voltages. Such a project could produce a theoretical study of great practical accuracy at any frequency, without

parasitic contributions being needed. Since this would be based on practical measurements, application of the theory could well be simplified in comparison with present methods.

Impedance analysis of a lossless short circuited transmission line

[illegible] the input impedance of a privacy [illegible] system in relation to that of an L-mesh two terminal circuit (a ladder). This can be worked out by Foster's theorem, involving an input impedance that is purely imaginary, with poles and zeros alternating along the frequency axis.

Two networks may be said to be equivalent if their poles and zeros correspond, and impedances are the same at any single non-resonant frequency. Fig 1 gives one example of this. The end loaded privacy consists of a short-circuited transmission line with a series lumped capacitance. The impedance of the transmission line is analysed overleaf, and considering the system used around the privacy resonance only (corresponding to the first pole of the equivalent circuit), we can approximate by lumping all non-resonant elements into one. (Figs 2 and 3). In the present case a single term approximately is adequate, since the next resonance is at three times the fundamental frequency.

Appendix 1

Impedance analysis of a lossless short circuited transmission line

For a TEM mode line of characteristic impedance Y_o and length ℓ, the input admittance is given by:-

$$Y = -jY_o \operatorname{Cot} \frac{\omega \ell}{c}$$

The admittance has poles at $\omega = n\omega_1$ where $n = 0, 1, 2, 3\ldots$, and $\omega_1 = \frac{\pi c}{\ell}$

Therefore $\frac{Y}{Y_o} = -j \operatorname{Cot} \frac{\pi \omega}{\omega_1}$

Expanding the Cot term we get

$$\frac{Y}{Y_o} = -j\frac{1}{\pi\frac{\omega}{\omega_1}} + j\frac{2}{\pi}\sum_{n=1}^{\omega} \frac{\frac{\omega}{\omega_1}}{n^2 - \left(\frac{\omega}{\omega_1}\right)^2}$$

The first term represents an inductance ($L_o = \frac{\ell}{cY_o}$) and the remaining terms of the series represent the admittance of series-tuned circuits

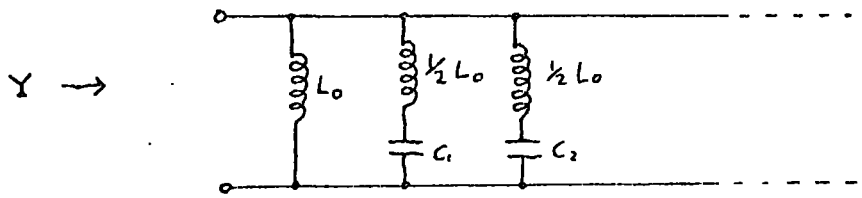

The effect of taking one, five and all the elements into account is plotted in Fig. 3.

Appendix 1

Fig. 1

Equivalent circuits for an n-mesh 2 pole with poles at w = 0 and ∞.

(a) Impedance form

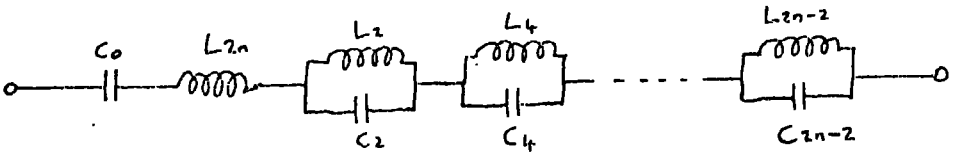

$$Z(\omega) = jA\omega \frac{(\omega^2-\omega_1^2/(\omega^2-\omega_3^2).....(\omega^2-\omega_{2H-1}^2)}{\omega^2(\omega^2-\omega_2^2)(\omega^2-\omega_4^2)...(\omega^2-\omega_{2H-2}^2)}$$

(b) Admittance form

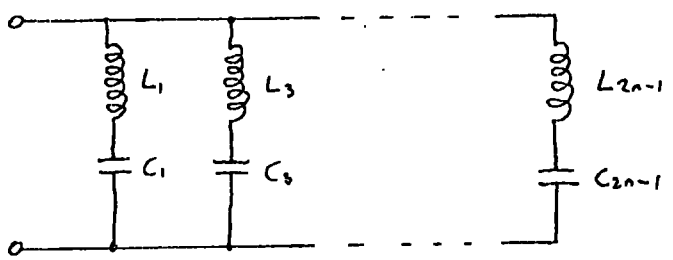

$$Y(\omega) = \mathbf{Z}(\omega)^{-1}$$

Fig. 2

Fig. 1 simplified at one pole $\omega = \omega_k$

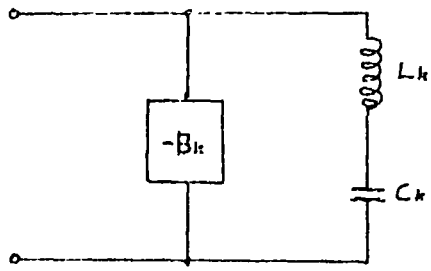

Fig. 3

Curves showing exact form of admittance function and two approximations.

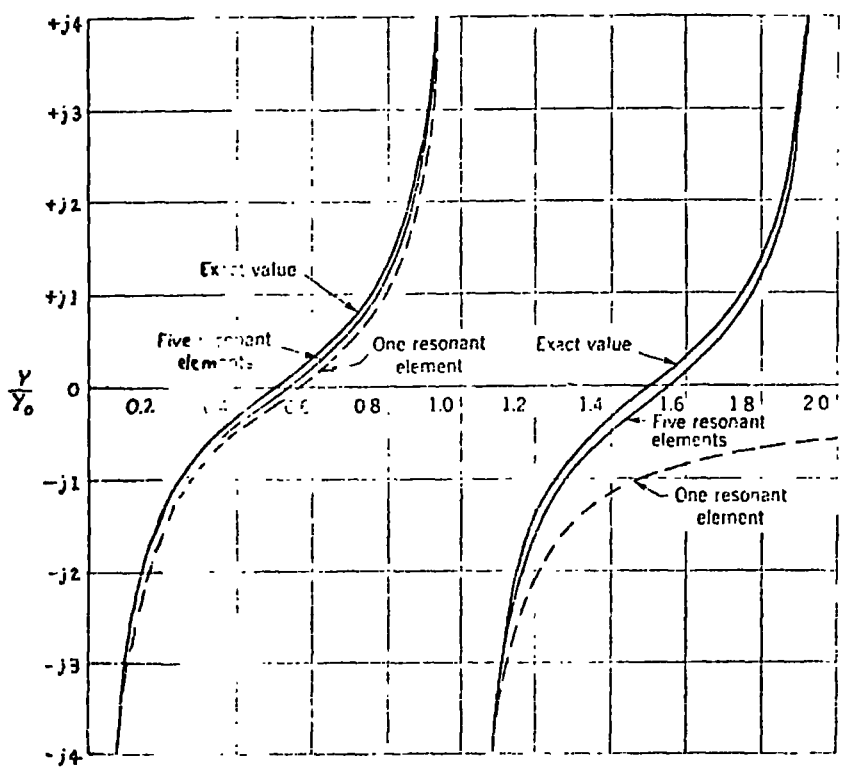

Appendix 2

Simplifications in the calculations for loop coupling

In Fig. 1d :-

$$R_e = \frac{X_m^2 R_s}{R_s^2 + X_\ell^2} \qquad \text{(i)}$$

and $$X_e = X_m \left(1 - \frac{X_\ell (2X_\ell - X_m)}{R_s^2 + X_\ell^2}\right)$$

In Fig. 1c using Kirchoff's Law at the points a - a' :-

$$R_s \approx \left(\frac{i_o}{i_1}\right) X_m$$

(Assuming $\frac{i_o}{i_1} > 1$ and $m \approx \sqrt{\ell \times L_o}$)

Therefore $R_s >> X_\ell$ and (i) becomes:-

$$R_e = \frac{X_m^2}{R_s}$$

also $X_e \approx X_m$ to a first approximation

Appendix 2

A Loop Coupled End-loaded Cavity

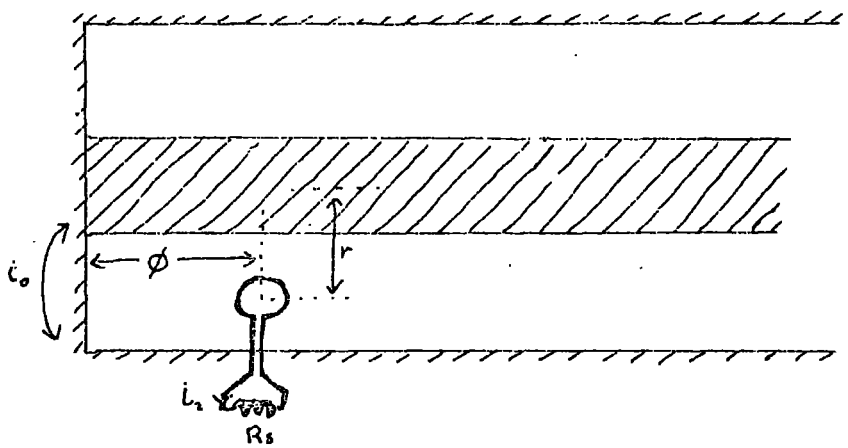

Fig. 1a Loop area A inserted in cavity

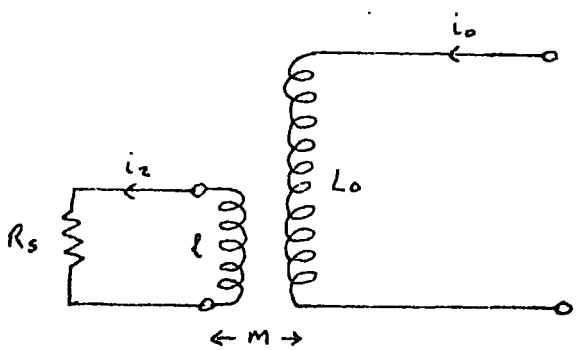

m = mutual inductance

ℓ = loop inductance

Fig. 1b Lumped equivalent circuit

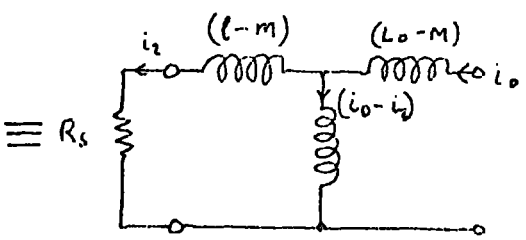

Fig. 1c

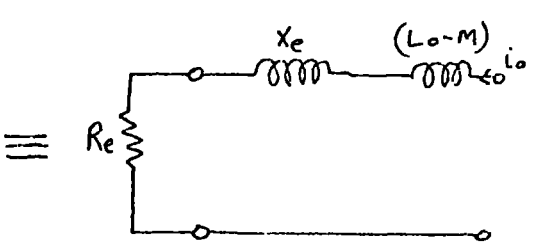

Fig.1d

Appendix I

Derivation of the inductive field in a Coaxial Cavity

$$X_m = \omega_o \times \frac{\text{lines of magnetic flux enclosed}}{\text{current induced}}$$

$$= \frac{\omega_o A \mu_o H}{i_1} \quad \text{in mks units}$$

From Fig. 2 :-

$$AH = \frac{i_1 \lambda_o}{4\pi^2} \int_o^{\phi} \int_a^{L} \frac{\cos\theta}{r} \, dr \, d\theta$$

$$= \frac{i_1 \lambda_o \sin\phi \ln(\frac{b}{a})}{4\pi^2}$$

Therefore

$$X_m = \frac{\mu_o \omega_o \lambda_o \sin\phi \ln \frac{b}{a}}{4\pi^2}$$

Now:-

$$\omega_o \lambda_o = \frac{2\pi c}{\sqrt{\varepsilon_r}}$$

where c = speed of light, ε_r = relative permeability of cavity filling.

For a concentric circular coaxial line:-

$$\ln \frac{b}{a} = 2\pi \frac{Z_o \sqrt{\varepsilon_r}}{\sqrt{\varepsilon_o \mu_o}}$$

Therefore $X_m = Z_o \sin^2\phi$

Appendix 3

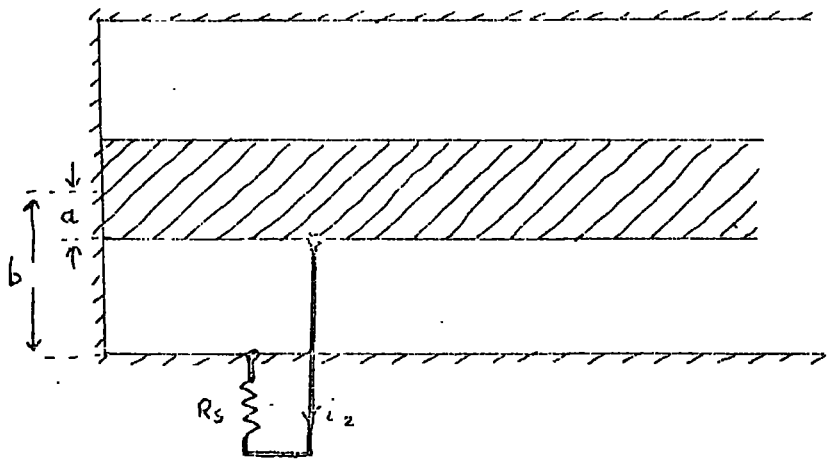

Fig. 1 Direct coupled cavity

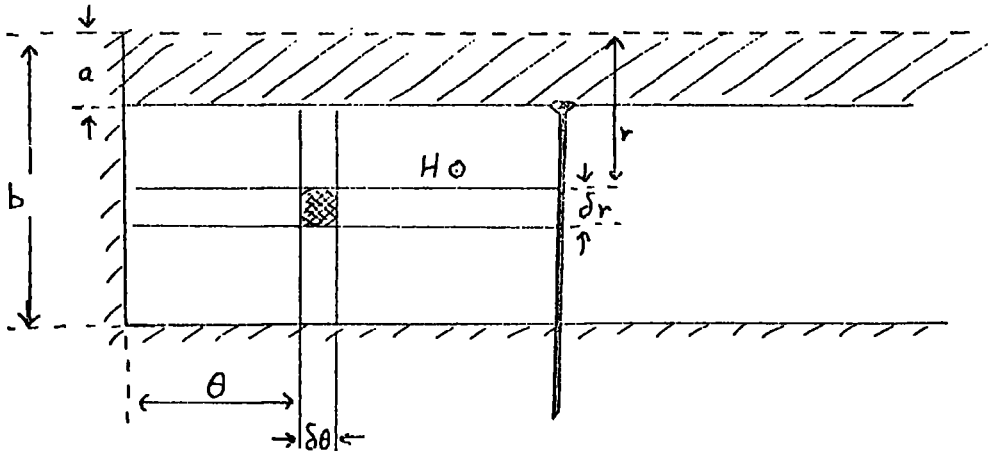

Fig. 2 Showing the magnetic flux density integration

APPENDIX 4

The loaded Q value of an End-loaded Cavity

$$Q_L = \frac{Z_o \pi}{4R_L}\left(\frac{i_o}{i_1}\right)^2 \quad \text{(Transmission line)} \quad .. \quad .. \quad .. \quad .. \quad (1)$$

$$Q_L = \frac{\omega_o L_o}{R_L}\left(\frac{i_o}{i_1}\right)^2 \quad \text{(Equivalent circuit)} \quad .. \quad .. \quad .. \quad .. \quad (2)$$

Therefore $$L_o = \frac{Z_o \pi}{4\omega_o} \quad .. \quad .. \quad .. \quad .. \quad .. \quad .. \quad (3)$$

$$\hat{I}_1 = \frac{V_{L_o}}{R_L - \frac{j}{\omega_o C}}$$

and $$\hat{I}_o = \left(I_1 - \frac{V_{L_o}}{\frac{-j}{\omega_o C_o}}\right)$$

$$= V_{L_o}\left(\frac{R_L + j\left(\frac{1}{\omega_o C} + \omega_o C_o R_L^2 + \frac{1}{\omega_o^2 C^2}\right)}{R_L^2 + \frac{1}{\omega_o^2 C^2}}\right)$$

separating Real and Imaginary ports $\left(\text{because } |I_o| = \sqrt{R^2 + I^2}\right)$

Therefore $$\frac{|I_o|^2}{|I_1|^2} = \frac{i_o^2}{i_1} = \frac{R_L^2 + \left[\frac{1}{\omega_o C} + \omega_o C_o\left(R_L^2 + \frac{1}{\omega_o^2 C^2}\right)\right]^2}{R_L^2 + \frac{1}{\omega_o^2 C^2}^2} \times \left(R_L^2 + \frac{1}{\omega_o^2 C^2}\right)$$

$$= 1 + \frac{2C_o}{C} + \omega_o^2 C_o^2 R_L^2 + \frac{C_o^2}{C^2} \quad .. \quad .. \quad .. \quad .. \quad .. \quad (4)$$

$$= \omega_o^2 C_o^2 R_L^2 + \left(1 + \frac{C_o}{C}\right)^2 \quad .. \quad .. \quad .. \quad .. \quad (4)$$

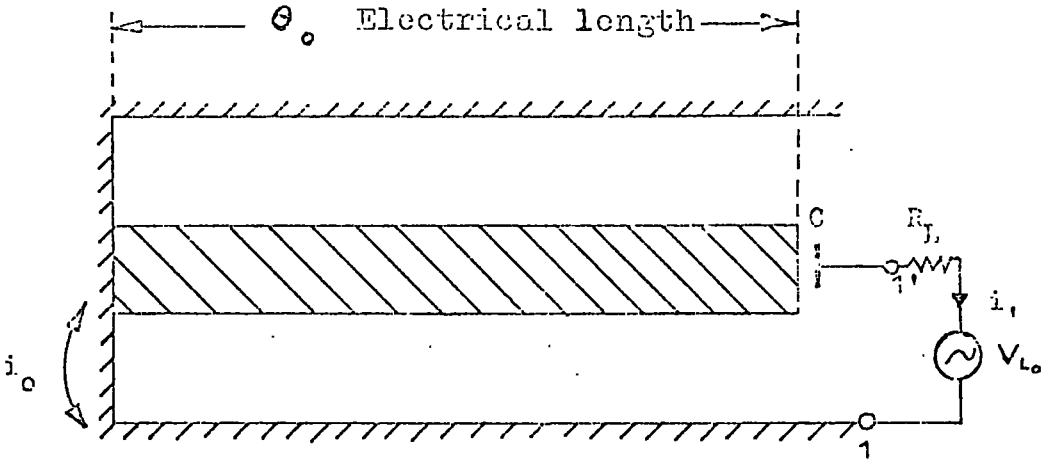

(Resonant frequency ω_0 , i_0, i_1 , rms values of $\hat{I}_0$, $\hat{I}_1$)

Fig. 1 Cavity fed by a Voltage Source

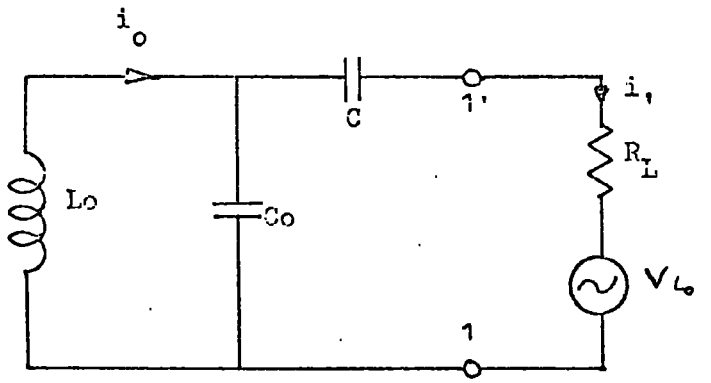

Fig. 2 Equivalent Circuit

Now:- $C = \frac{1}{\omega_o Z_o \tan \theta_o}$ and $C + C_o = \frac{1}{\omega_o^2 L_o}$

from transmission line and equivalent circuit resonance conditions respectively.

Therefore $\left(1 + \frac{C_o}{C}\right)^2 = \left(\frac{C + C_o}{C}\right)^2 = \frac{16\tan^2 \theta_o}{\pi^2}$ .. .. (5)

$R_L \omega_o C_o << 1$ for Q values > 1

Therefore $(R_L \omega_o C_o)^2$ can be neglected in comparison with $\frac{16\tan^2 \theta_o}{\pi^2}$

for practical values of Q_L.

Therefore substituting (5) into (1)

$$Q_L \simeq \frac{4Z_o}{\pi R_L} \tan^2 \theta_o$$

APPENDIX 5

Output Components of Balanced and Double-Balanced Mixers

Balanced:-

Switching function $S(t)$ $\begin{matrix}1\\0\end{matrix}$

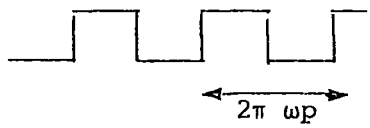

Fourier Series:- $S(t) = \frac{1}{2} + \frac{2}{\pi}(\cos \omega p - 1/3 \cos 3\omega p + 1/5 \cos 5\omega p$ ..... etc.)

Signal:- $A \cos \omega q$

Output = $A \cos \omega q \; S(t)$

$$= \frac{A \cos \omega q}{2} + \frac{2A}{\pi}(\cos \omega p \cos \omega q - 1/3 \cos 3\omega p \cos \omega q + \text{etc})$$

(1) (2) (3)

$$= \frac{A}{2}\cos \omega q + \frac{2A}{\pi}(\cos(\omega p - \omega q) + \cos(\omega p + \omega q))$$

$$- \frac{2A}{3\pi}(\cos(3\omega p - \omega q) + \cos(3\omega p + \omega q)) \text{ etc.}$$

Output terms:-

1 Signal

2 I.F. (difference frequency)

3 Sum frequency

Double Balanced:-

Switching function S(t) :-

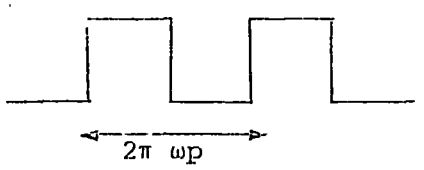

Fourier series:- $S(t) = \frac{4}{\pi} (\cos \omega p - 1/3 \cos 3\omega p + 1/5 \cos 5\omega p$ ..... etc.)

Signal:- $A \cos \omega q$

Output = $A \cos \omega q \; S(t)$

$$= \frac{4A}{\pi} (\cos \omega p \cos \omega q - 1/3 (\cos 3\omega p \cos \omega q) + \text{etc.})$$

$$= \frac{4A}{\pi} (\underset{(2)}{\cos (\omega p - \omega q)} + \underset{(3)}{\cos (\omega p + \omega q)}$$

$$- \frac{4A}{\pi} (\cos (3\omega p - \omega q) + \cos (3\omega p + \omega q)) + \text{etc.}$$

Note increased coefficients of term (2) (I.F. output) in case of double-balanced configuration, and lack of unwanted signal (term (1)) at output.

REFERENCES

1. Lord Kelvin "On the Theory of the Electric Telegraph" Maths. Phys. Papers 2. P.61 Proc. Roy. Soc. 1855

2. G. Kirchoff "Über dic Bewegung der Electrizitat in Drahten Pogg. Ann. 100, P.193, 1857

3. O. Heavyside Electric Papers 2, Pp.19 and 307, 1886-71

4. J.J. Thomson Math. Soc. Proc. 17, P.310, 1886

5. Lord Rayleigh "Sound I", 1894

6. E.G. Richardson "Sound", Edmond Arnold 1927

7. E.J. Jordan "Wireless World", 76. 1423, January 1971

8. W.L. Barrow "Transmission of Electromagnetic Waves in Hollow Tubes on Metal", Proc. I.R.E. 24, P.1298, October 1936

9. G.C. Southworth "Hyper-frequency Wave Guides", Bell System Technical J. 15, P.284, April 1936

10. W.W. Hansen "A type of Electrical Resonator," J. Appl. Phys. 9, P.654, October 1938

11. A.L. Schanlow and C.H. Townes "Infrared and Optical Masers", Phys. Rev. 112, Pp.1940-1949, December 1958

12. A.G. Fox and T. Li "Resonant Modes in a Maser Interferometer", Bell System Tech. J. 40, Pp. 53-458, March 1961

13. D.J.E. Ingram "Microwave Spectroscopy", Butterworth 1955

14. P.H. Smith "Optimum Coax Diameters", Electronics, Pp. 111-114, February 1950

15. S.B. Cohn "Direct Coupled Resonator Filters", Proc. I.R.E. Pp. 187-196, February 1957

16. W.W. Mumford "Maximally Flat Filters in Waveguide", Bell System Technical J. 22, Pp. 648-714, October 1948

17. R.M. Fano, A.W. Lawson Jnr. "Microwave Filters using Quarter Wave Couplings", Proc. I.R.E. 35, Pp.1318-1323, November 1947

18. G.L. Matthaei, L. Young, E.M.T. Jones "Microwave Filters, Impedance-Matching Networks and Coupling Structure", Chapter 4 McGraw-Hill, 1964

19. E.V.D. Galzier, H.R.L. Lamont "Services Textbook of Radio", 5, P. 252, H.M.S.O. 1958

20. Morena, Theodore "Microwave Transmission Design Data" Pp. 11-41, Dover 1958

21. H.T. Friis "Noise Figures of Radio Receivers", Proc. Inst. Radio Engrs. 32, Pp. 419-422, 1944

22. B.L.J. Kulesza "General Theory of a Lattice Mixer", Proc. IEE 118, Pp. 864-870, 1971

23. Torrey and Whitmer "Crystal Rectifiers" M.I.T. Press, P.15, 1948

24. D.G. Tucker "Modulation and Frequency Changers", MacDonald 1953

25. Penfield and Rafuse "Varactor Applications", M.I.T. Press 1962

26. R.A. Pucel "Theory of the Esaky Diode Frequency Converter", Sol. St. Electronics, 3, Pp. 167-207, 1961

27. H.E. Rowe "Some General Properties of Non-linear Elements", Part II, Proc. I.R.E., 46.5, Pp.850-860, 1958

28. A.M. Saleh Adel "Theory of Resistive Mixers", M.I.T. Press 1971

29. H.S. Block "Modulation Theory", Van Nostrand, P.147, 1953

30. J.P. Wright Internal Report 5 of the Solid State Microwave Research Group, University of Durham. (Also Report 13 in preparation)

31. Standards on Electron Devices : Methods of Measuring Noise Proc. I.R.E. Vol. 41, 7, Pp. 890-896

32. J. Gregory Ph.D. Thesis (in preparation)

33. Handbook of Microwave Measurements, Vol.1 P.379, Wiley 1963

34. W.W. Mumford "A Broad-band Microwave Noise Source", Bell System Technical J. 28, Pp. 608-618

35. F.E. Terman Radio Engineers Handbook, Pp. 210-215, McGraw-Hill 1950

36. B.L.J. Kulesza Ph.D. Thesis, Department of Electronic & Electrical Engineering, University of Birmingham, Birmingham, England

4.5 GHz NARROW-BAND OPEN-CIRCUIT LATTICE MIXERS

by

J.P. Wright J.R. Emmett B.L.J. Kulesza

Paper read at the

European Microwave Conference

August 1971

Stockholm

4.5 GHz NARROW-BAND OPEN-CIRCUIT LATTICE MIXERS

J.P. Wright
Newcastle Pol. & U. of Durham U.K.

J.R. Emmett
U. of Durham U.K.

B.L.J. Kulesza
U. of Durham U.K.

1. Introduction

The previous paper presented a summary of the general theory of a lattice mixer and specifically dealt with the solutions of special cases in which the circuit was assumed to be purely resistive. The conclusion was that a narrow-band open-circuit mixer offers the lowest c.p.l. even at quite low image-rejection ratios. The aim of this project was to construct such a mixer at 4.5 GHz and investigate its performance.

The basic circuit of the lattice mixer shown in Fig.1 of the preceding paper was used as the starting point. The main difficulty was to find a microwave equivalent for the balanced arrangement of the two series resonances in the mixer input. From among the available microwave components the resonant cavity was chosen since it offers the highest Q and hence the highest image-rejection ratio. At the frequency of 4.5 GHz its physical size is not prohibitive and is comparable to the remaining components of the mixer circuit.

2. Two-cavity balanced system

It is well known that a coaxial transmission line of just under a quarter of a wavelength long, shorted at one end and capacitively-loaded at the other, will behave as a resonant element. In the usual applications, because of the way in which the two coupling loops and/or probes are introduced, such a cavity can be represented as a parallel resonant circuit. The series-resonance behaviour was achieved by utilising the cavity end-capacitance also as the coupling element to the load.

Two, identical, end-loaded cavities were finally combined to form a balanced system as shown in Fig.1. The signal is fed via the two coupling loops in parallel forming a figure of eight on the diagram. The local-oscillator current through the diodes produces opposing voltages across each loop also across C_1 & C_2 capacitors. Accordingly, under the ideal balance conditions, there should not be any local-oscillator breakthrough into the signal or the intermediate-frequency circuits. The capacitor C_3 is provided for fine adjustment of the 'longitudinal' resonance at the local-oscillator frequency and thus to ensure a sinusoidal current waveform during the forward-conducting periods of the diodes as required by the theory.

The transfer characteristics of the two cavities are shown in Fig.2. In each case, the image frequency component is attenuated by more than 14 dB. At the signal frequency the loss is about 0.6 dB per cavity giving a total loss of about 1.2 dB in the input.

3. Mixer diodes

If a semiconductor diode is considered as a time-varying resistance, there are essentially three constants which characterise its performance. These are, r_b the incremental resistance at the origin, r_s the spreading resistance, and I_s the reverse saturation current constant. Furthermore, to assess its potential in a microwave circuit the diode depletion and package capacitances must also be known. The ratio r_s/r_b, denoted by r_s', is used to describe the quality of the diode and I_s is incorporated in the definition of the local-oscillator current drive X.

The information supplied by manufacturers on the mixer diodes is usually inadequate and further measurements are necessary to establish their parameters accurately. These measurements, carried out at d.c., r.f. and microwave frequencies, are essential not only to find out whether the assumed diode law is satisfied but also to obtain a matched set of four diodes.

There are two types of semiconductor diodes which are normally considered for use in a mixer circuit. The modern point-contact diode with its relatively low capacitance, and the hot carrier diode characterised by a low reverse-current constant I_s and greatly reduced storage effects. Various independent techniques were employed to determine r_b and I_s, the key parameters of the diode. These included a.c. bridge measurements, graphical extrapolation methods, and computer-aided calculations of all the diode constants from the I/V forward characteristics. In lattice mixers the reverse characteristic is of no interest if the incremental resistance is greater than r_b. The relation $r_b = kT/qI_s$ provided an additional check on the validity of the individual measurements.

The results obtained on point-contact diodes have produced a wide range of values for the constants. Magnitudes as low as 7.5K for the r_b, and as high as 3.2μA and 12 ohms for I_s and r_s, respectively, were recorded for one type of diode. It had a low capacitance and was recommended by the manufacturer as a possible mixer diode at X-band. However, because its quality factor was poor (ab. 10^{-3}) its use in a lattice mixer even at 4.5 GHz cannot produce a satisfactory low-loss performance. Other point-contact diodes had more acceptable parameters, r_b in the order of 100K, I_s of about 0.3μA and r_s of 1 to 3 ohms.

The measurements obtained on hot carrier diodes have produced better results. The constants of the Si devices, HP2970, DC1502 and HP2815 gave quality factors of $4.7\ 10^{-6}$, $0.83\ 10^{-6}$ and $0.3\ 10^{-6}$, respectively. The total capacitance in some cases was just above 1 pf.

An exceptional set of constants was obtained for the unencapsulated GaAs hot carrier junction 148CAY/A, manufactured by Mullards, resulting in a quality factor of about $4\ 10^{-11}$ and the total capacitance of about 0.1 pf. Graphical-extrapolation methods had to be employed to deduce r_b and I_s of $1.3\ 10^{11}$ ohms and $2\ 10^{-13}$ amps, respectively.

4. The effect of the depletion capacitance on the c.p.l. and Z_i

It is apparent that as higher operational frequencies are utilised diode capacitances cannot be ignored, and their effect must be included in the analysis. This was achieved by replacing the time-varying resistances with the time-varying impedances. Since the external-to-junction capacitance is determined by the type of encapsulation used and circuit strays, it was decided initially to consider only the depletion capacitance at the origin. Consequently, the K_1, K_2 & K_3 parameters became not only functions of the local-oscillator drive and the quality factor of the diodes, but also of the depletion capacitances. Because of good image-rejection ratios obtained with the double-cavity system (Fig.2), and for mathematical simplicity, the termination at the image frequency was assumed to be infinite.

The calculated total loss for the lattice mixer using Si and GaAs diodes at various local-oscillator powers is shown in Fig.3. The loss due to the depletion capacitance is given by the reading above the reference level, i.e. C = 0.

It is seen in Fig.4 that the capacitance has a considerable effect on the magnitude of the input impedance at the signal frequency. Similar effect is predicted for the output impedance at the intermediate frequency.

5. Results and comparison with the theory

The results obtained on the two mixers are encouraging not only because of their low-loss performance but also because a close agreement with the theoretical predictions was achieved. Most of the excess loss can be accounted for, within the experimental error, in each mixer circuit.

Although the image frequency rejection was good (Fig.2) we found that the total loss of the cavities at the signal frequency was still too high at about 1.2 dB. The losses incurred in the matching networks amounted to about 0.9 dB. The remaining loss of 1 dB is attributed to the diode capacitances and diode inductance. The effect of the package and stray capacitances on the c.p.l. is being analysed but the results are not yet available for comparison.

On comparing the two mixer circuits in Fig.5 it is noted that to obtain the same c.p.l. higher local-oscillator power is required for the Si devices. The reason for this, verifiable by the analysis, is that the quality factor for the Si diodes is much worse than that for the GaAs diodes.

A complete elimination of diode reactances or their neutralisation by circuit techniques is difficult, if not impossible, at higher frequencies. Microwave integrated circuits may be a solution to the problem in which junctions can be placed directly on suitable substrates. In our mixers improvements in the design of cavities and matching networks should produce a further reduction of at least 1.5 dB in the total loss. This means that for a lattice mixer using GaAs hot carrier diodes a measured c.p.l. of about 1.5 dB should be possible.

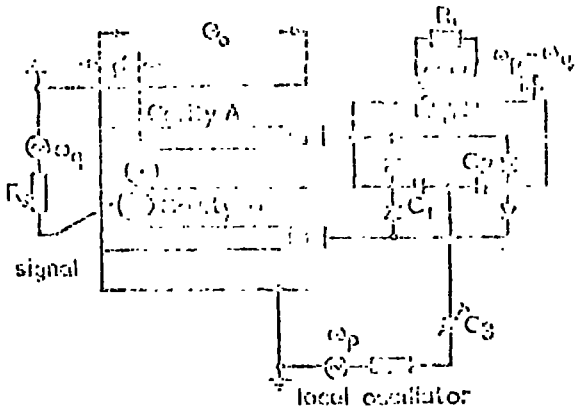

Fig.1 Diagrammatic Representation of a 4·5 GHz Lattice Mixer.

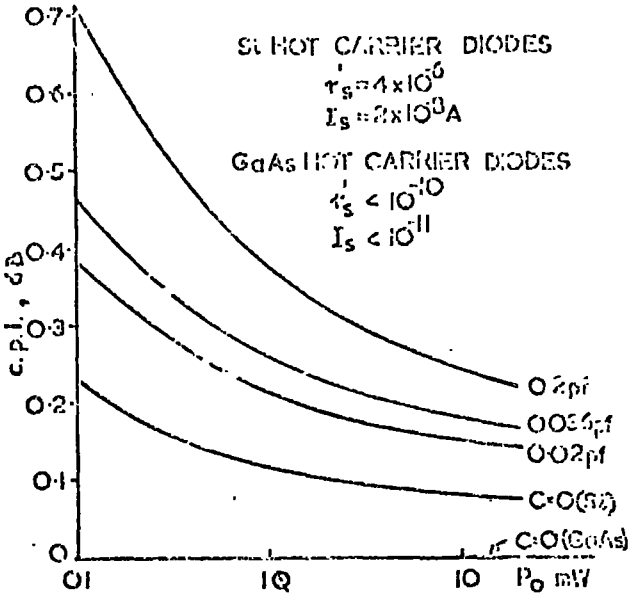

Fig.3 Predicted loss due to diode depletion capacitances.

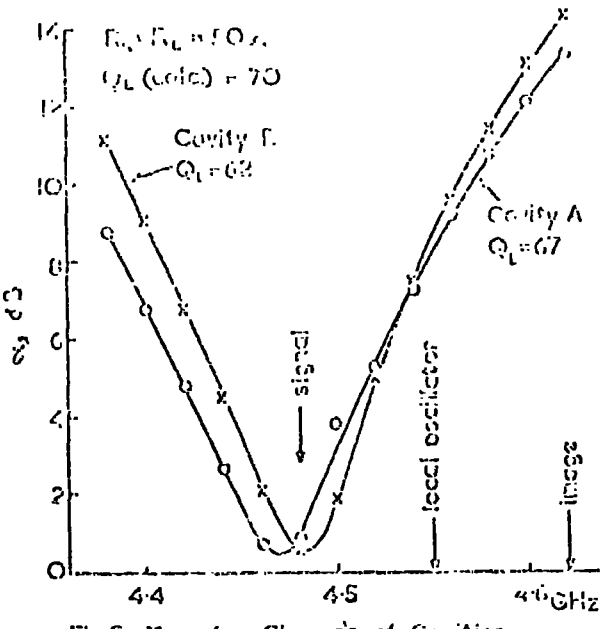

Fig 2. Transfer Charac's of Cavities

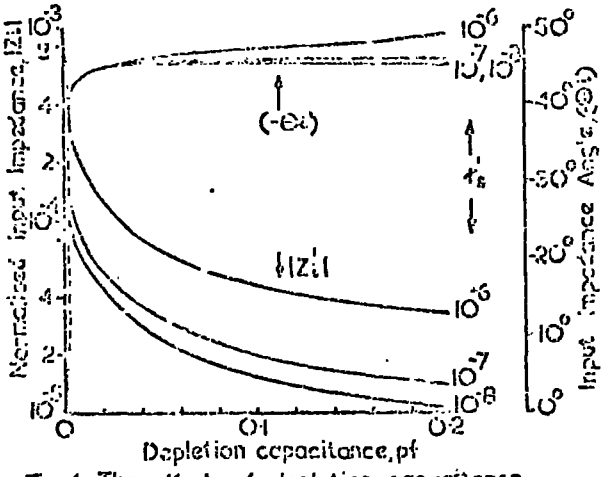

Fig.4 The effect of depletion capacitance on input impedance.

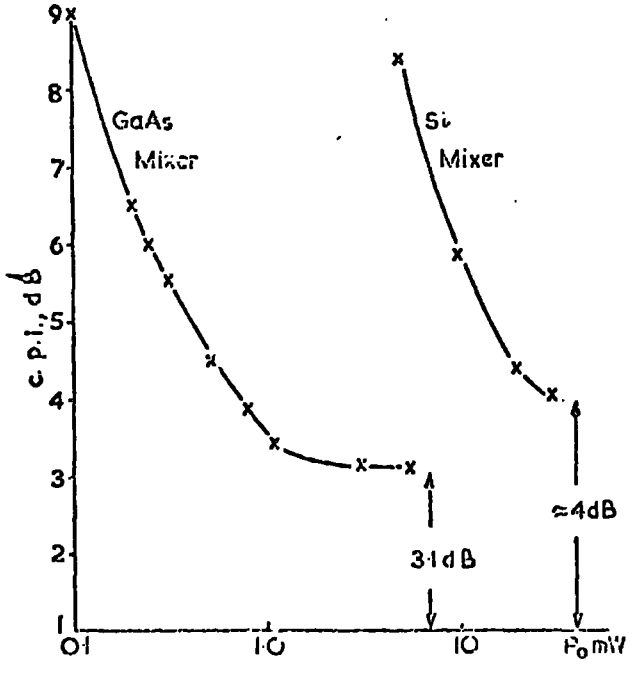

Fig 5 Measured optimum c.p.l. as a function of local-oscillator power

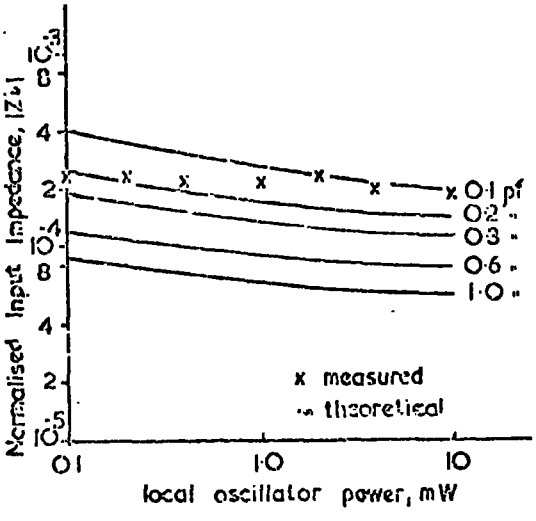

Fig 6. Magnitude of input impedance under matched conditions